Inferring magnetic fields in galaxy clusters

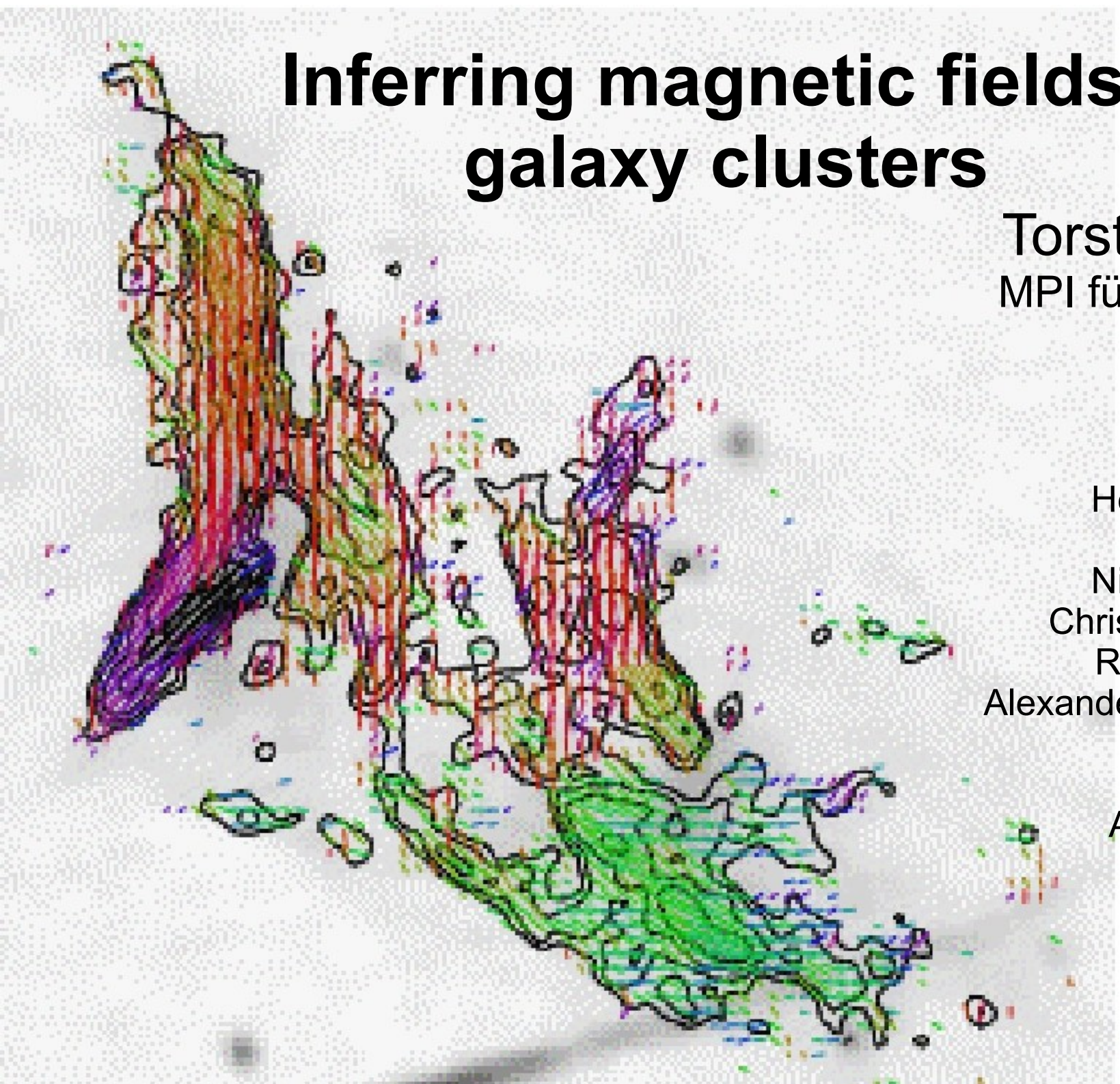

Torsten Enßlin
MPI für Astrophysik

collaborators:
Tracy Clarke
Martin Jubelgas
Henrik Junklewitz
Petr Kuchar
Niels Oppermann
Christoph Pfrommer
Rodion Stepanov
Alexander Schekochihin
Volker Springel
Corina Vogt
Andre Waelkens

Outline:

Cluster radio emission
& magnetic turbulence

Faraday rotation
& magnetic spectrum inference

Stokes correlators
& tension forces

Faraday-Stokes correlations
& magnetic helicity

Outline:

Cluster radio emission
& magnetic turbulence
T. Clarke, C. Pfrommer, V. Springel

Faraday rotation
& magnetic spectrum inference

Stokes correlators
& tension forces

Faraday-Stokes correlations
& magnetic helicity

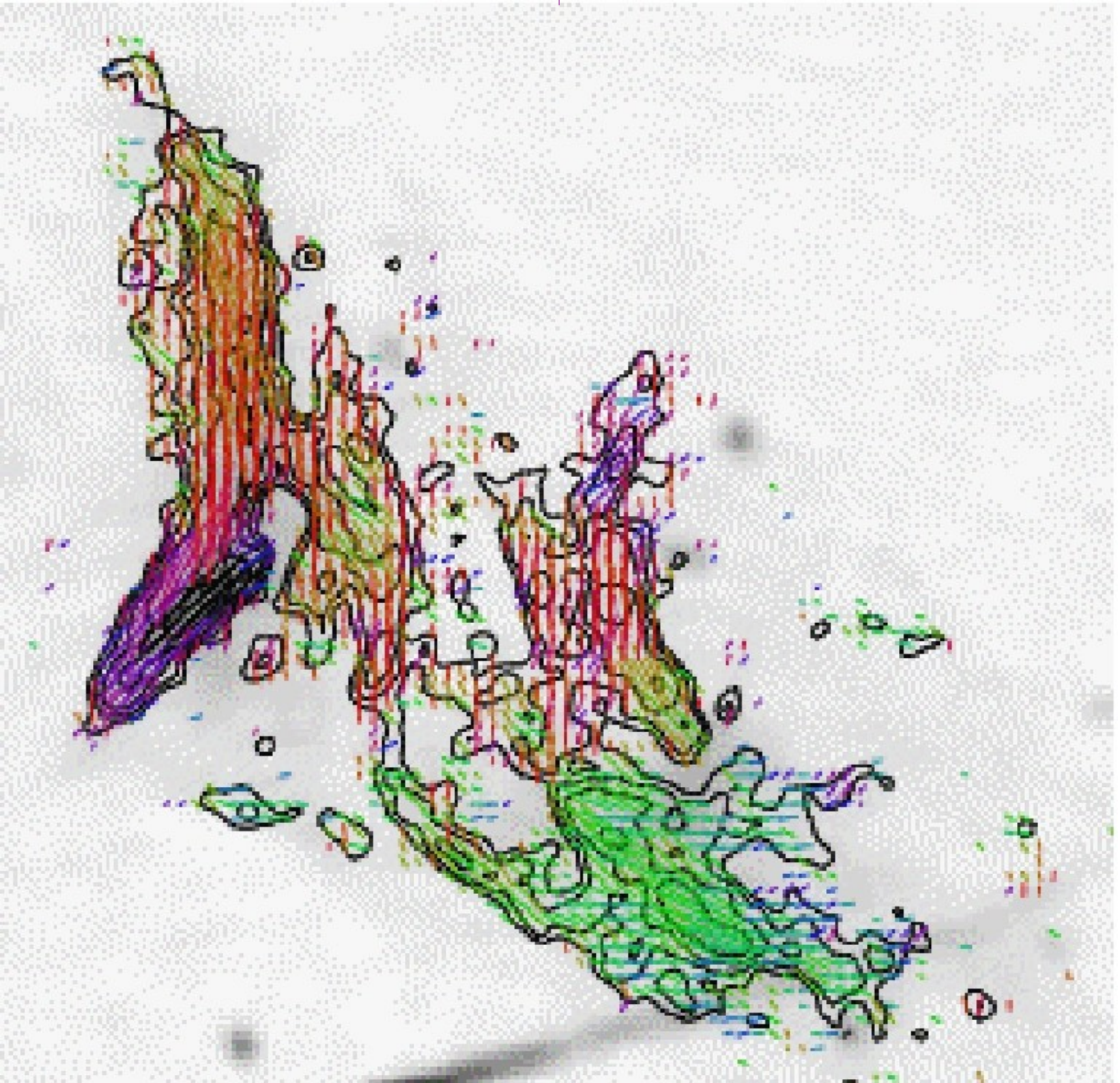

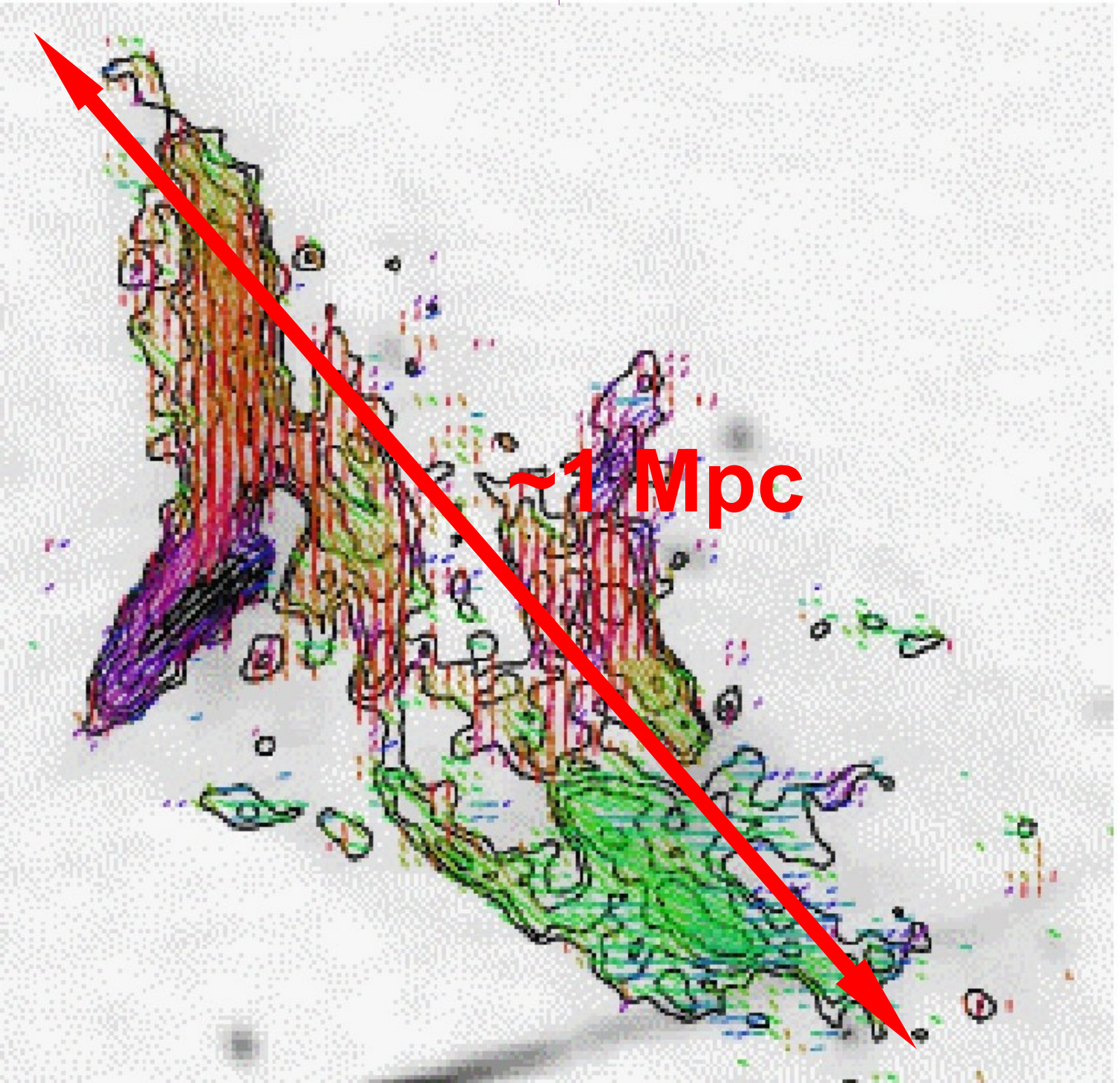
~1 Mpc

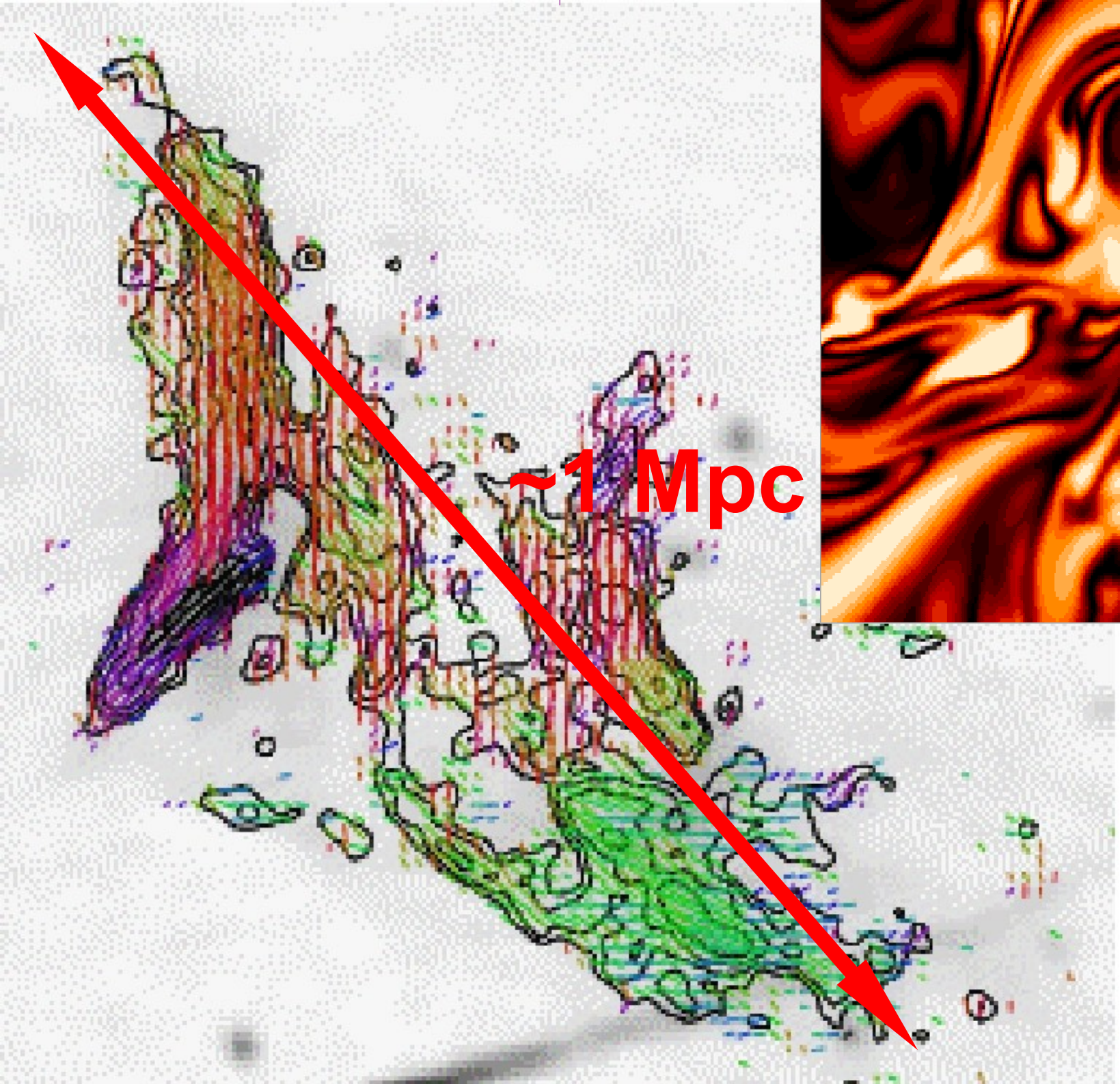

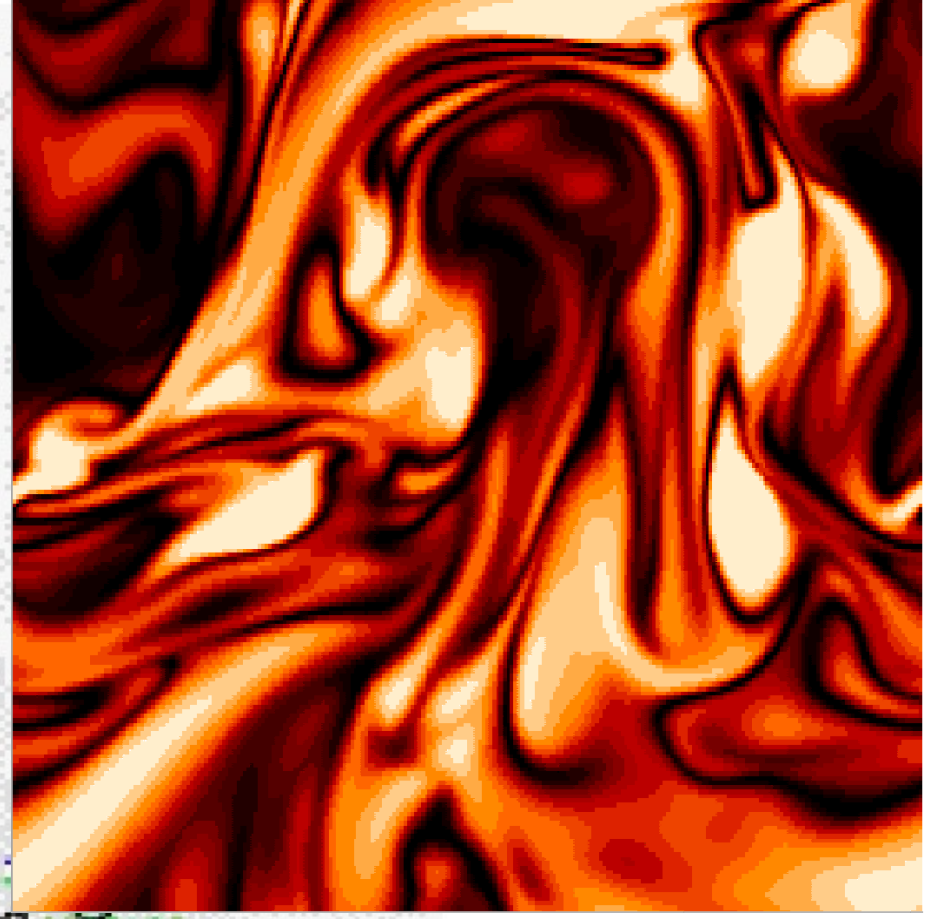

Schekochihin et al.

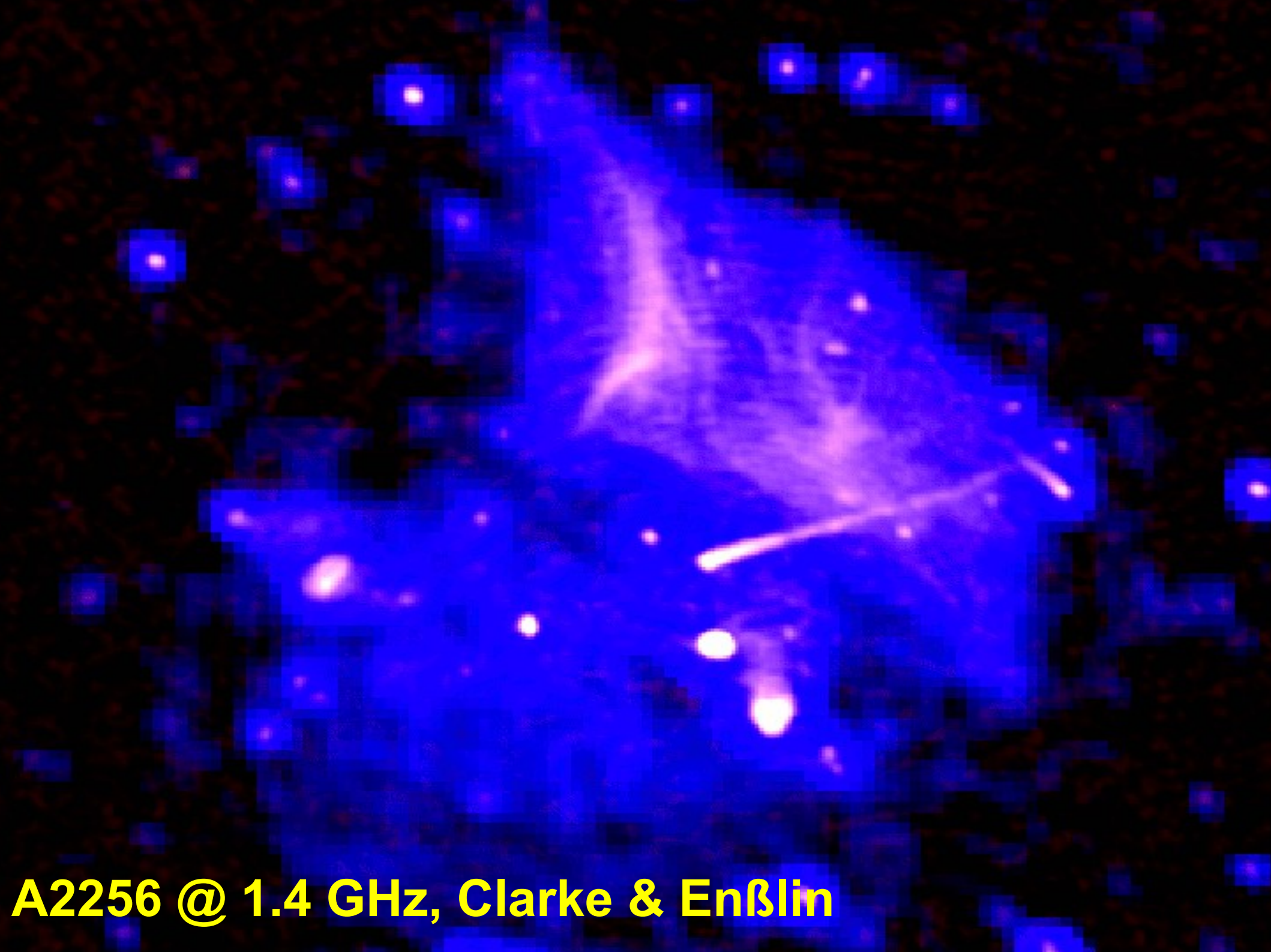
A2256 @ 1.4 GHz, Clarke & Enßlin

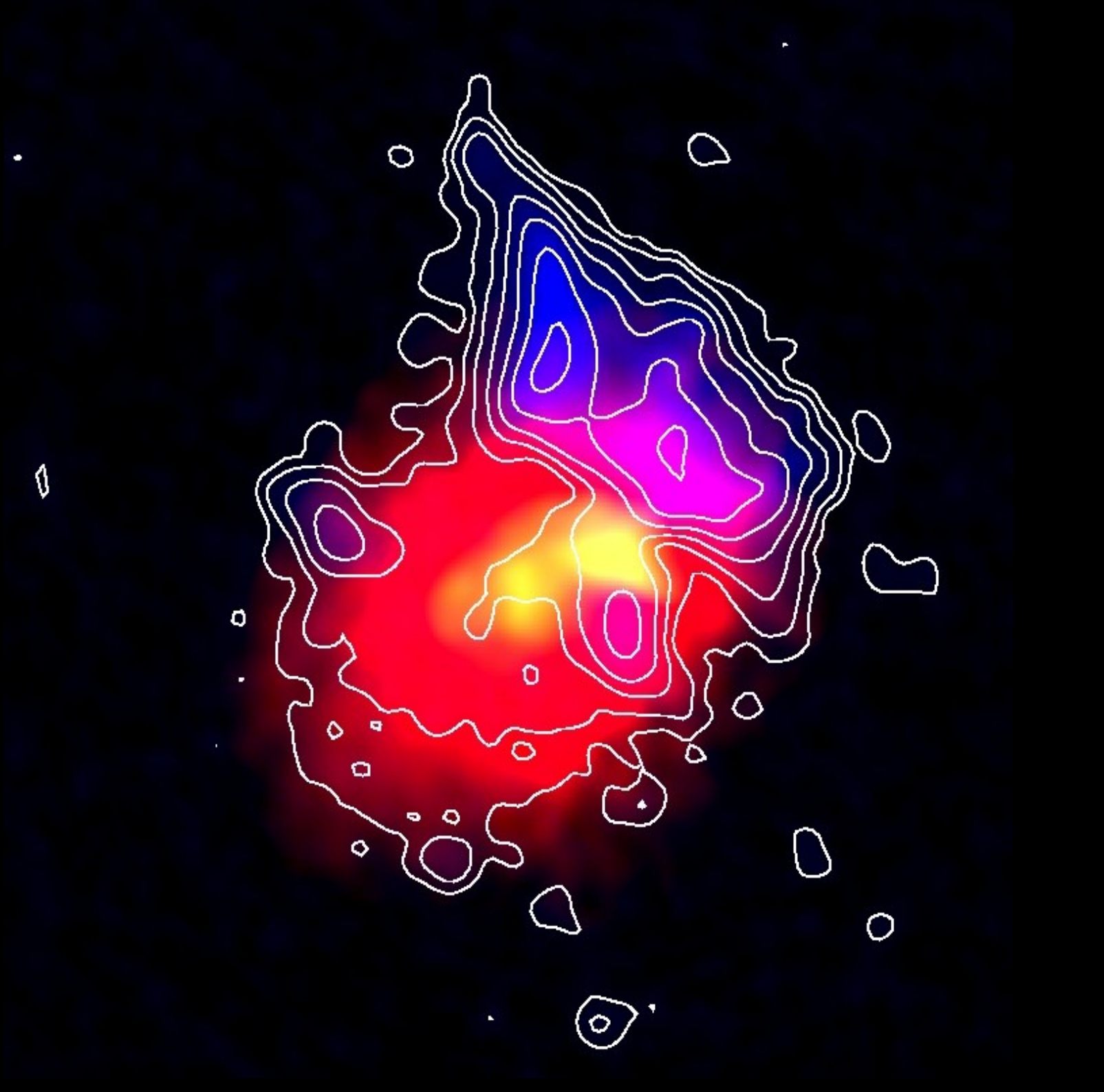

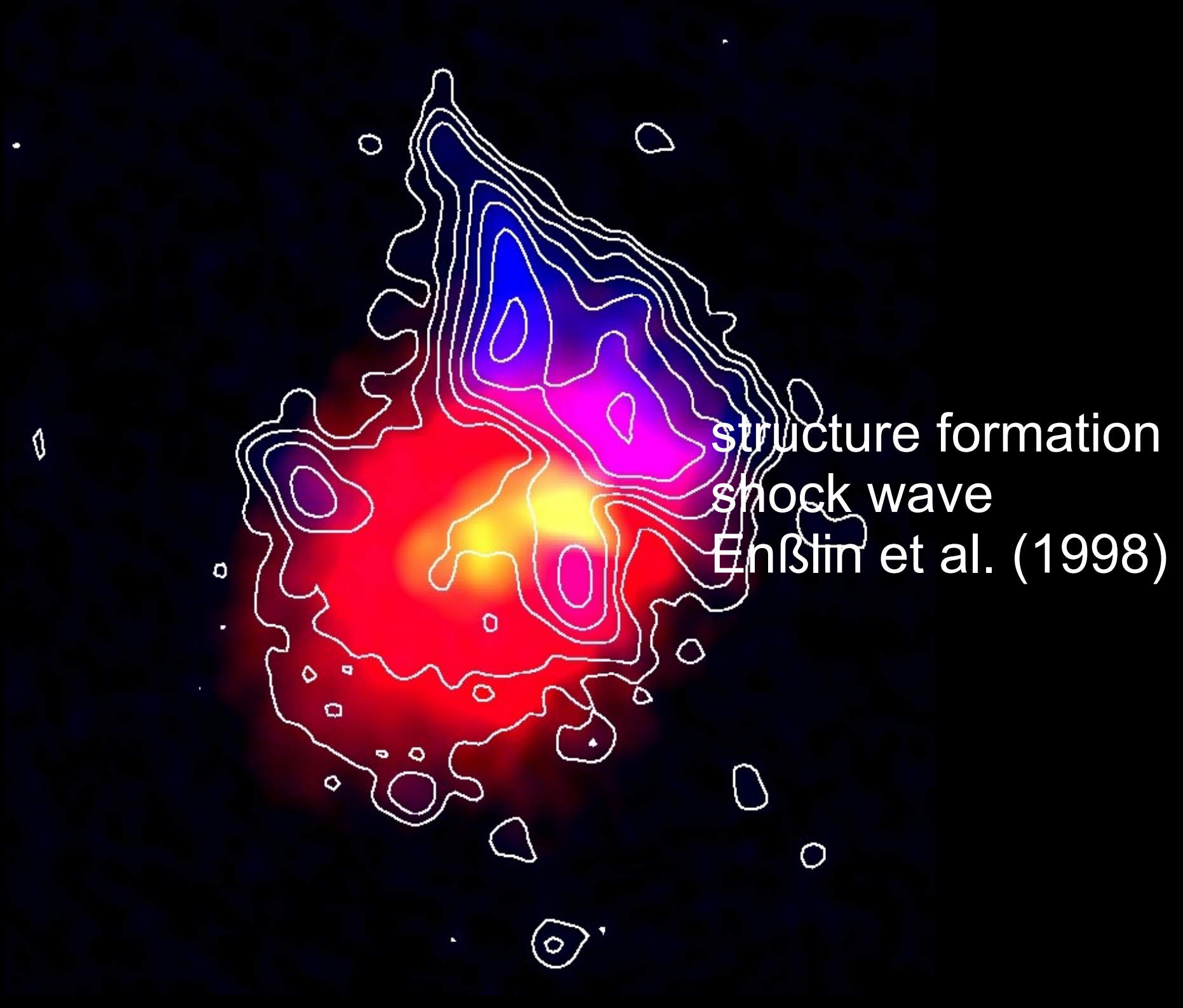
structure formation
shock wave
Enßlin et al. (1998)

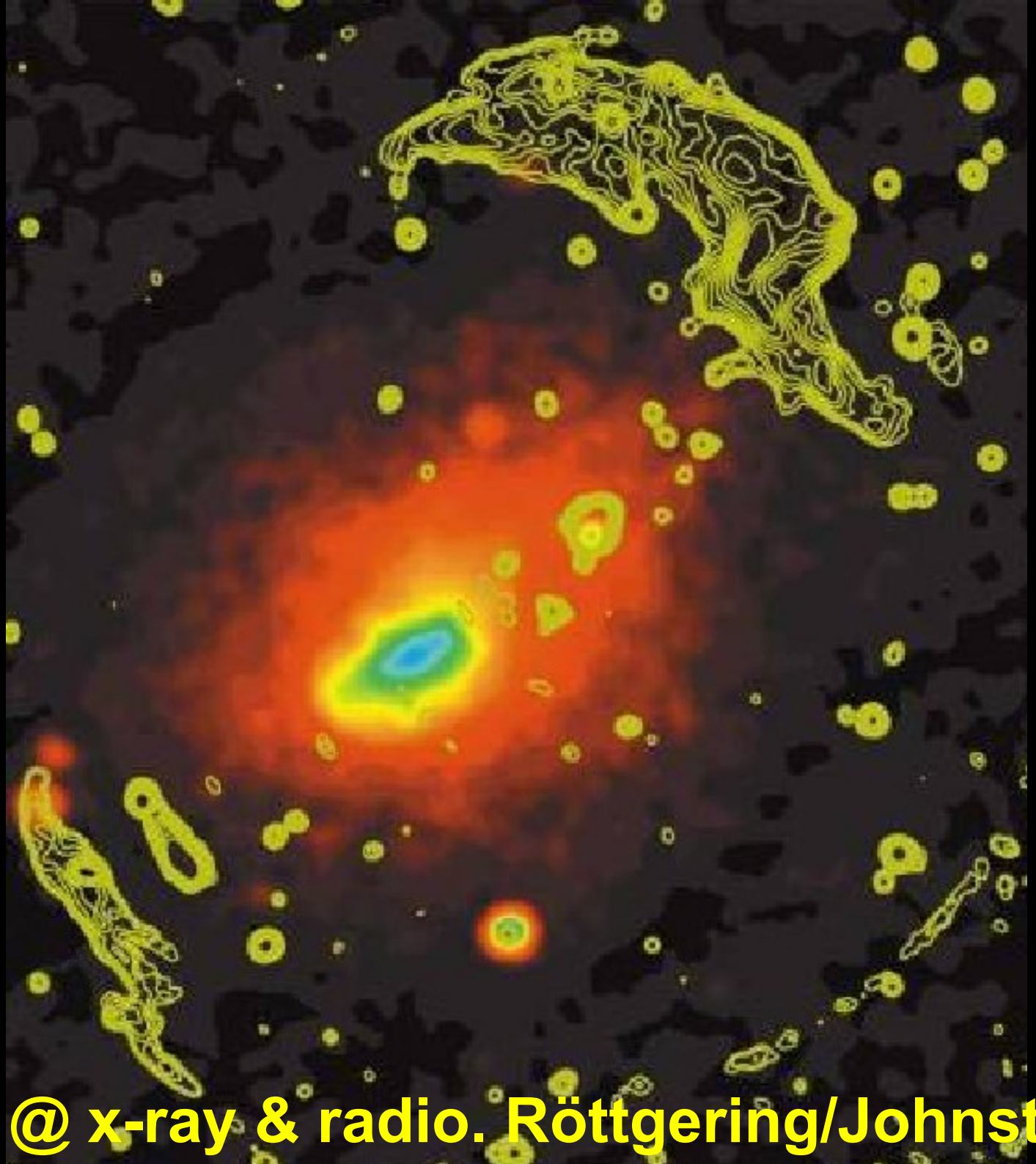

A3667 @ x-ray & radio. Röttgering/Johnston-Hollit

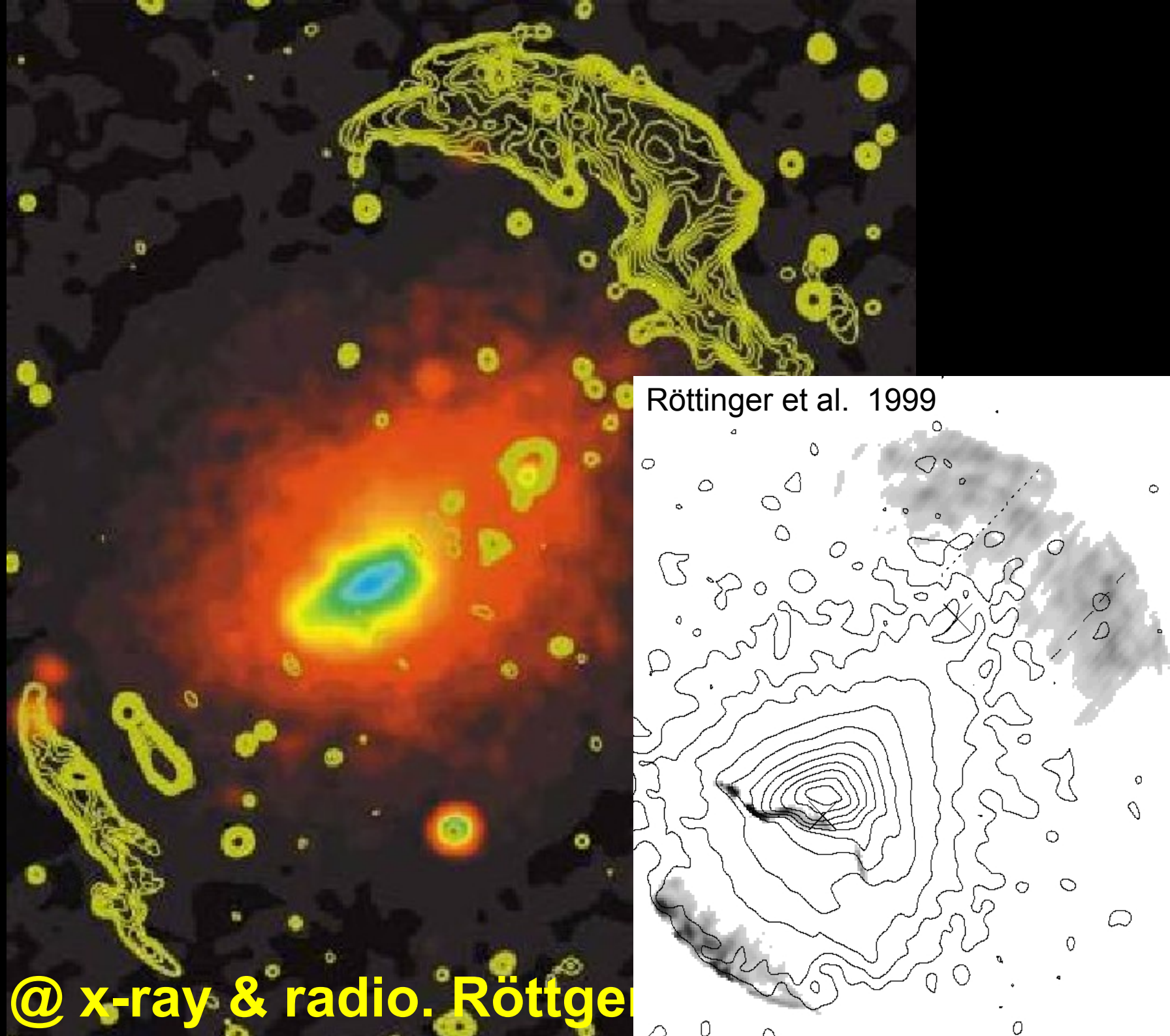

A3667 @ x-ray & radio. Röttge

giant radio halo & relic

Coma cluster

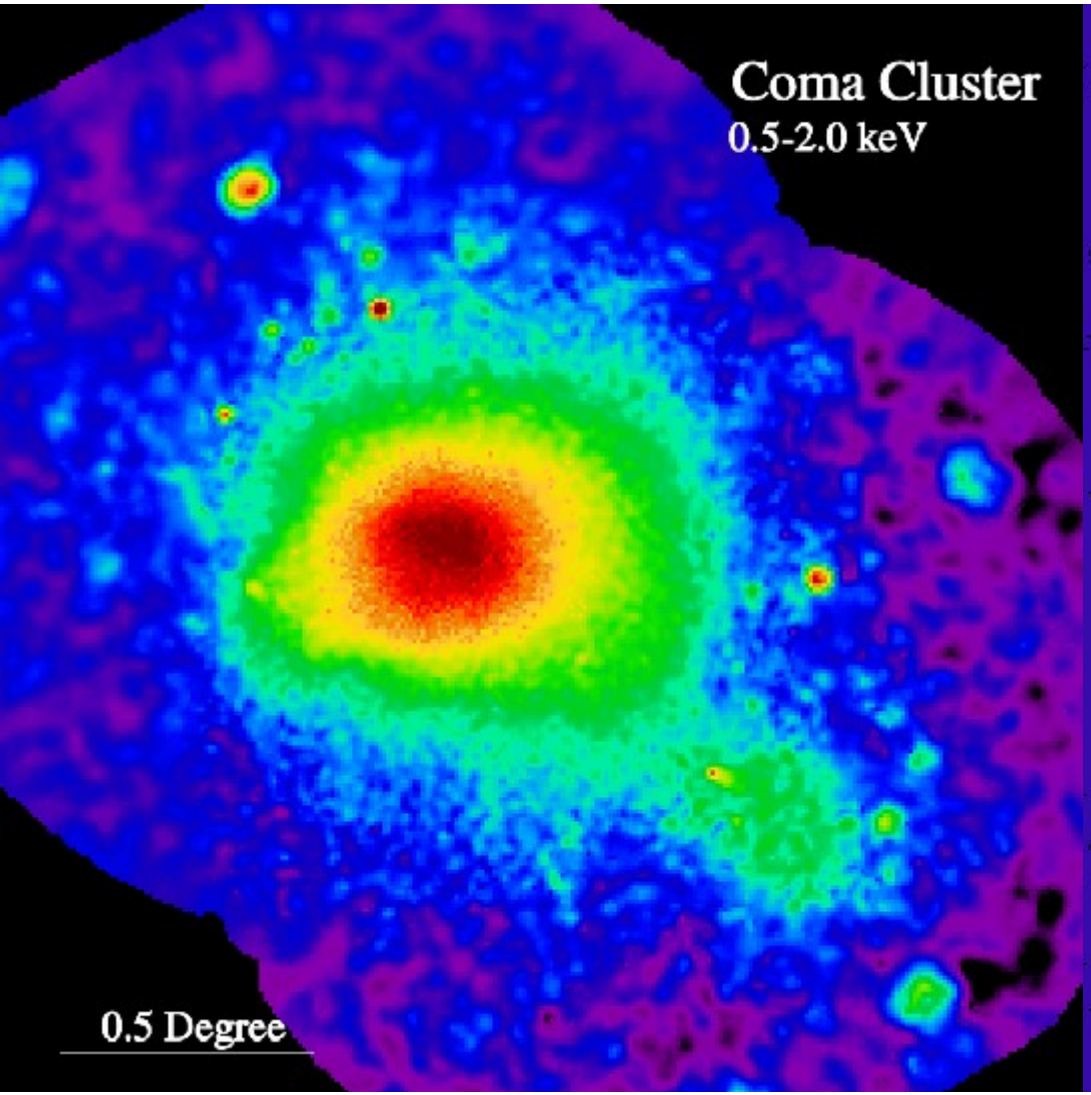

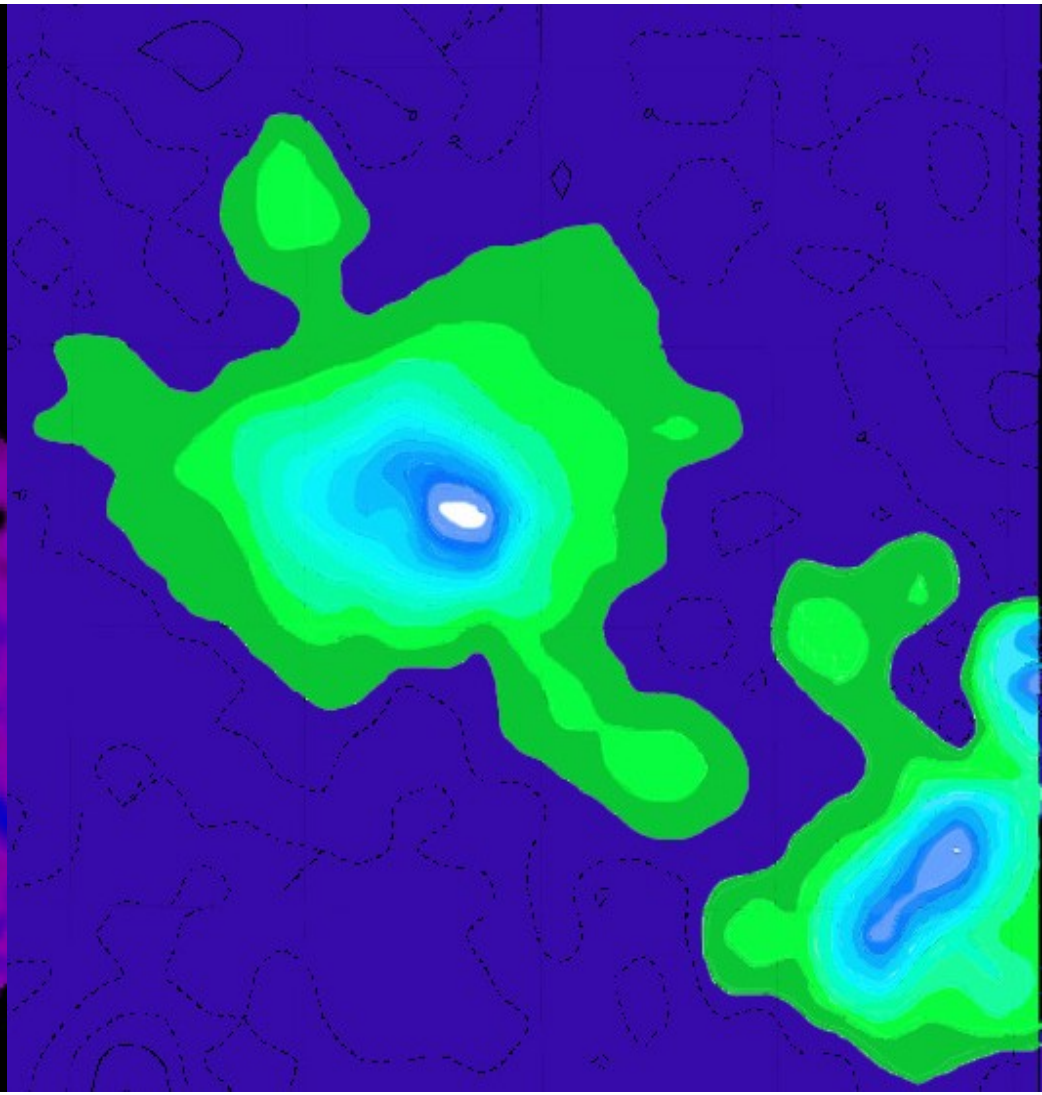

X-ray

1.4 GHz, Deiss et al.

giant radio halo & relic

g72a

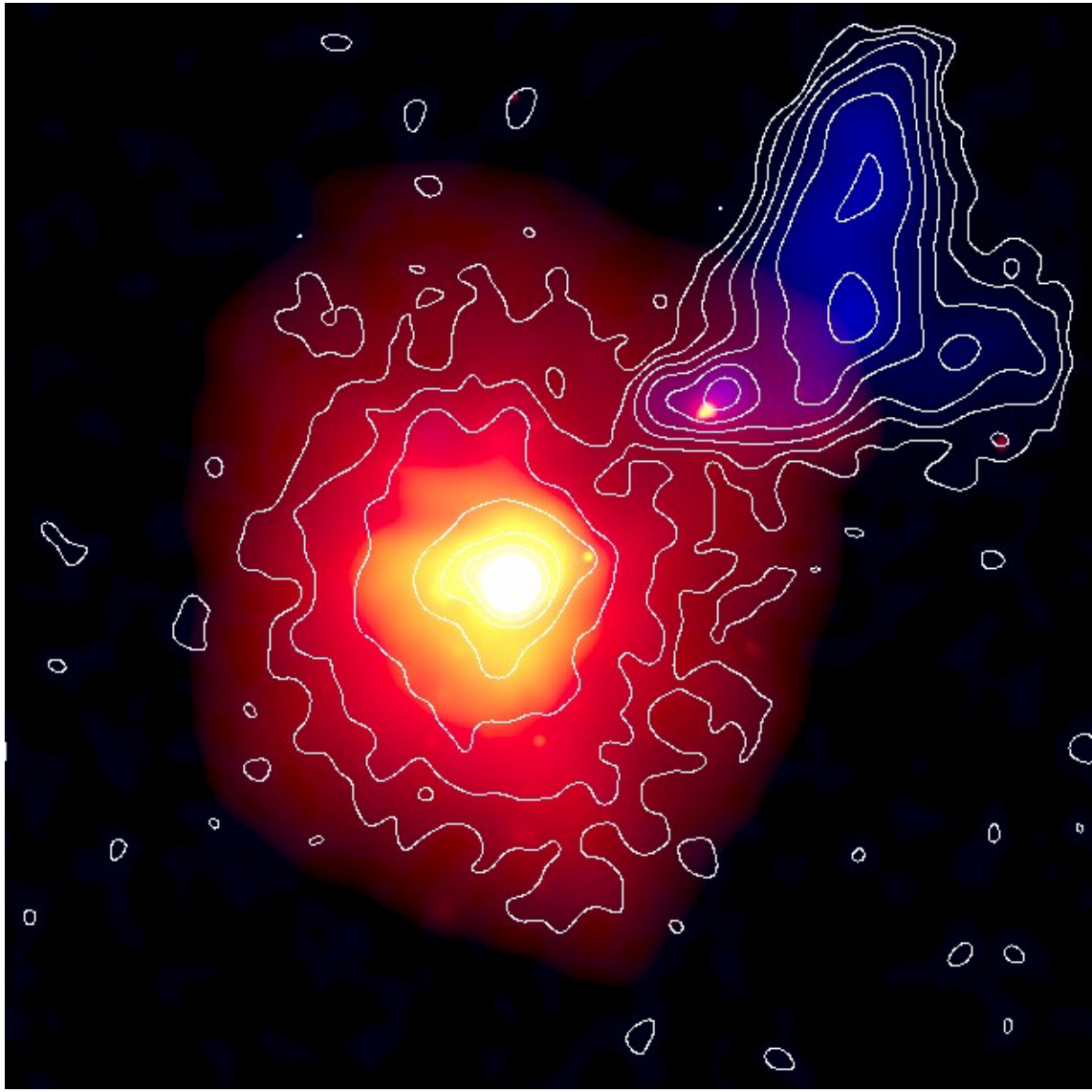

X-ray + radio

giant radio halo & relic

A 2256

g72a

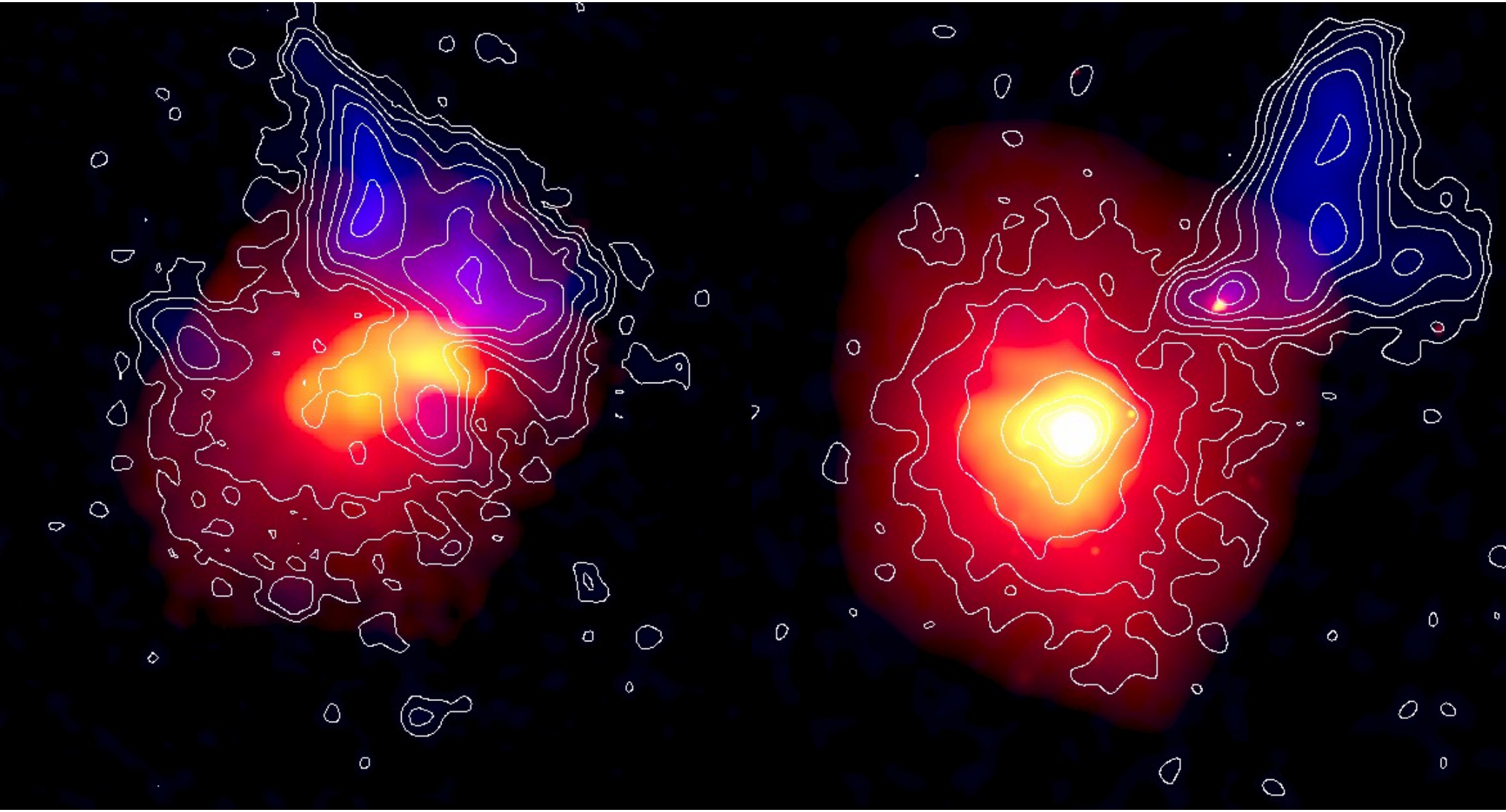

X-ray + radio

giant radio halo & relic

A 2256

g72a

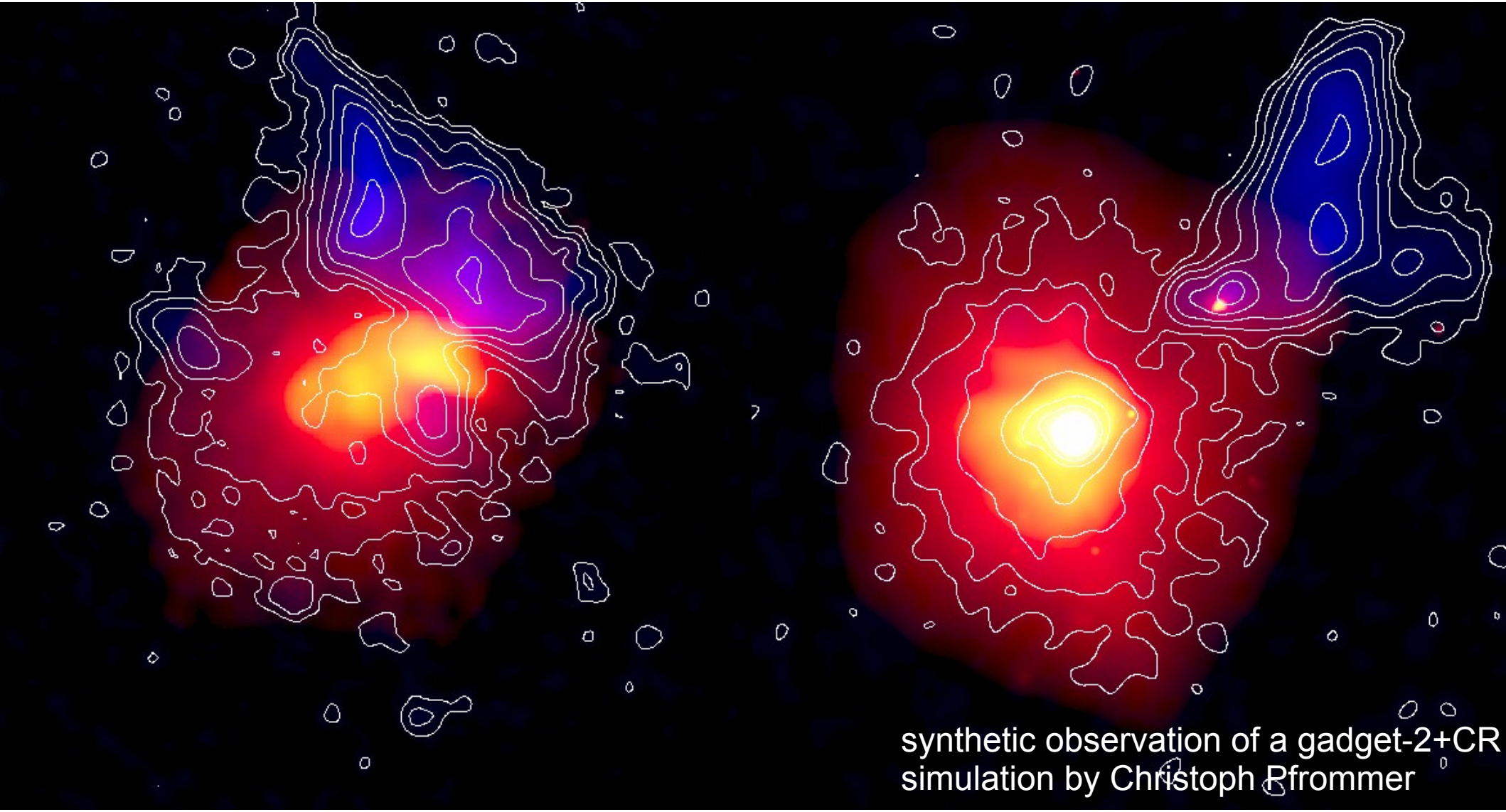

X-ray + radio

giant radio halo & relic

g72a

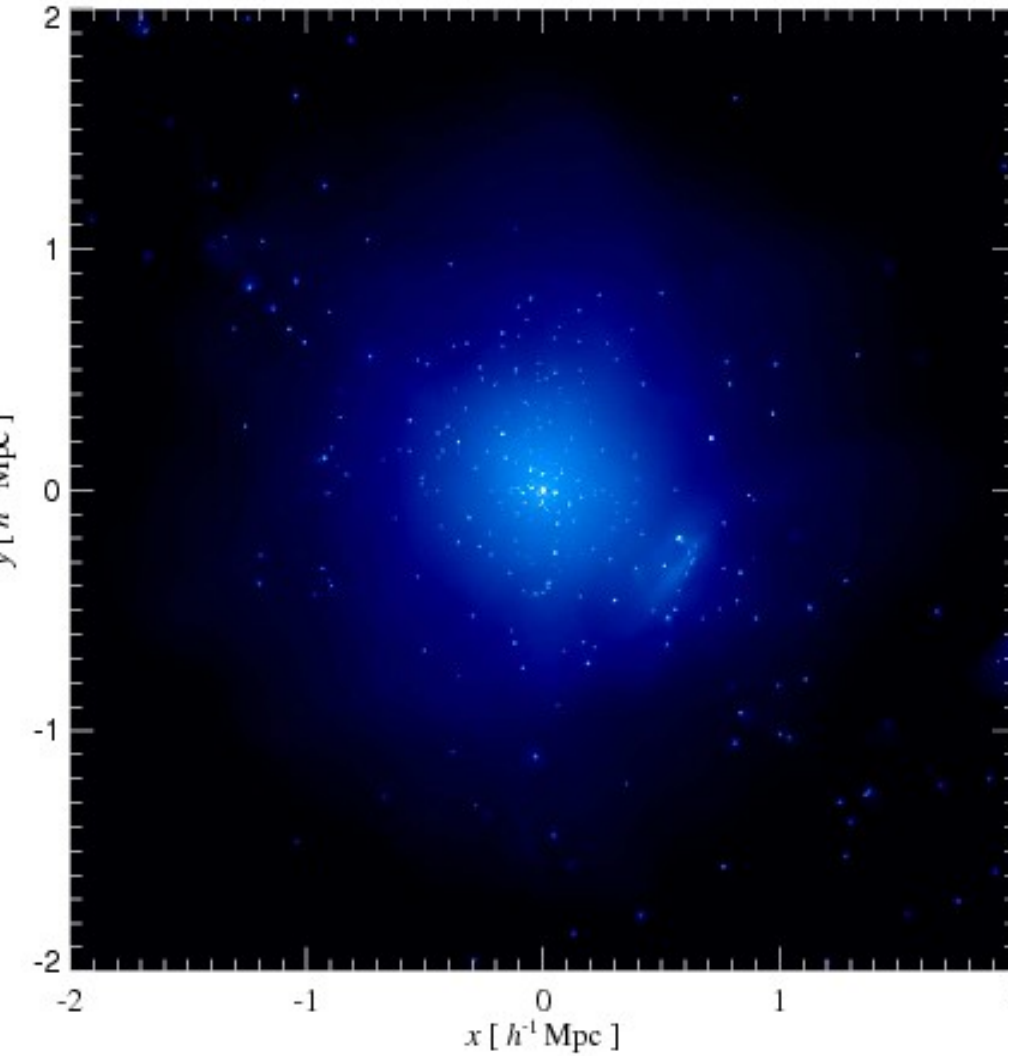

X-ray

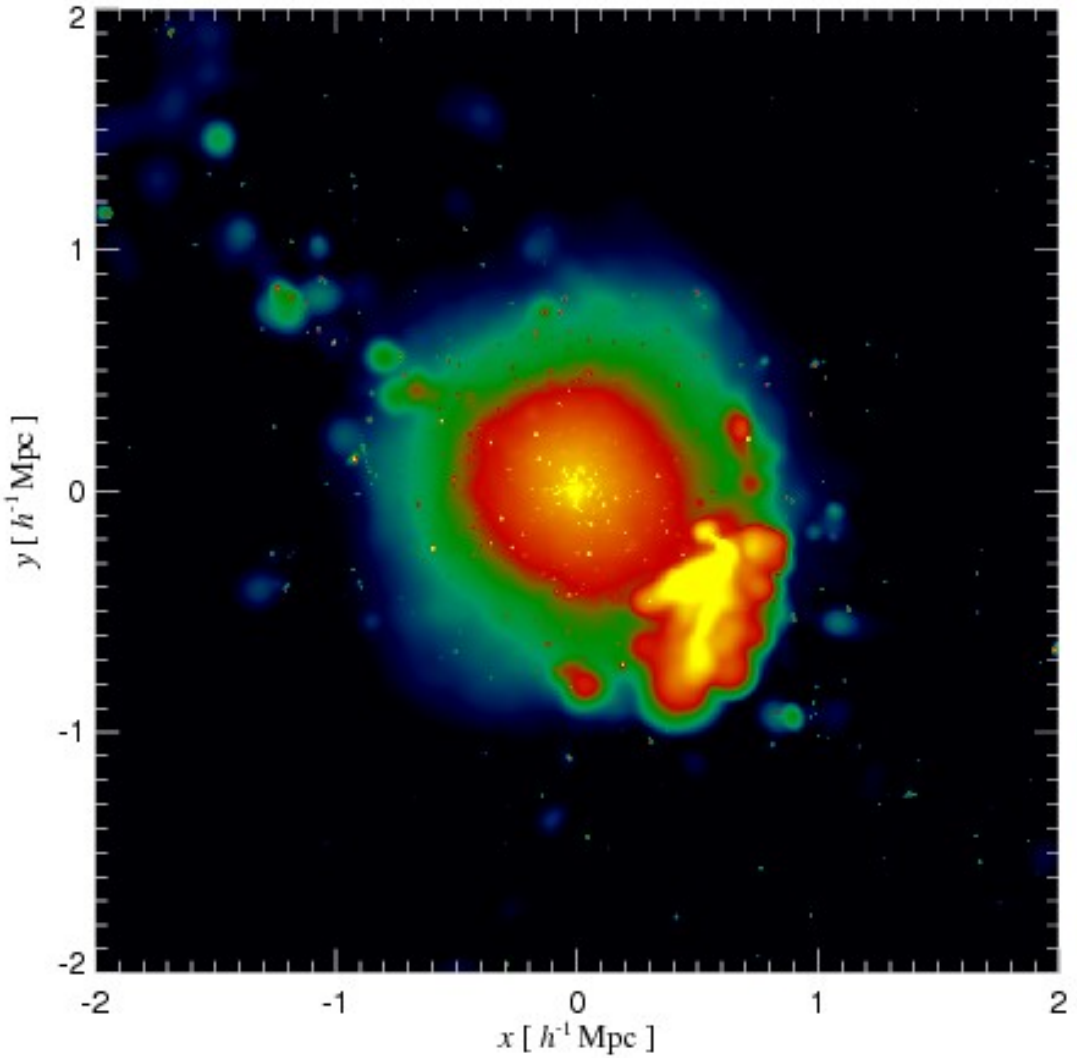

radio

hadronic particle reactions

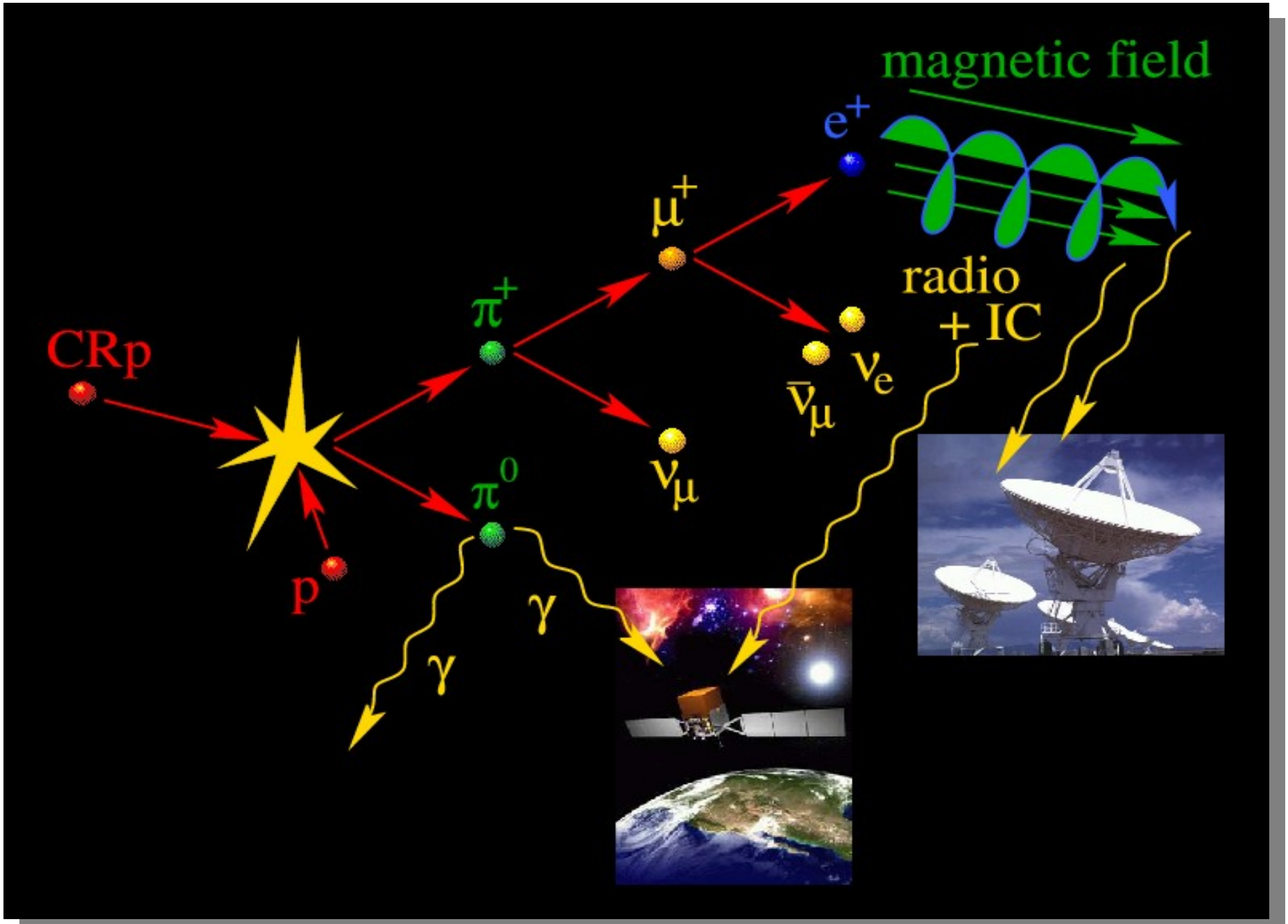

gadget-2 code

Cluster observables: Physical processes in clusters:

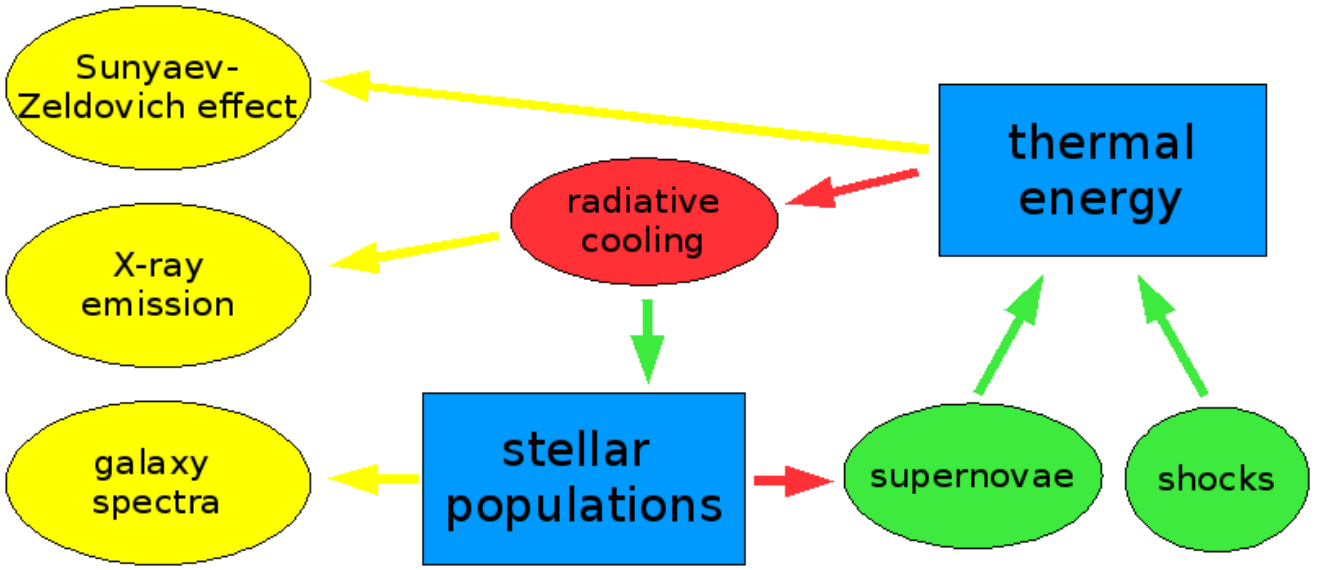

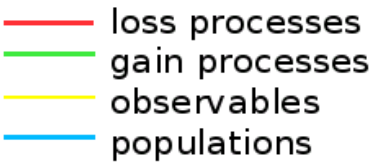

giant radio halo

What is the origin of the relativistic particles ?

What maintains the magnetic fields ?

Available energy sources:

- **galactic winds**
- **radio galaxies**
- **structure formation flows**

giant radio halo

What is the origin of the relativistic particles ?

What maintains the magnetic fields ?

Available energy sources:

- **galactic winds**
- **radio galaxies**
- **structure formation flows**

Mach numbers of dissipated energy

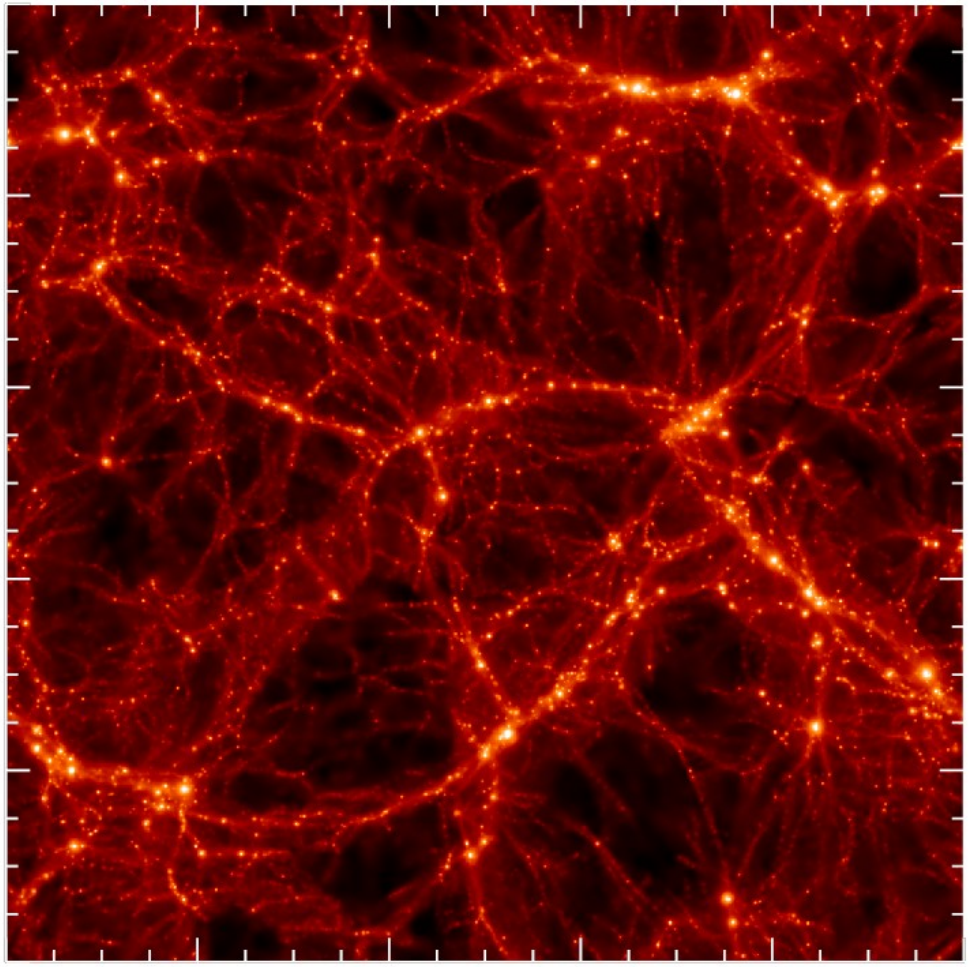

$\langle 1 + \delta_{\rm gas} \rangle_{\rm los}$

10^{-1} 10^{0} 10^{1} 10^{2}

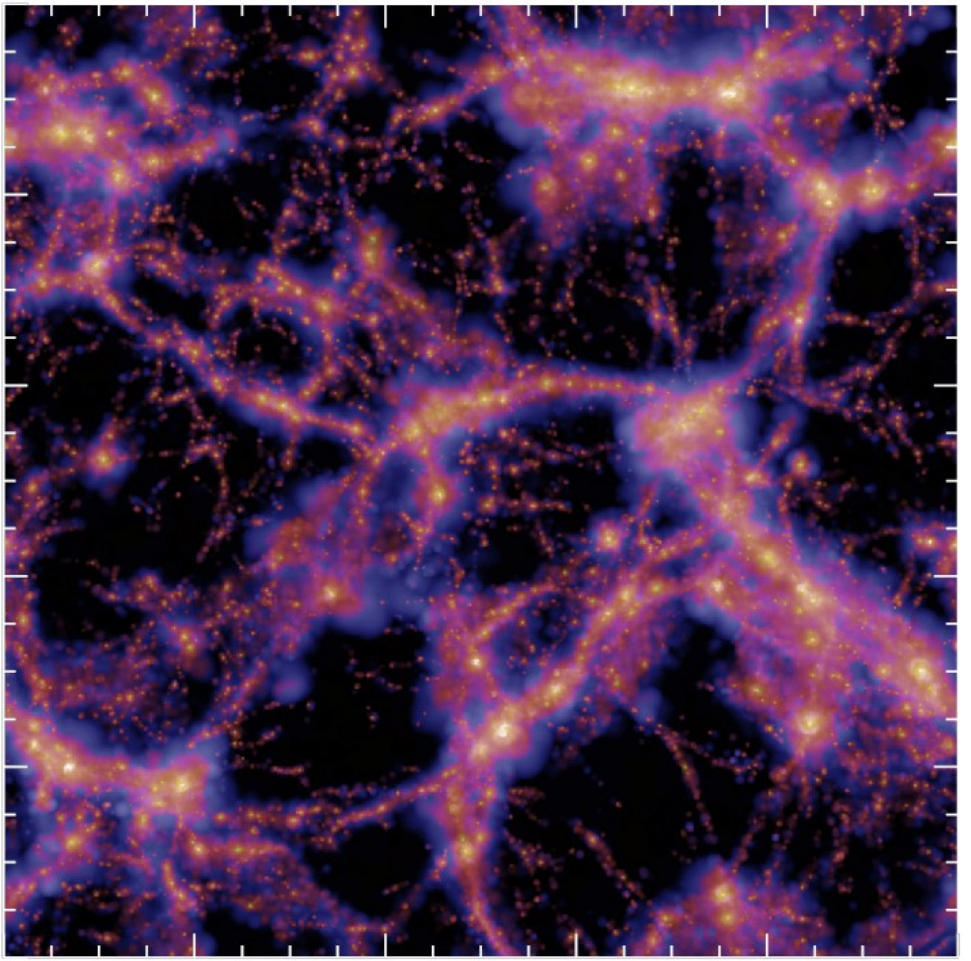

$$\frac{\langle \mathcal{M}\, \mathrm{d}\varepsilon_{\rm diss}/(\mathrm{d}\log a)\rangle_{\rm los}}{\langle \mathrm{d}\varepsilon_{\rm diss}/(\mathrm{d}\log a)\rangle_{\rm los}}$$

1 10

Pfrommer, Springel, Enßlin, Jubelgas (2006)

Mach number statistics

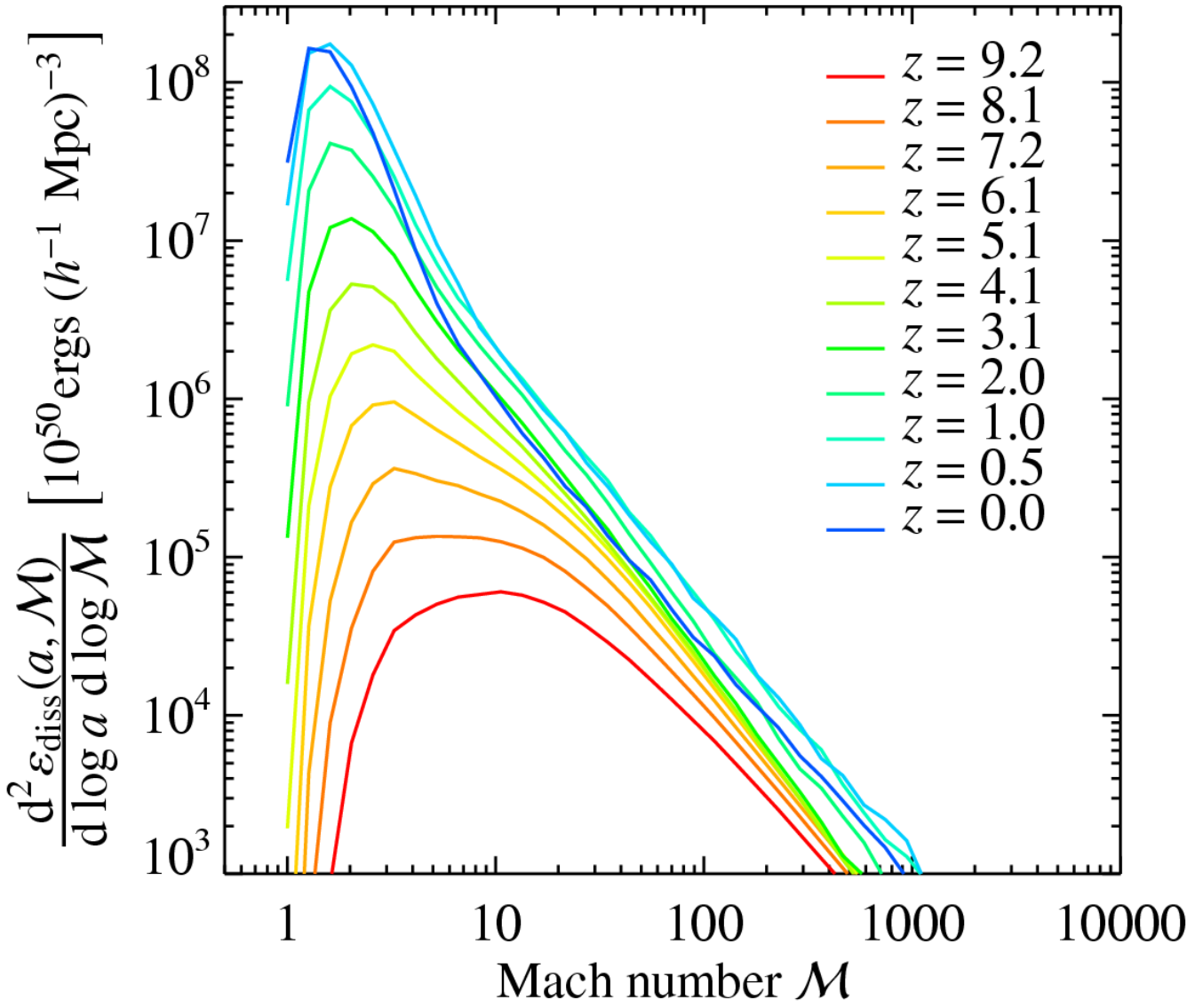

Pfrommer, Springel, Enßlin, Jubelgas (2006)

simulated galaxy cluster

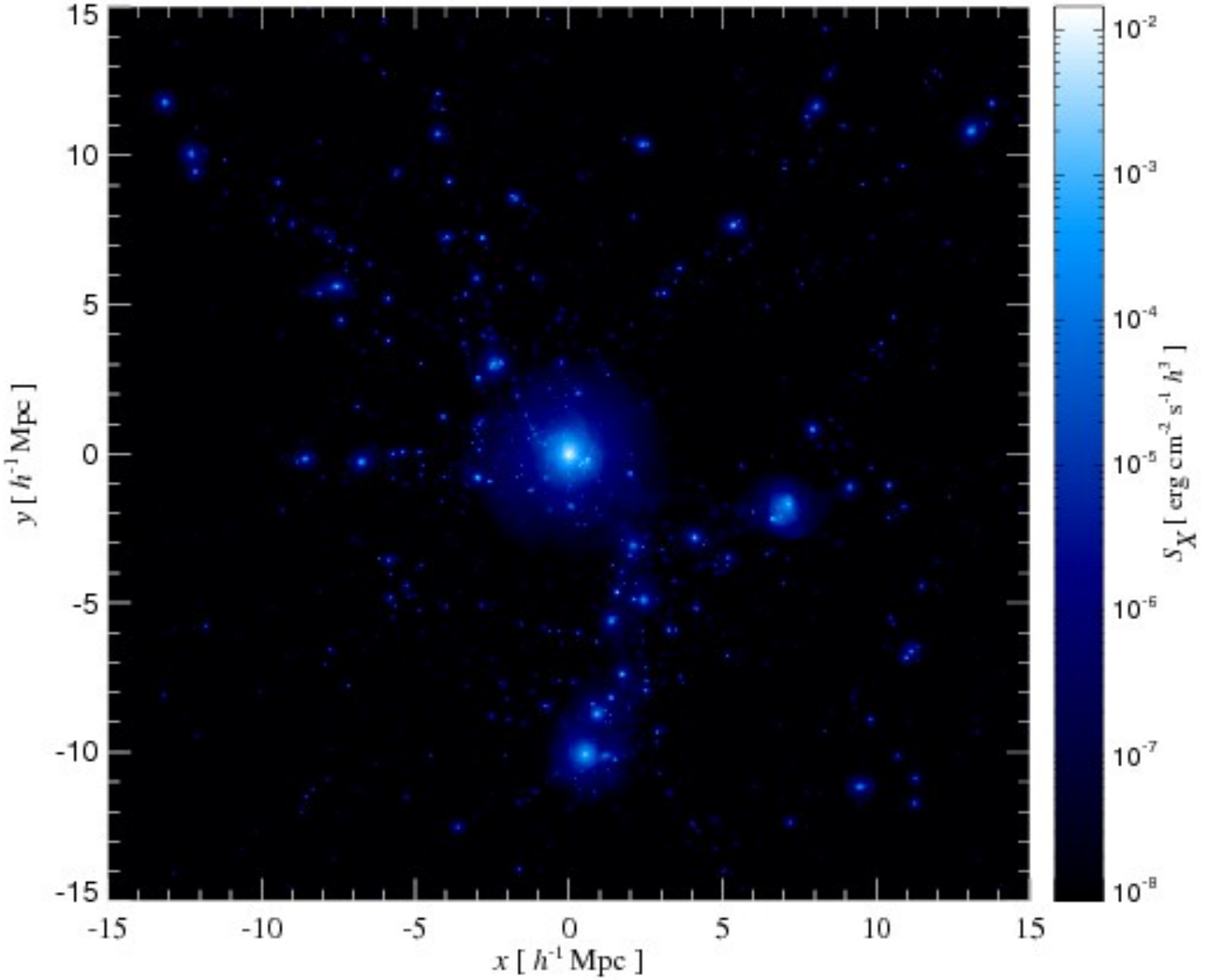

X-ray

Pfrommer et al.

radio relics

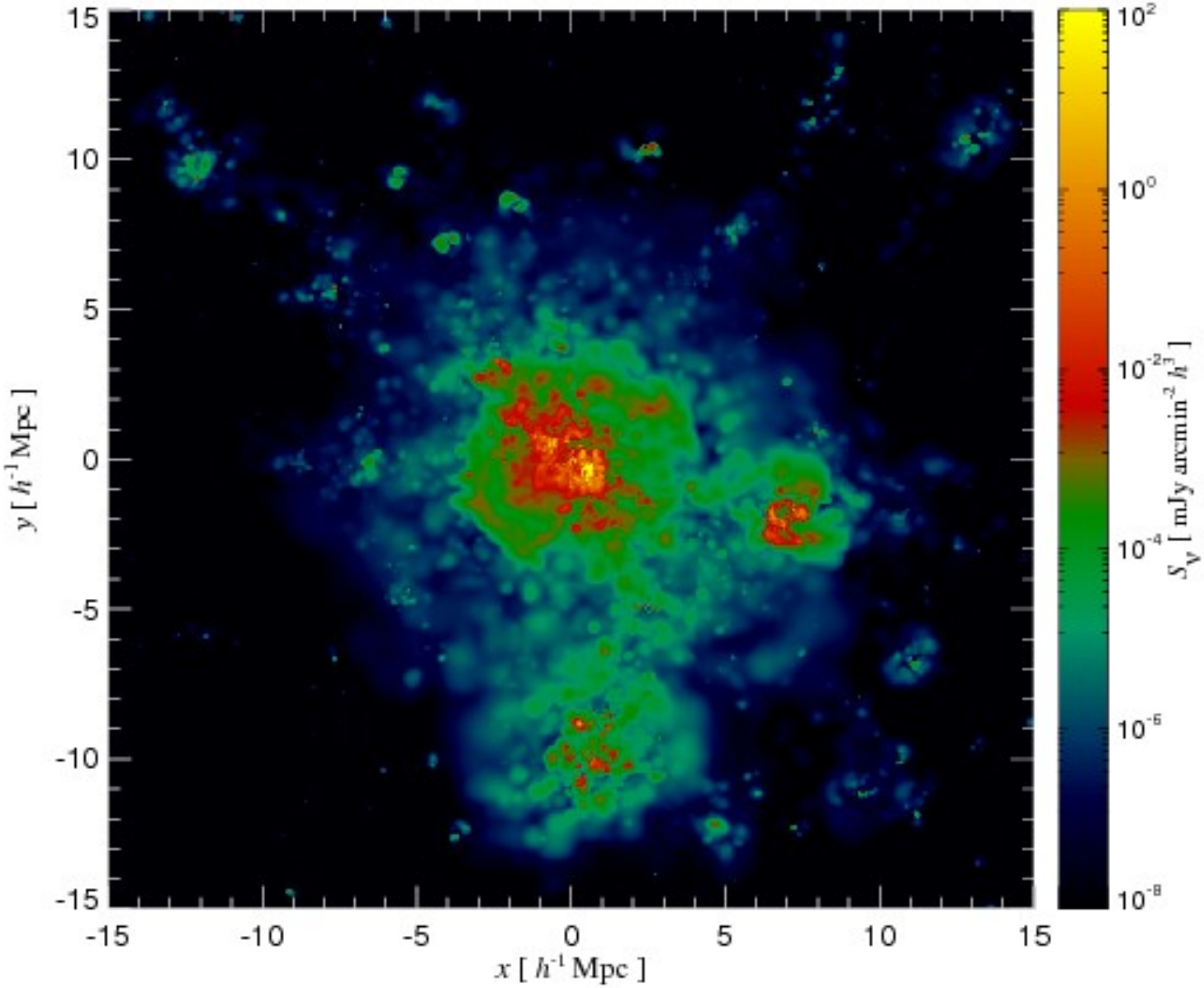

150 MHz

Pfrommer et al.

hadronic radio halo

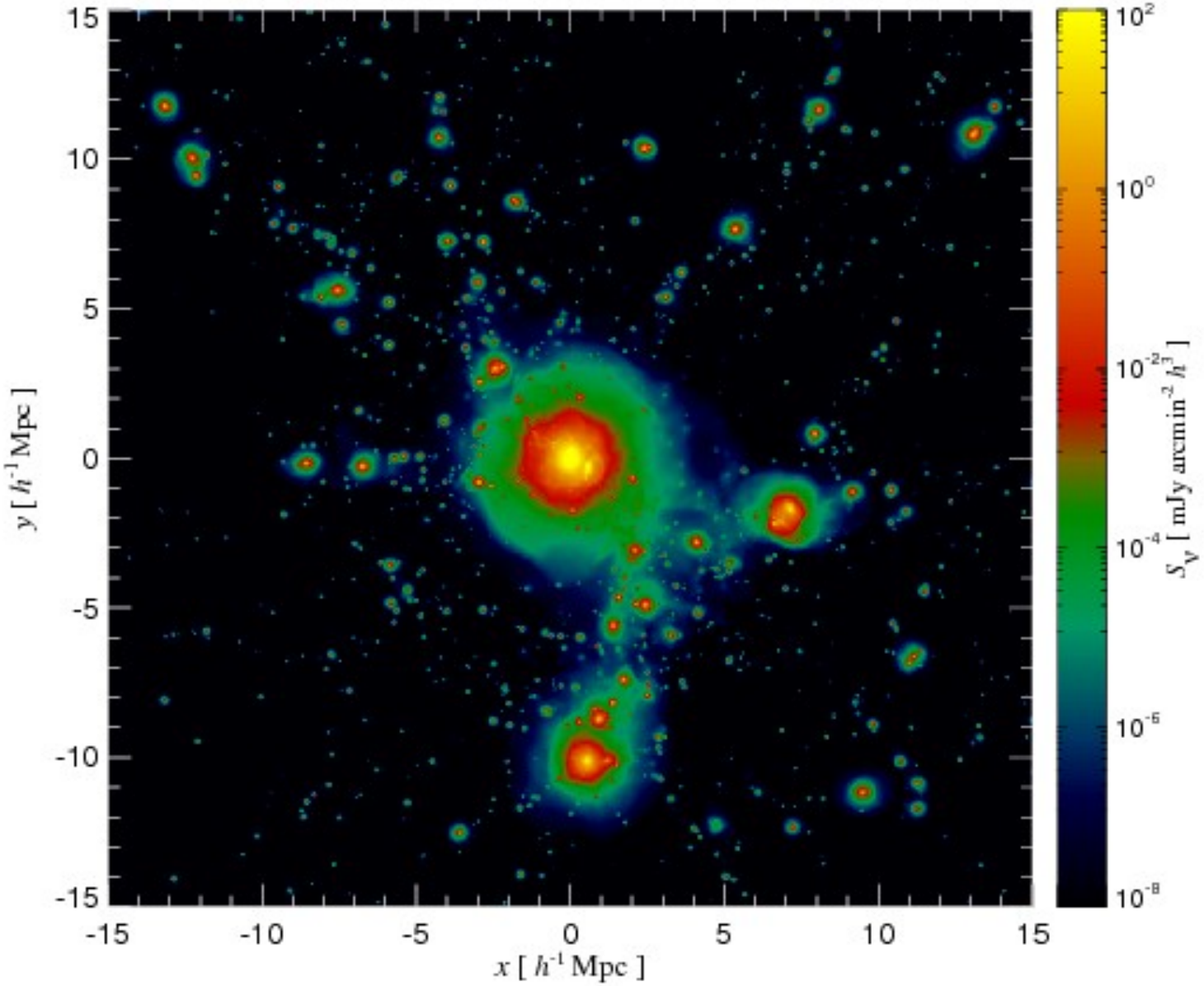

150 MHz

Pfrommer et al.

radio web: halos & relics

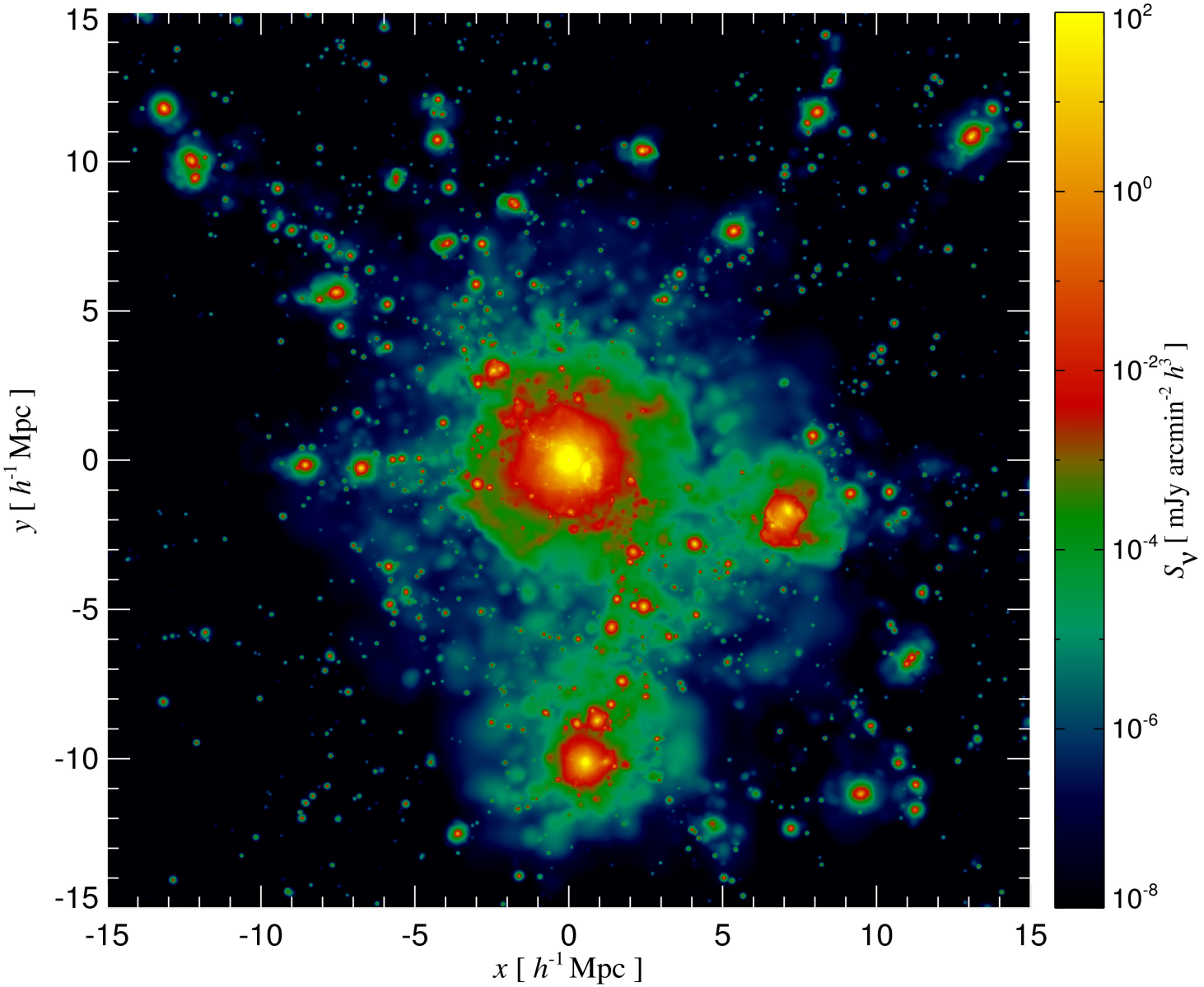

150 MHz

Pfrommer et al.

Radio gischt illuminates cosmic magnetic fields

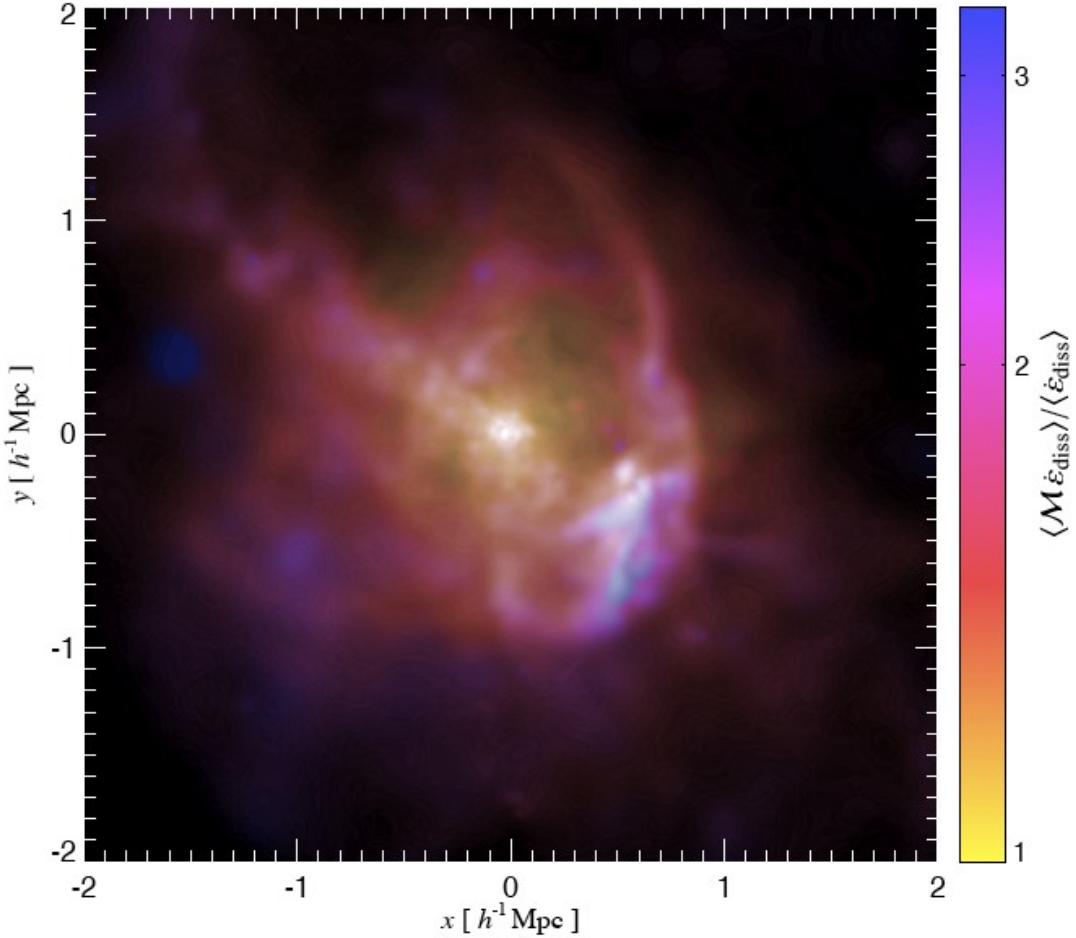

Structure formation shocks triggered by a recent merger of a large galaxy cluster.

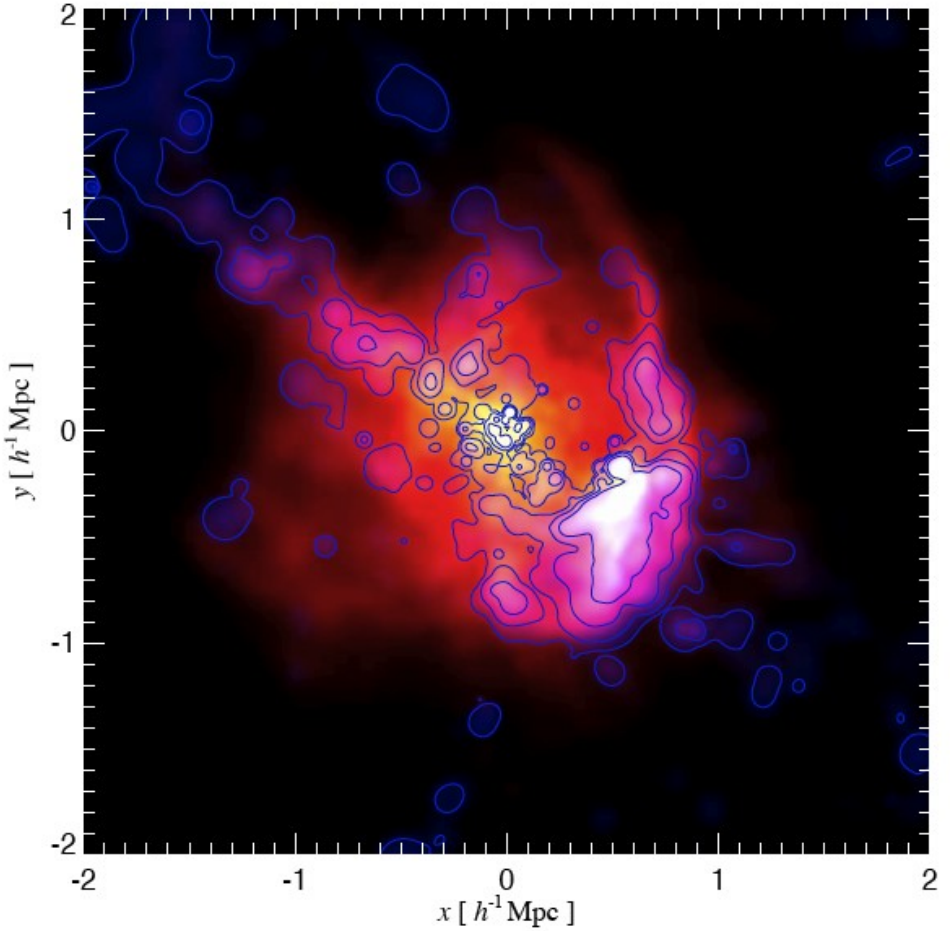

red/yellow: shock-dissipated energy,

blue/contours: 150 MHz radio gischt emission from shock-accelerated CRe

CITA–ICAT

Christoph Pfrommer

Population of faint radio relics in merging clusters

Probing the large scale magnetic fields

Finding radio relics in 3D cluster simulations using a friends-of-friends finder with an emission threshold → relic luminosity function

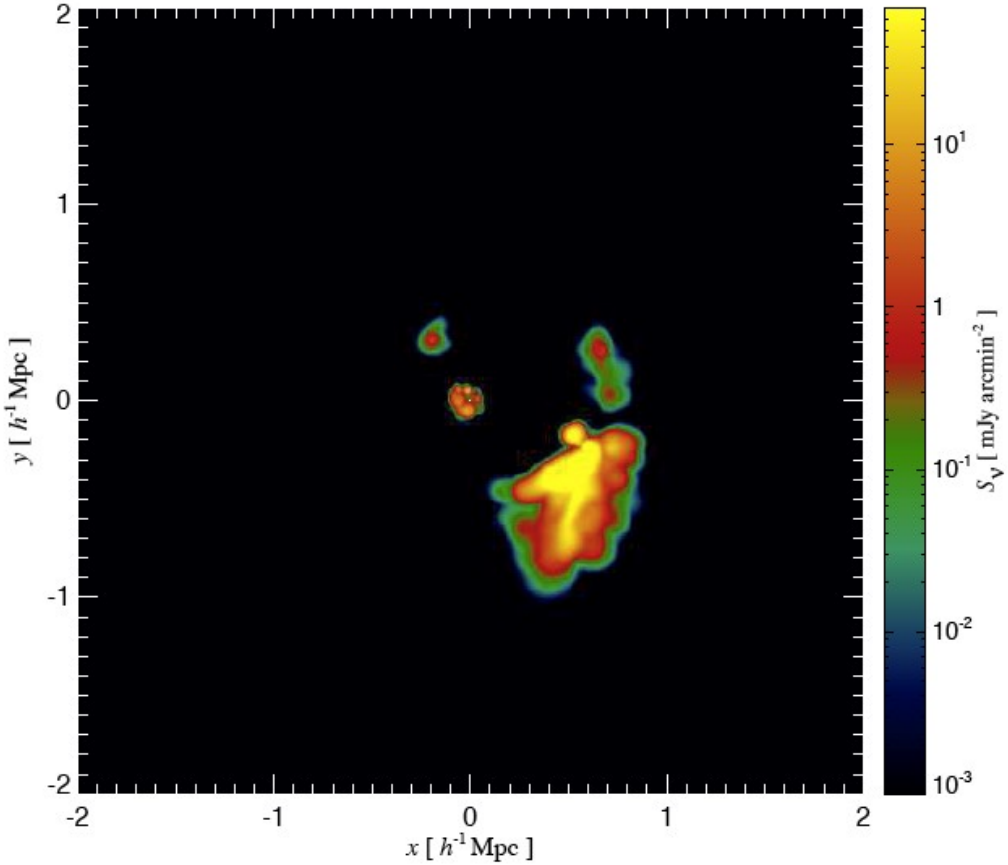

radio map with GMRT emissivity threshold

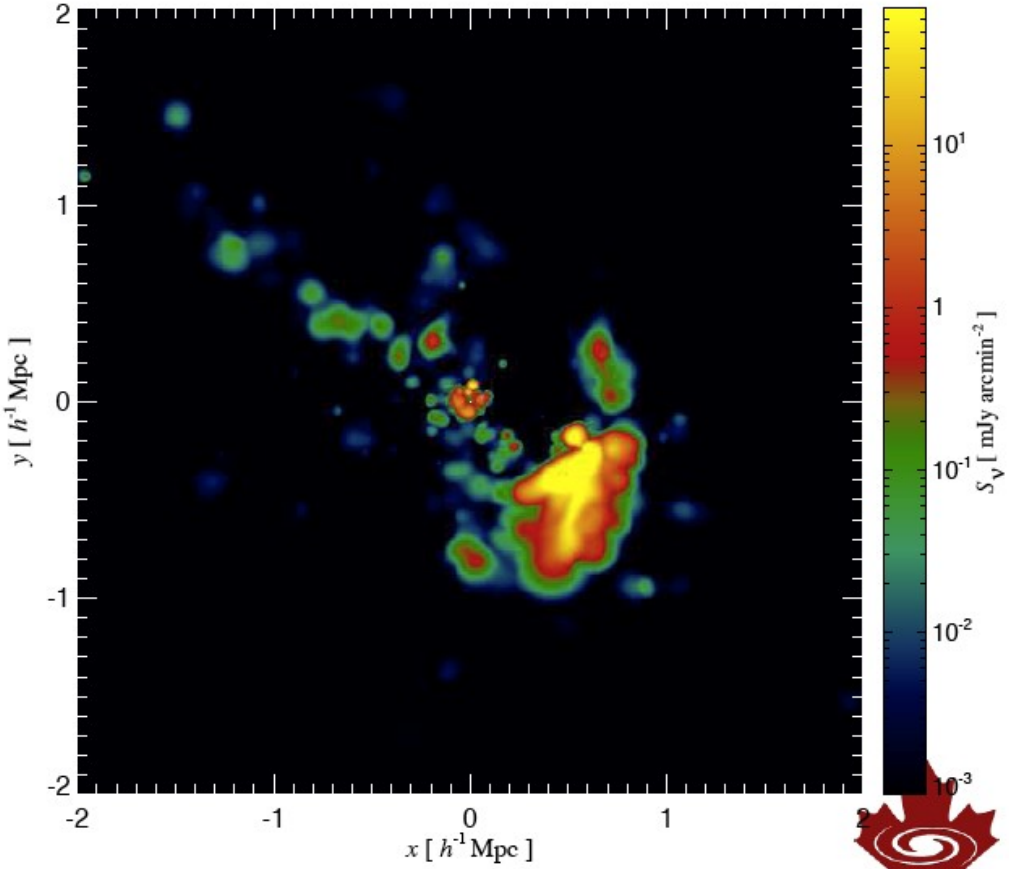

"theoretical" threshold (towards SKA)

CITA–ICAT

gadget-2 code

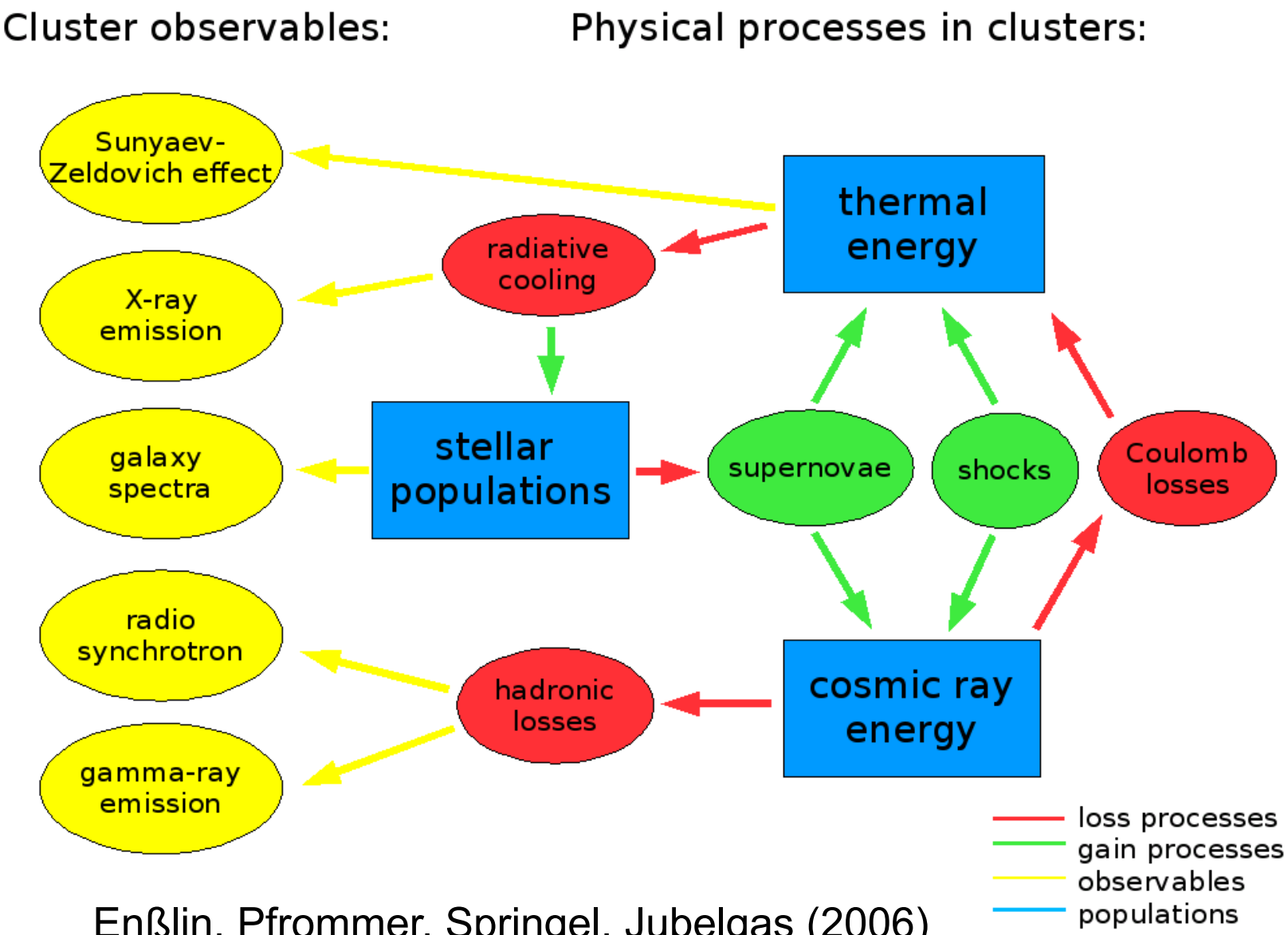

Enßlin, Pfrommer, Springel, Jubelgas (2006)
Jubelgas, Springel, Enßlin, Pfrommer (2006)
Pfrommer, Springel, Enßlin, Jubelgas (2006)

shock dissipation

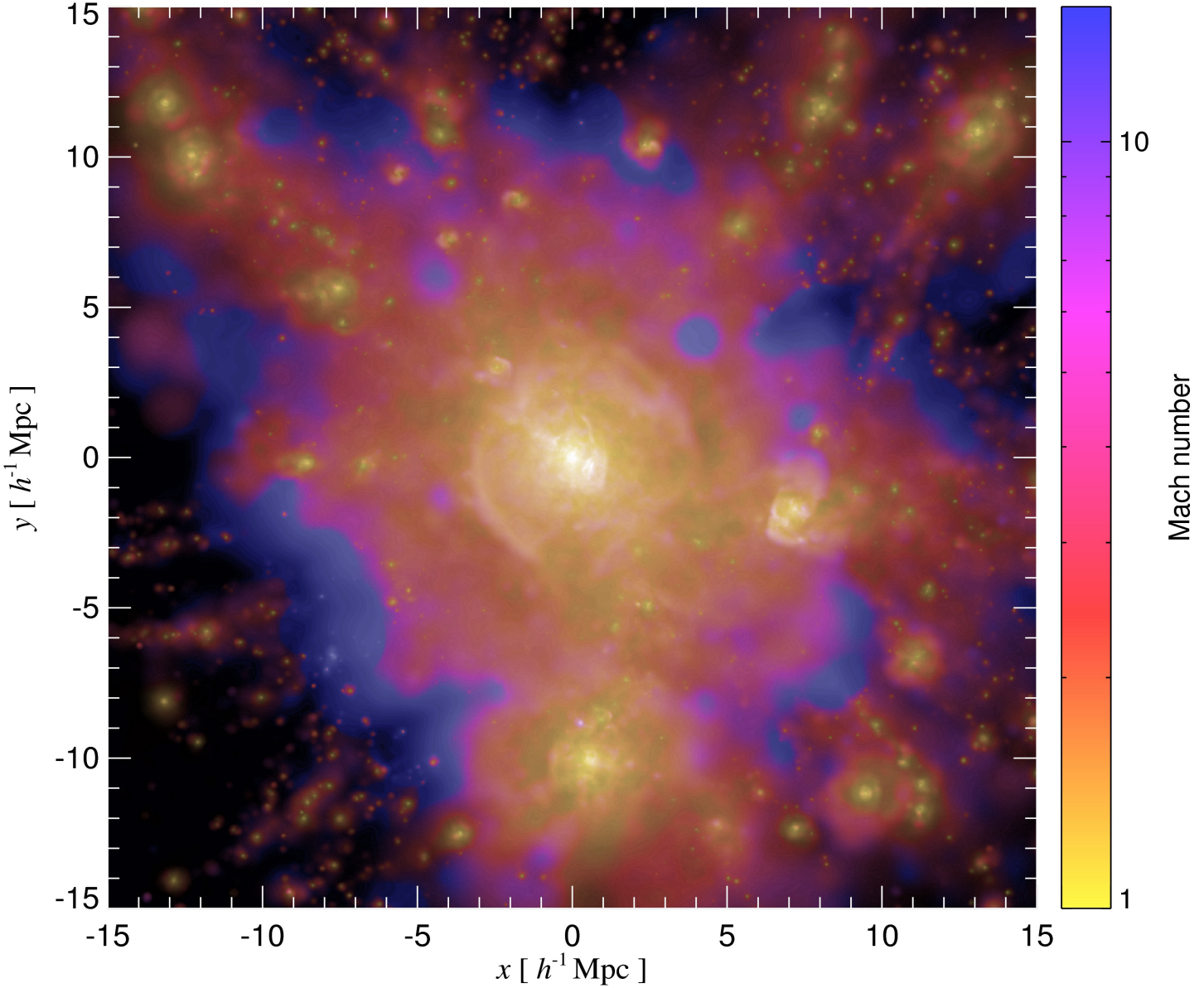

energy dissipation & Mach number

Pfrommer in prep.

Outline:

Cluster radio emission
& magnetic turbulence

Faraday rotation
& magnetic spectrum inference
C. Vogt, P. Kuchar

Stokes correlators
& tension forces

Faraday-Stokes correlations
& magnetic helicity

Galaxy Cluster Fields

Hydra A cluster

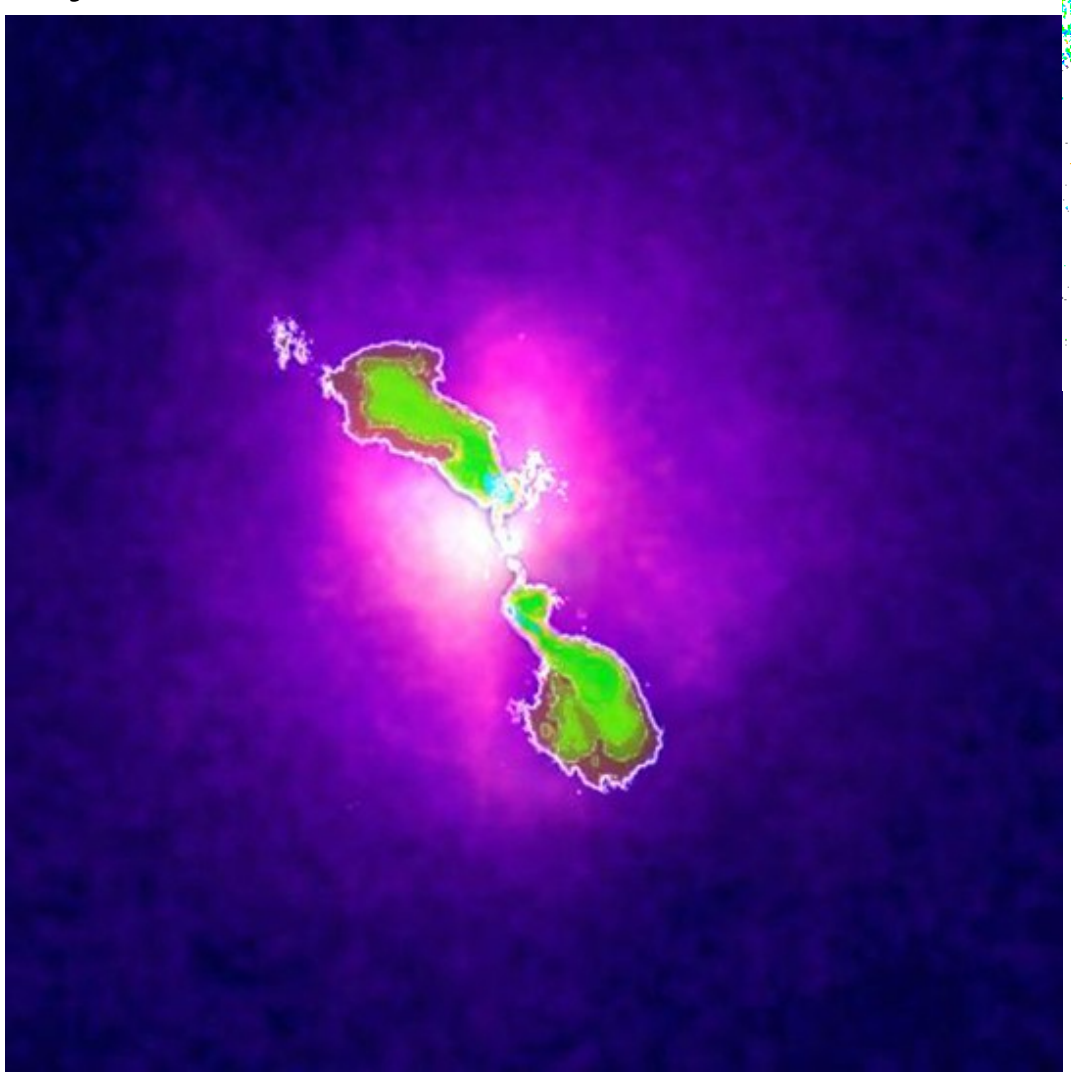

RM

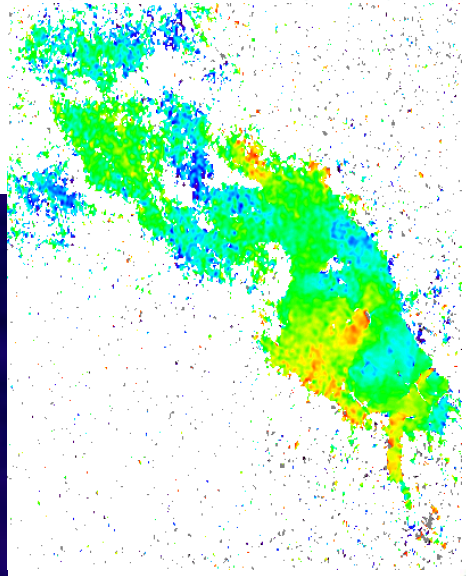

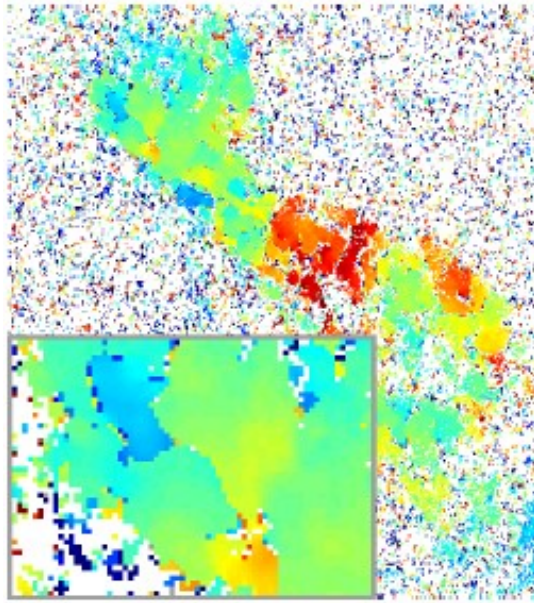

Taylor & Perley (1993)
VLA/Chandra

PACERMAN

Dolag et al. (2005)
Vogt et al. (2005)

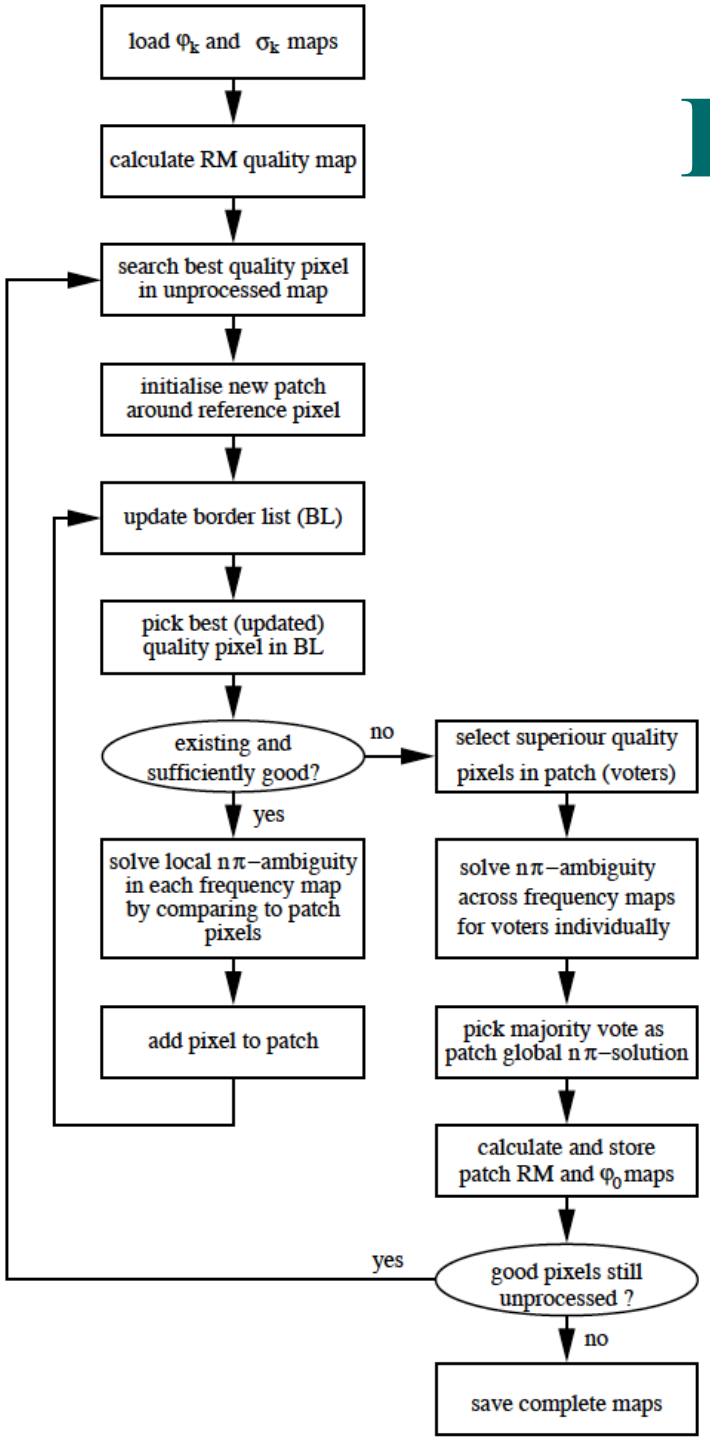

n-π-ambiguity in RM fitting

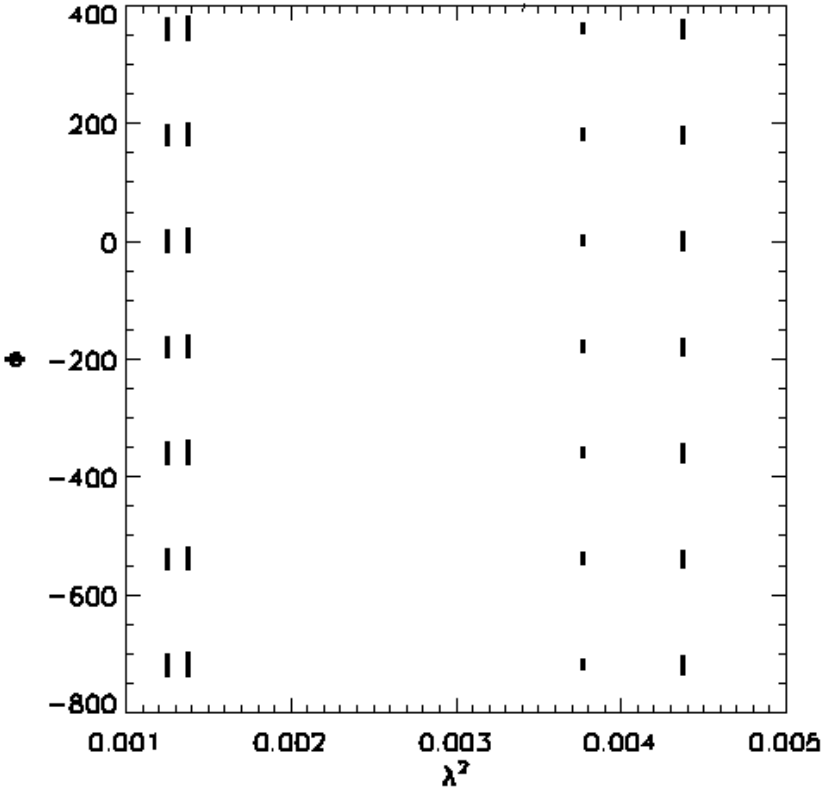

PACERMAN

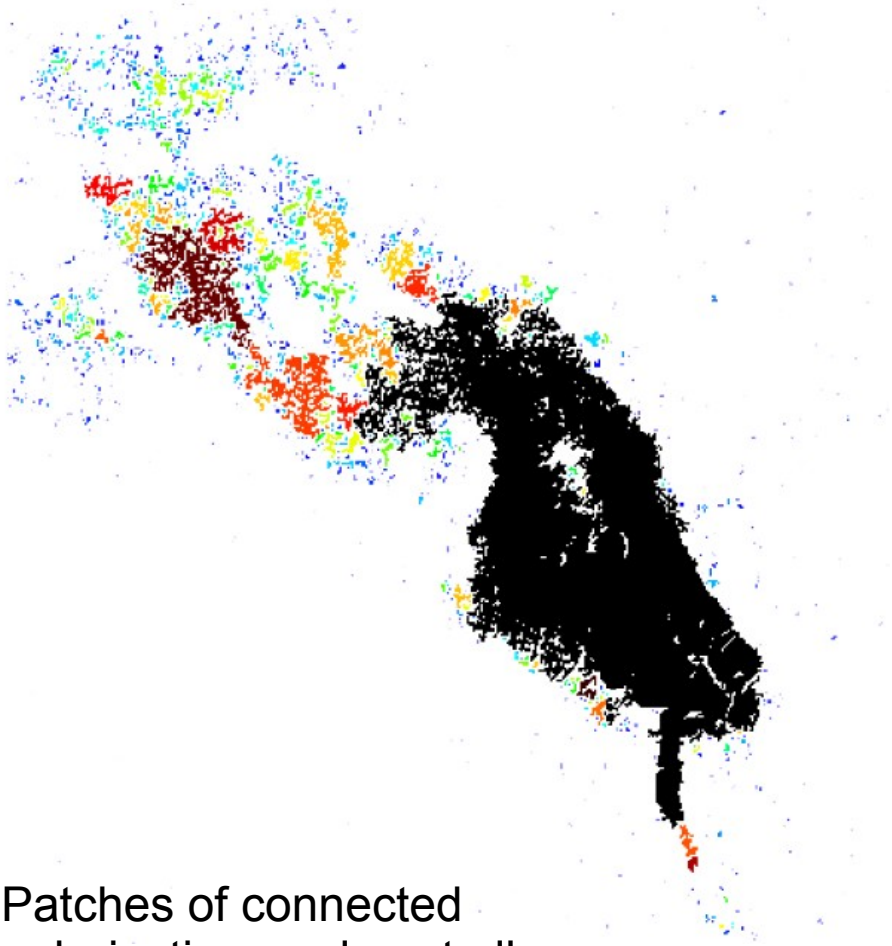

Patches of connected polarisation angles at all frequencies

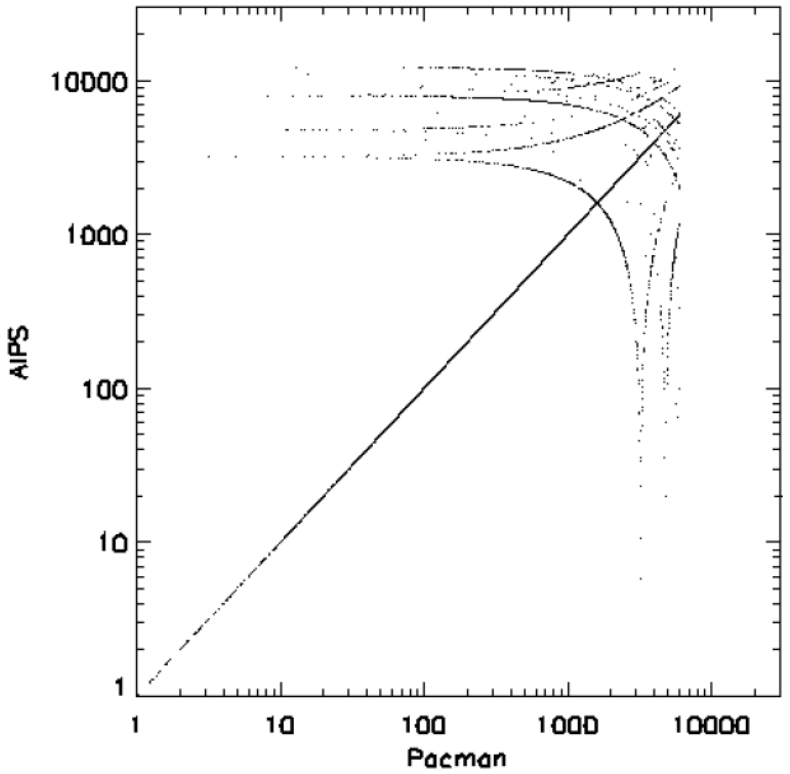

AIPS vs PACERMAN RM values

RM-Maps

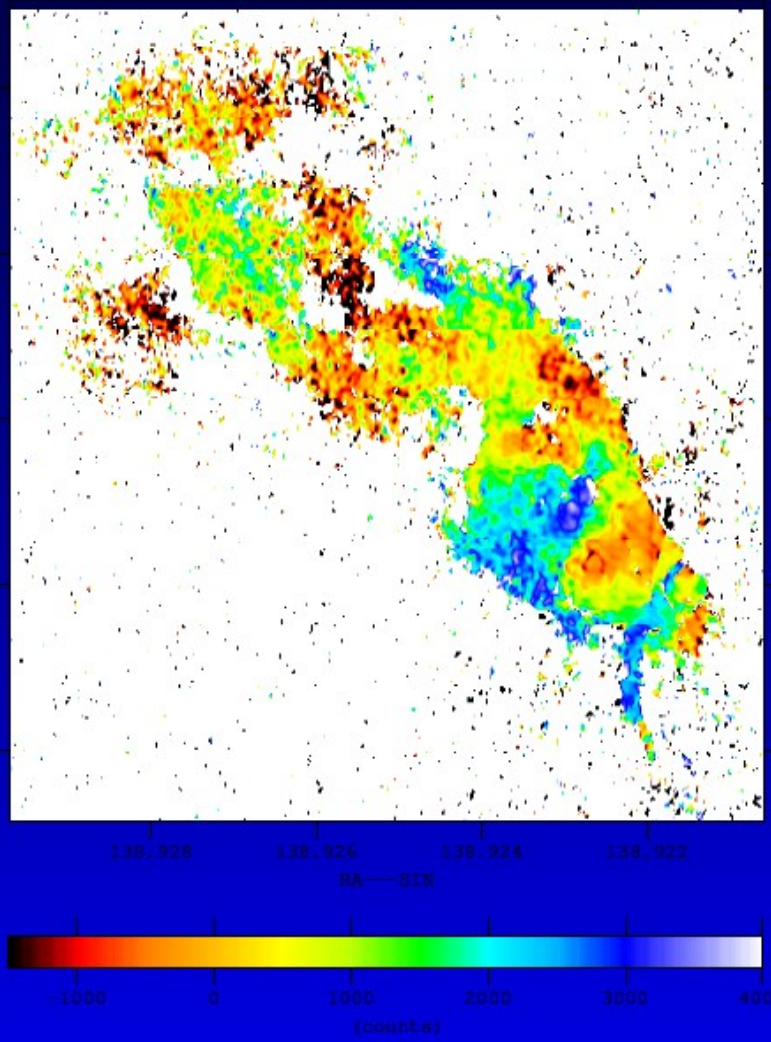
138.928
138.926
138.924
138.922
RA---SIN
-1000
0
1000
2000
3000
4000
(counts)
HYDRA-4.ROTMES.FITS_0 Colorbar

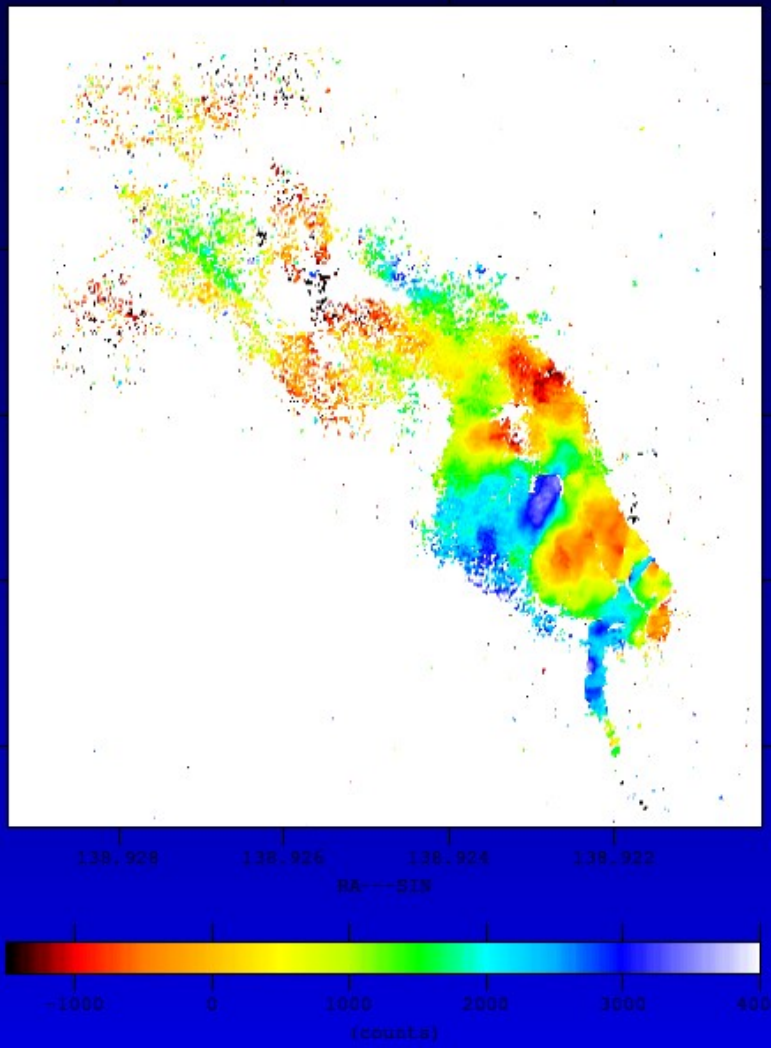
138.928
138.926
138.924
138.922
RA---SIN
-1000
0
1000
2000
3000
4000
(counts)
hydra5.fits_0 Colorbar

PACERMAN

RM error map

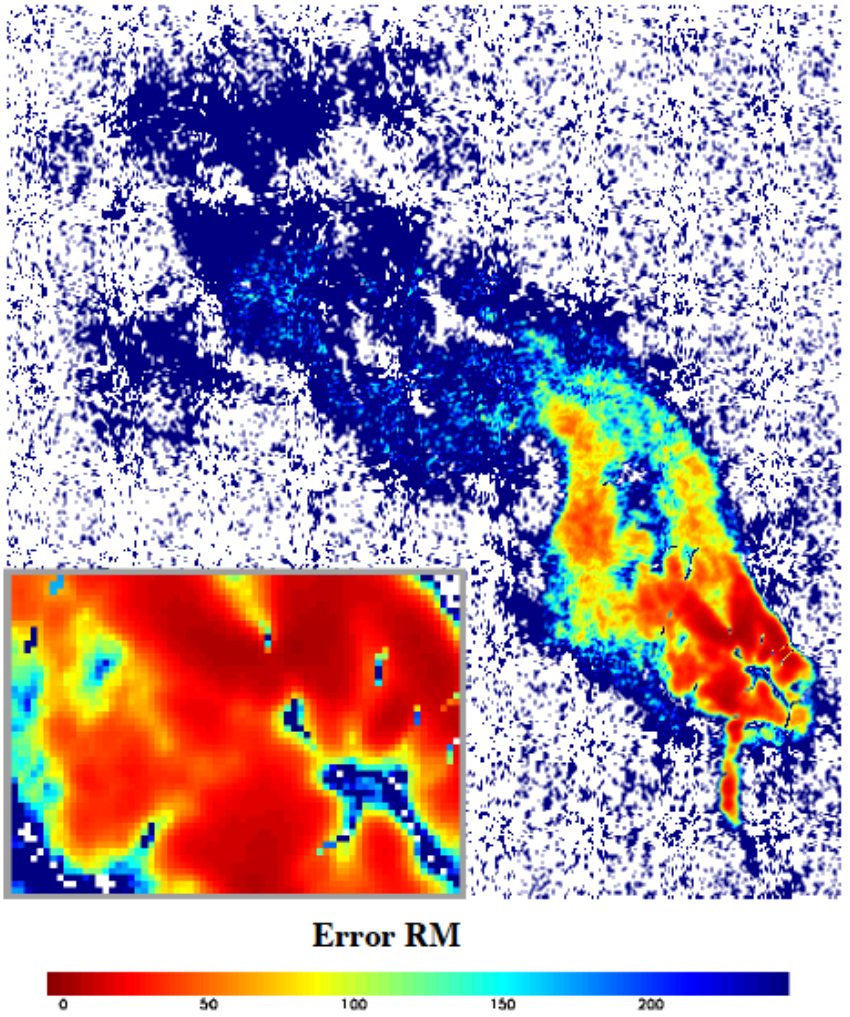

RM-PA gradient alignment map

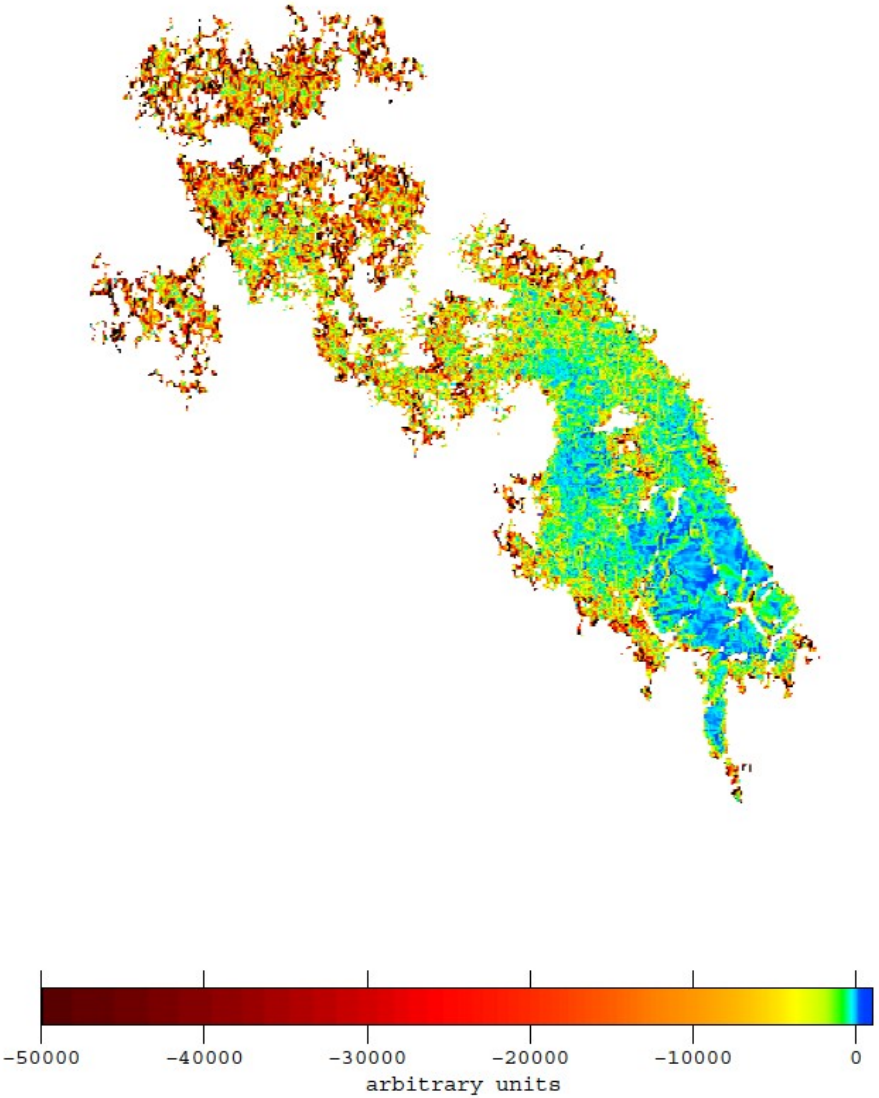

Galaxy Cluster Fields

Hydra A cluster

RM

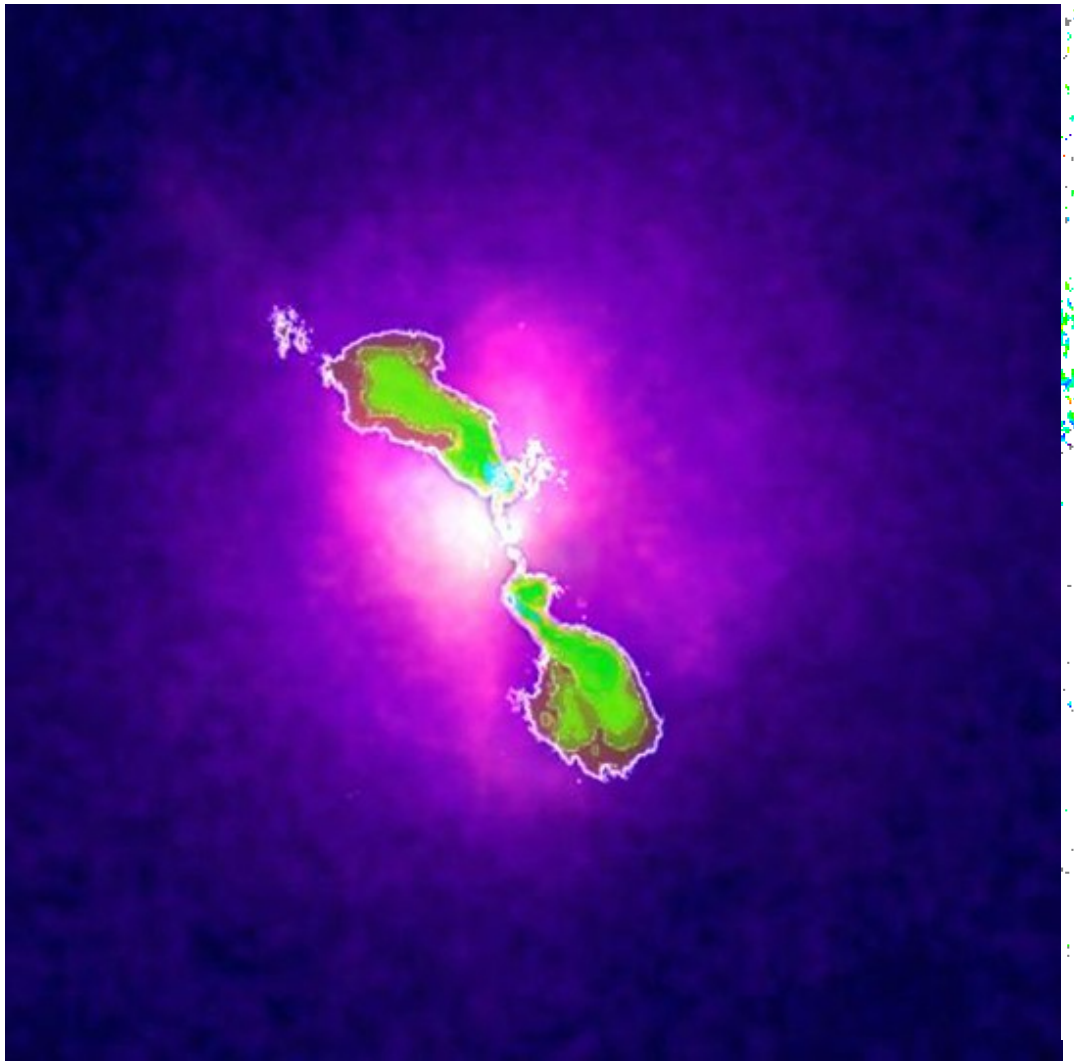

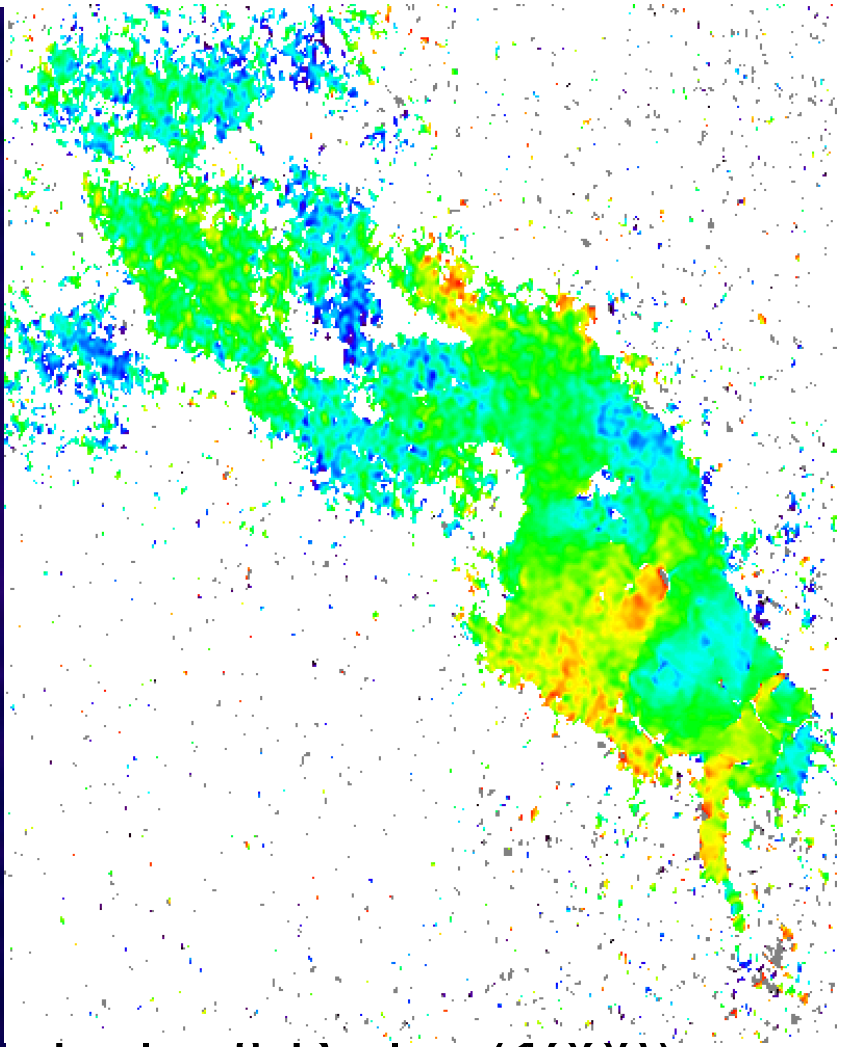

Taylor & Perley (1993)
VLA/Chandra

Observational Setup

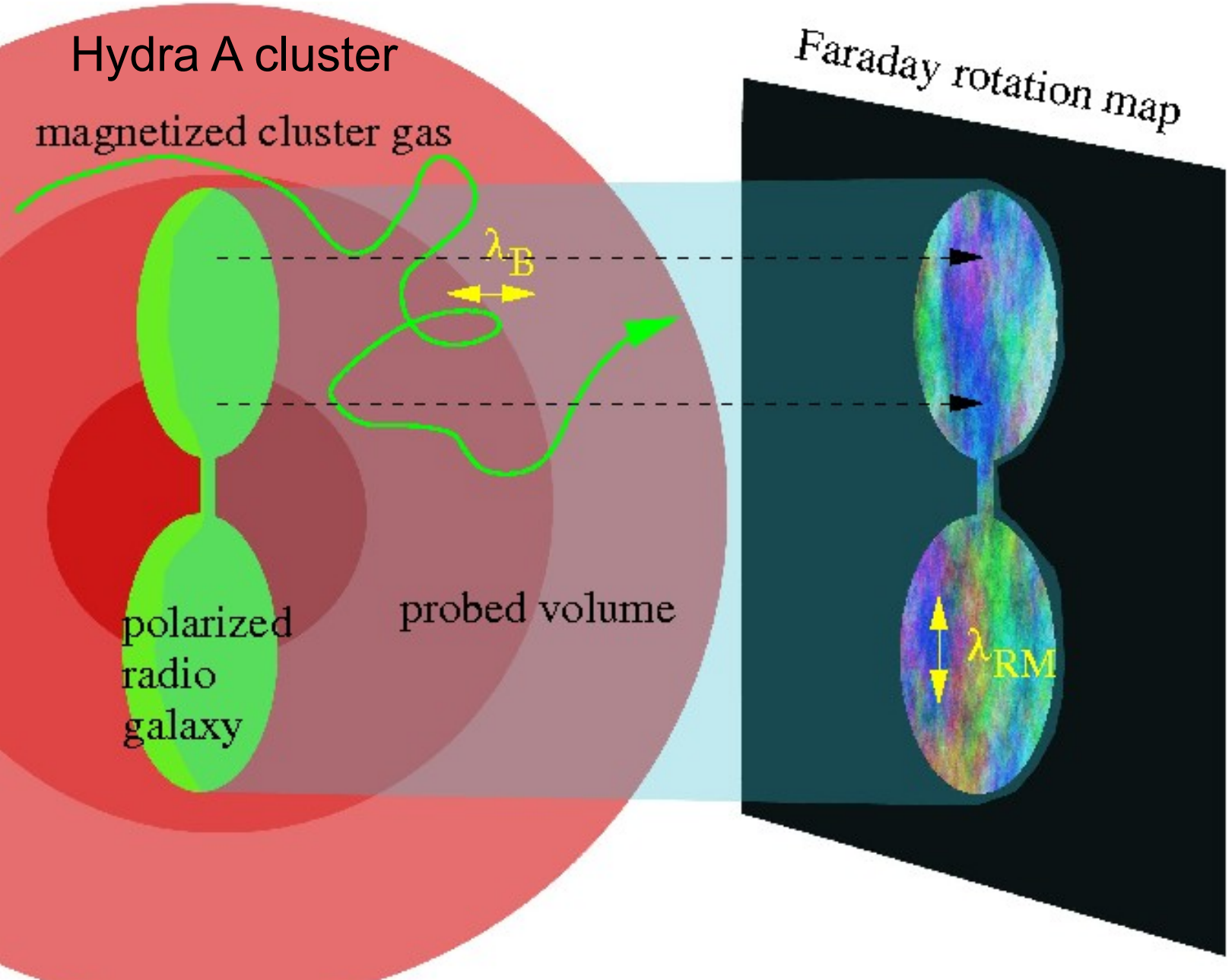

Observational Setup

Hydra A cluster

$w(r) = \langle B(x)\, B(x+r) \rangle$

$C_{RM}(r) = \langle RM(x)\, RM(x+r) \rangle$

Assumptions:

- statistical isotropy
- div B = 0

$C_{RM}(k) \sim w(k)/2$

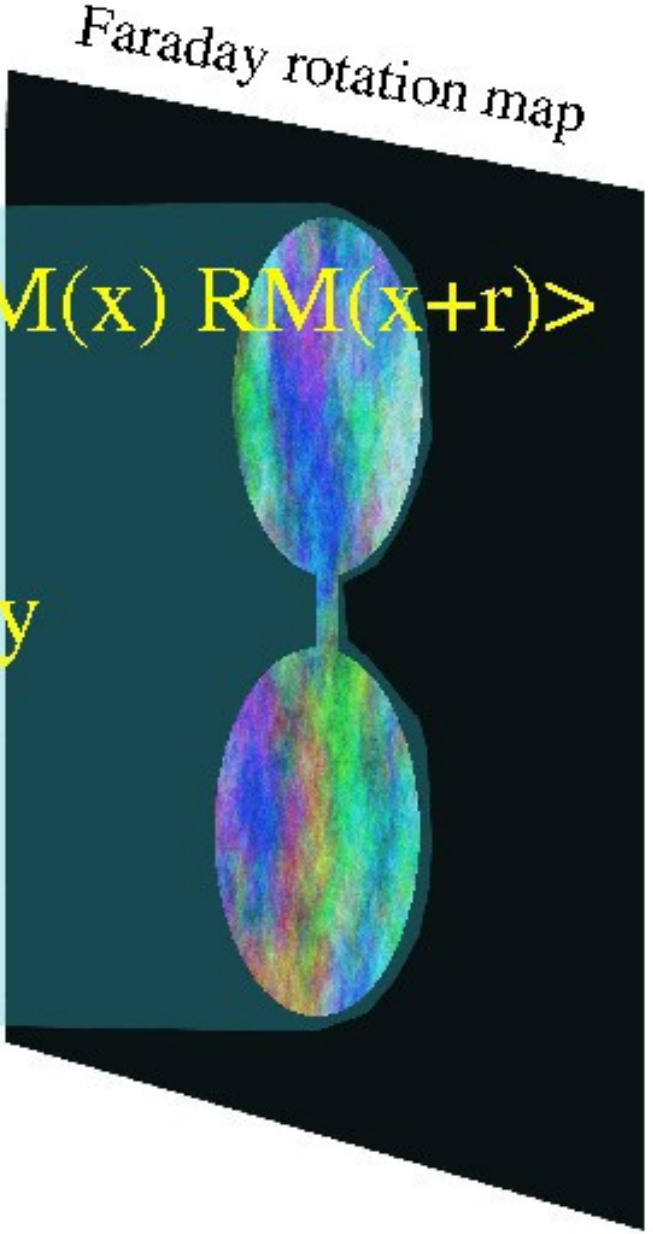

Magnetic power spectrum in Hydra A cool core cluster

Kuchar & EnBlin (2009)

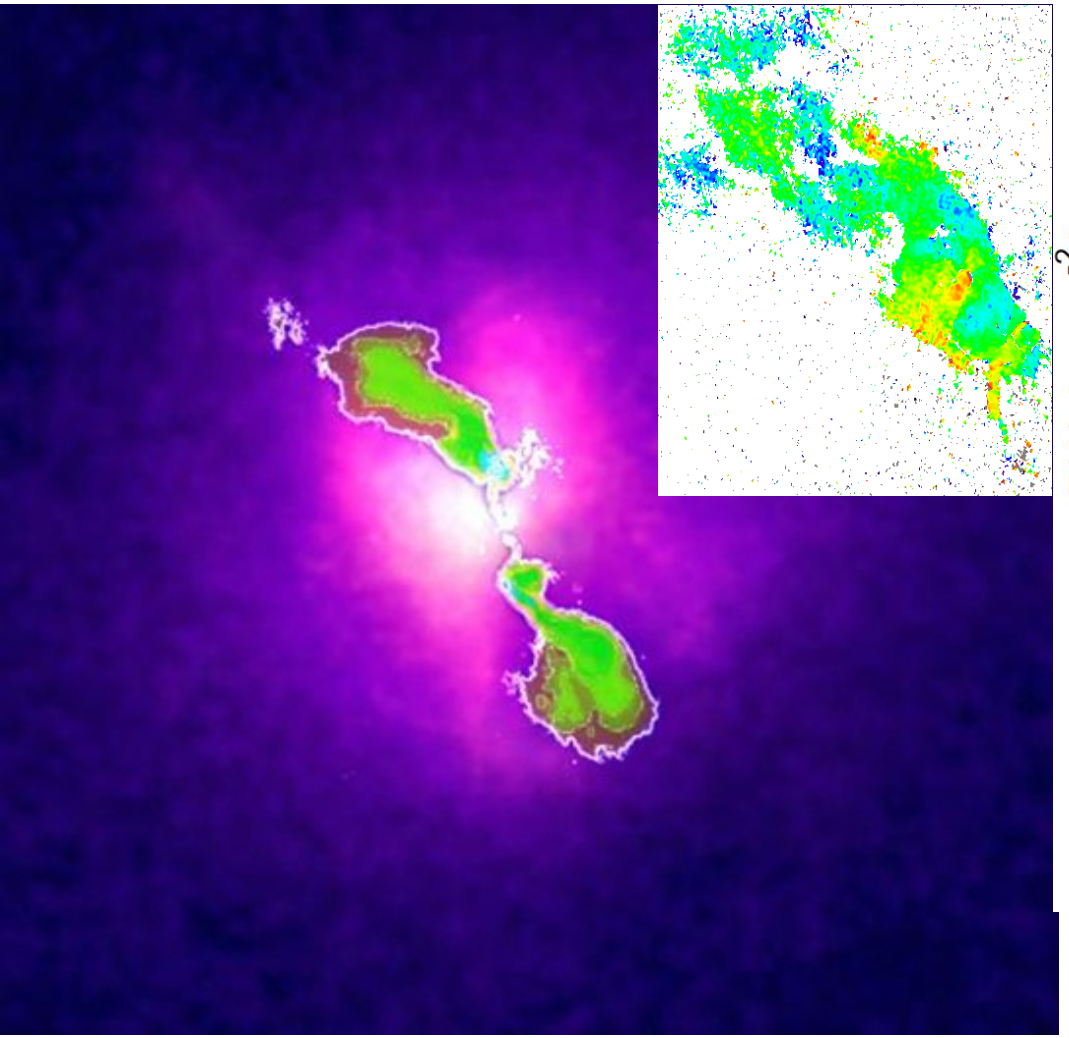

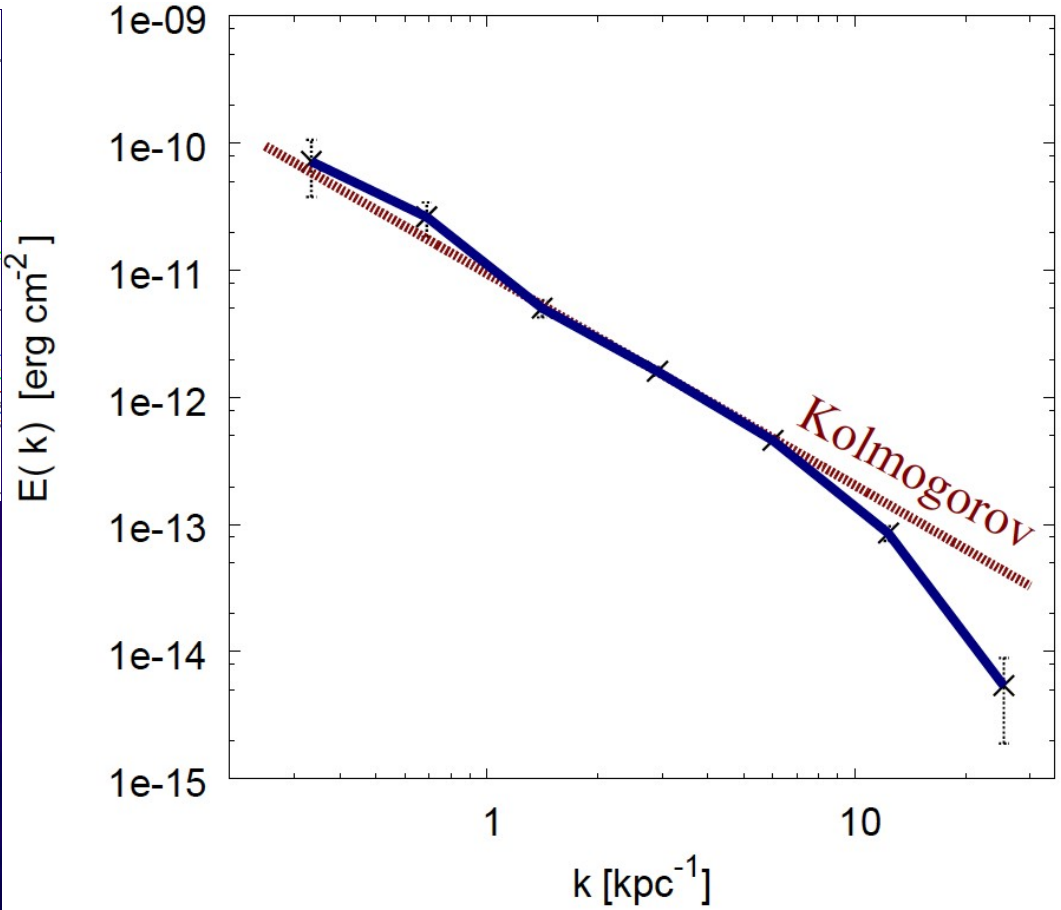

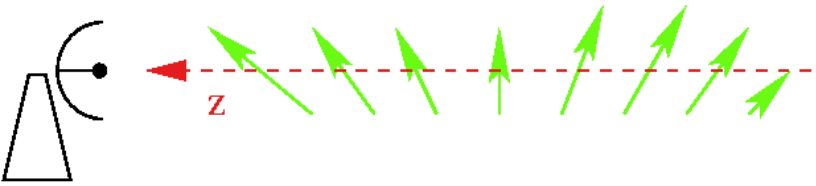

inference

realities

data space

model space

$$\omega(k) = \langle \mathbf{B}(\mathbf{k}) \cdot \overline{\mathbf{B}}(\mathbf{k}) \rangle$$

$$\omega(k) = \sum_i s_i w_i(k)$$

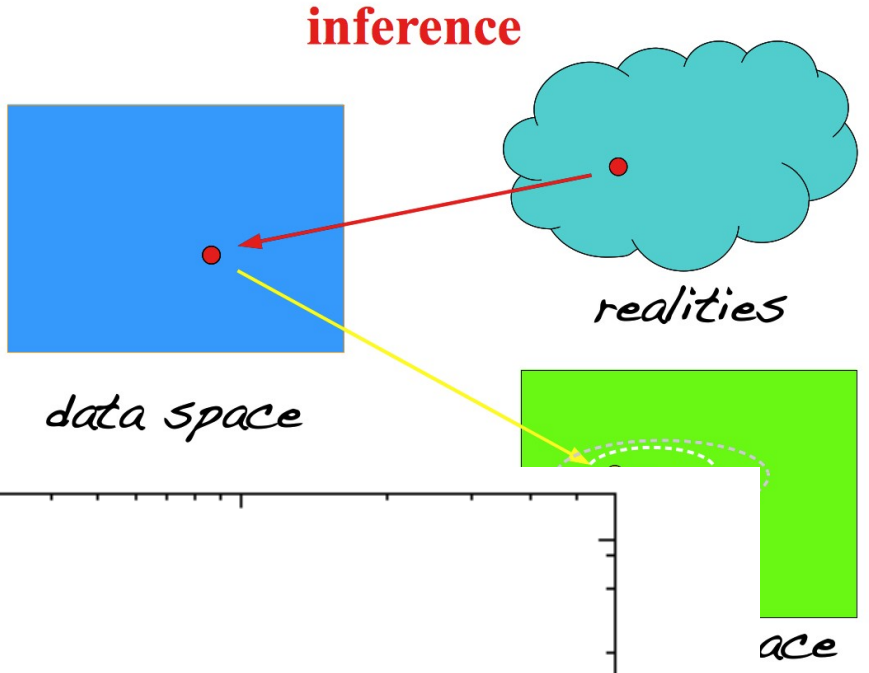

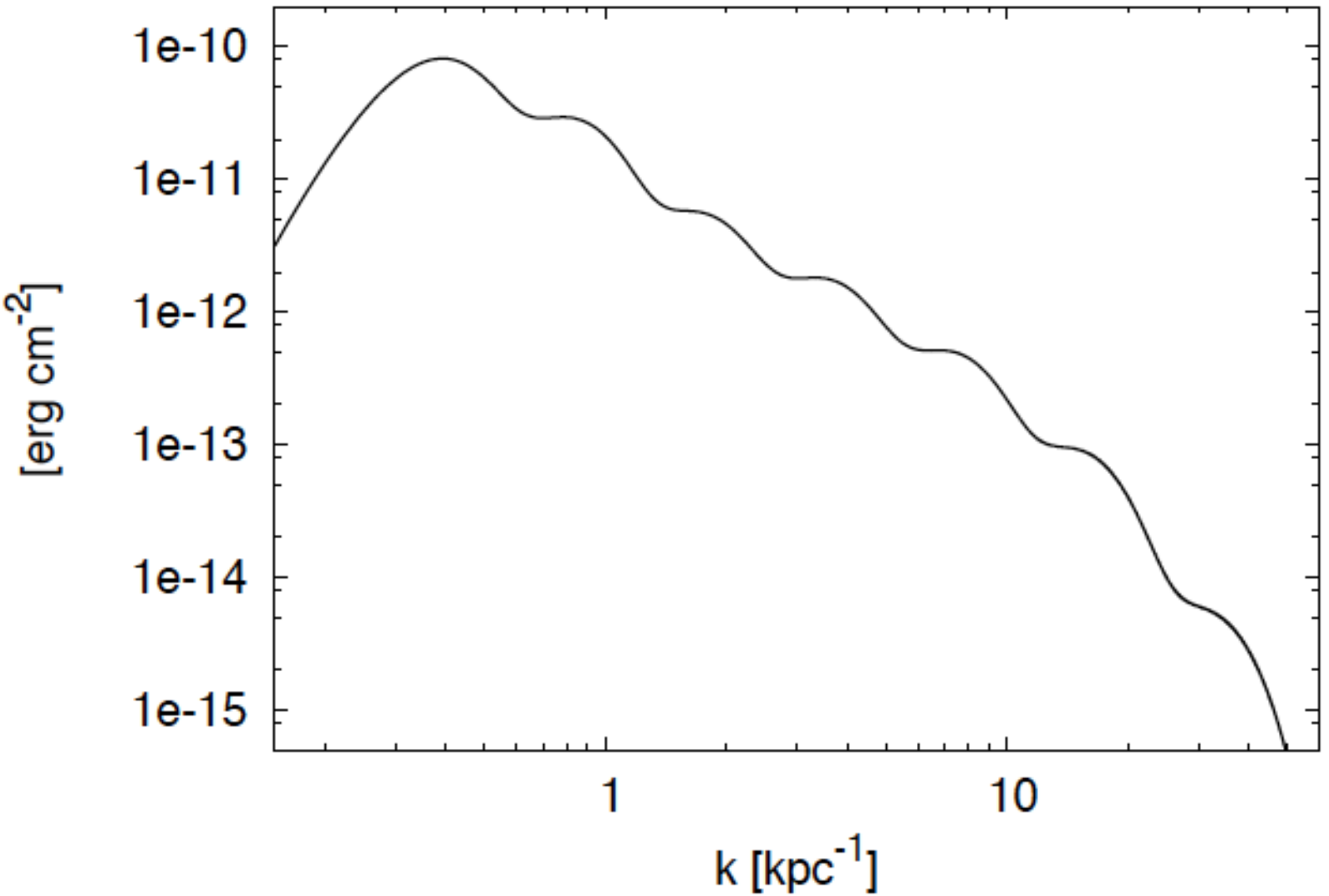

$$C \equiv C(s) = \langle d_i \, d_j \rangle$$

$$C(s) = \langle (RB + n)(RB + n)^T \rangle$$

$$= R\langle BB^T \rangle R^T + \langle nn^T \rangle$$

$$\equiv \widetilde{C}(s) + N$$

$$\widetilde{C}(\mathbf{x}_\perp, \mathbf{x}'_\perp) = \langle \, a_o^2 \int_{z1}^{\infty} n_e(\mathbf{x}) B_z(\mathbf{x}) dz \int_{z2}^{\infty} n_e(\mathbf{x}') B_z(\mathbf{x}') dz' \, \rangle$$

$$\langle B^2(\mathbf{x}) \rangle = B_o^2 (n_e(\mathbf{x})/n_o)^{2\alpha}$$

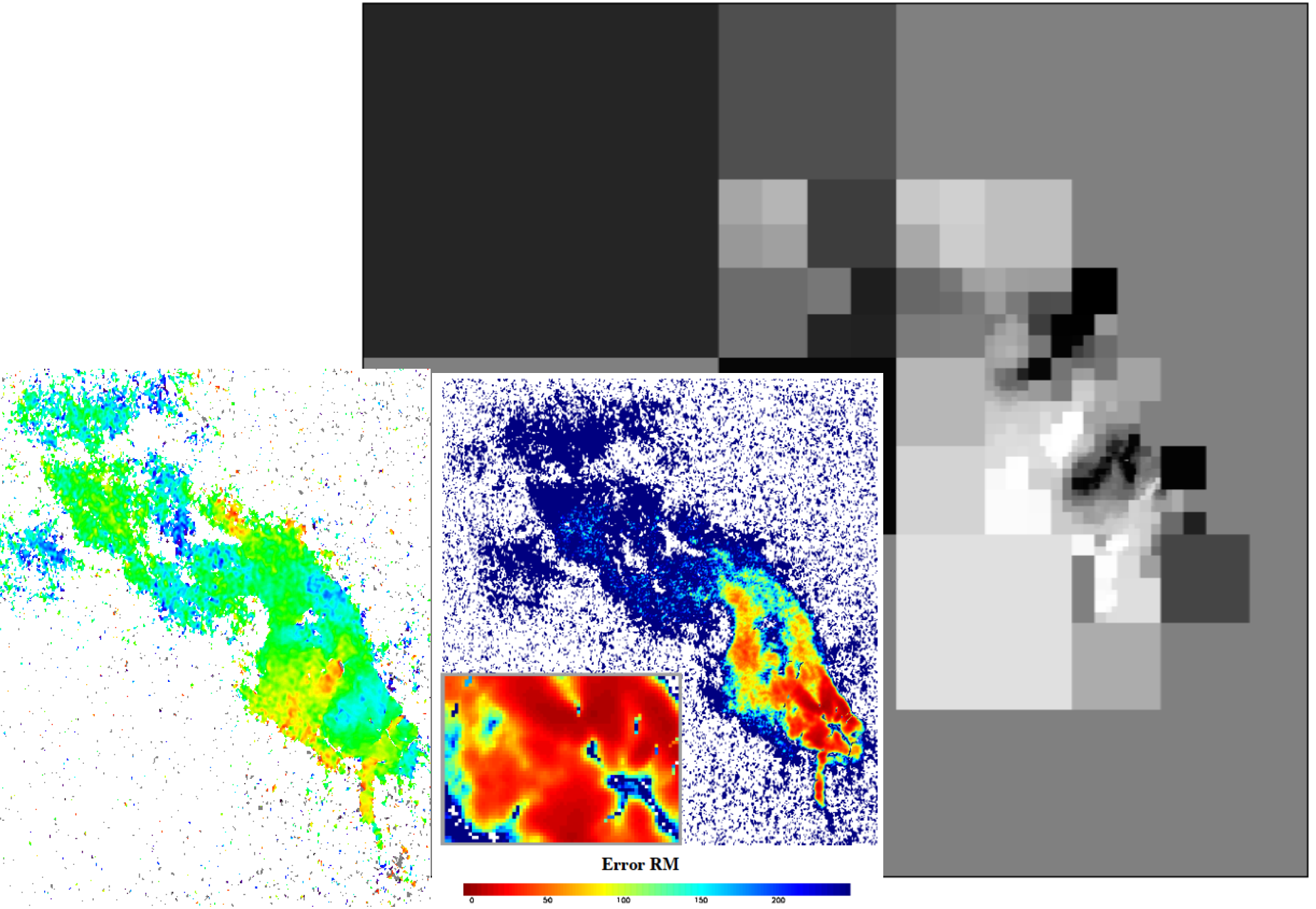

Fig. 3: Merged data map of Hydra A for 1000 data points. The RM values range between -1700 rad/m^2 (dark) and 2800 rad/m^2 (light). The map has a size of about 40 kpc.

Used information & assumptions

- The rotation measure map and its error map,
- knowledge of the geometry of the Faraday active volume, which depends also on the projection angle θ of the jet and the cavity size,
- knowledge of the electron density profile n_e,
- assuming that the magnetic field strength B follows the electron density profile like $B \propto n_e^{\alpha}$ (e.g. Dolag et al. 2001),
- assuming statistical isotropy of B,
- assuming solenoidal fields
- assuming that there is no polarized radio emission inside of the Faraday active volume in front of the radio bubble,
- assuming a Gaussian probability distribution of the rotation measure map.

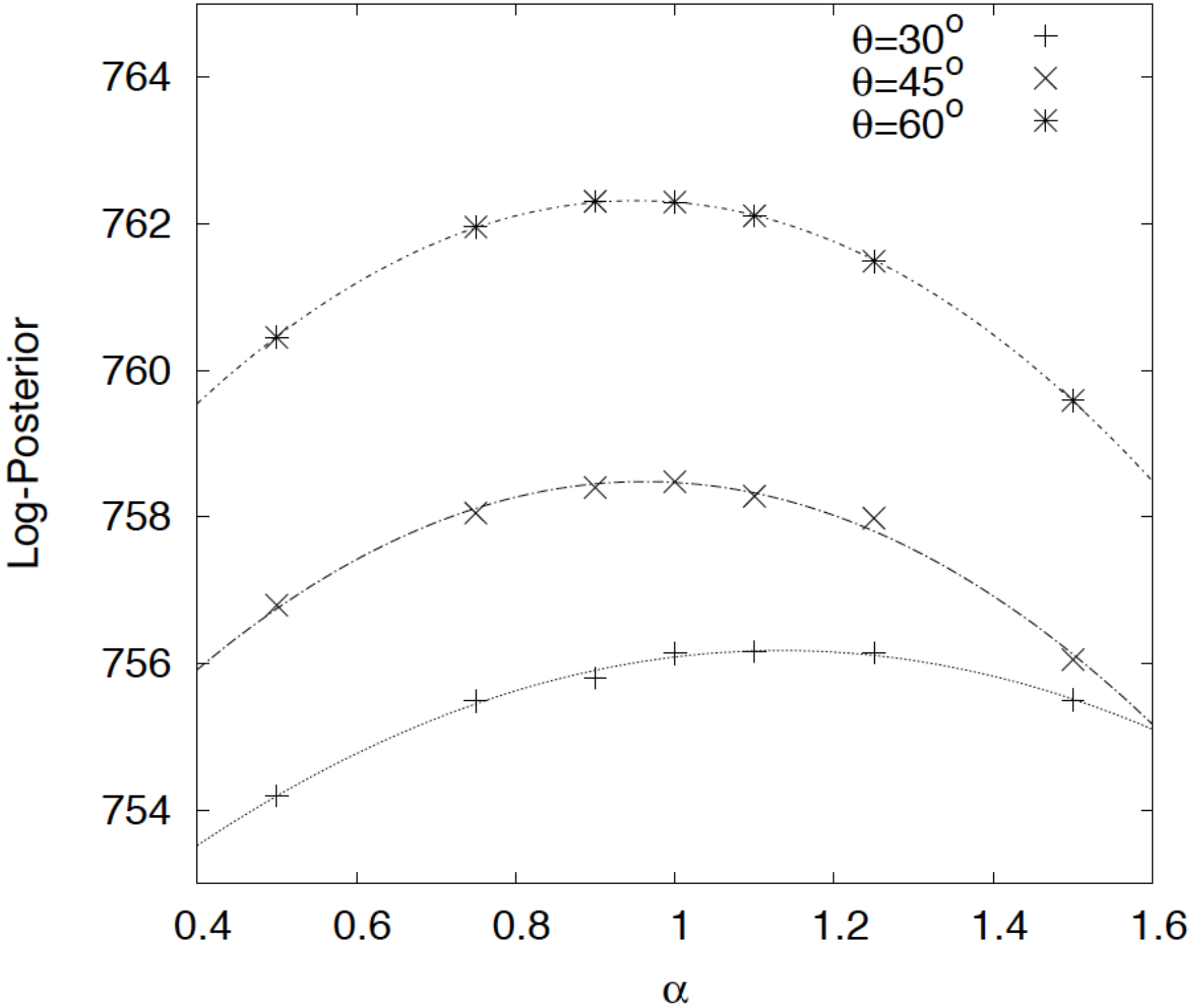
θ=30°
θ=45°
θ=60°
764
762
760
758
756
754
Log-Posterior
0.4
0.6
0.8
1
1.2
1.4
1.6
α

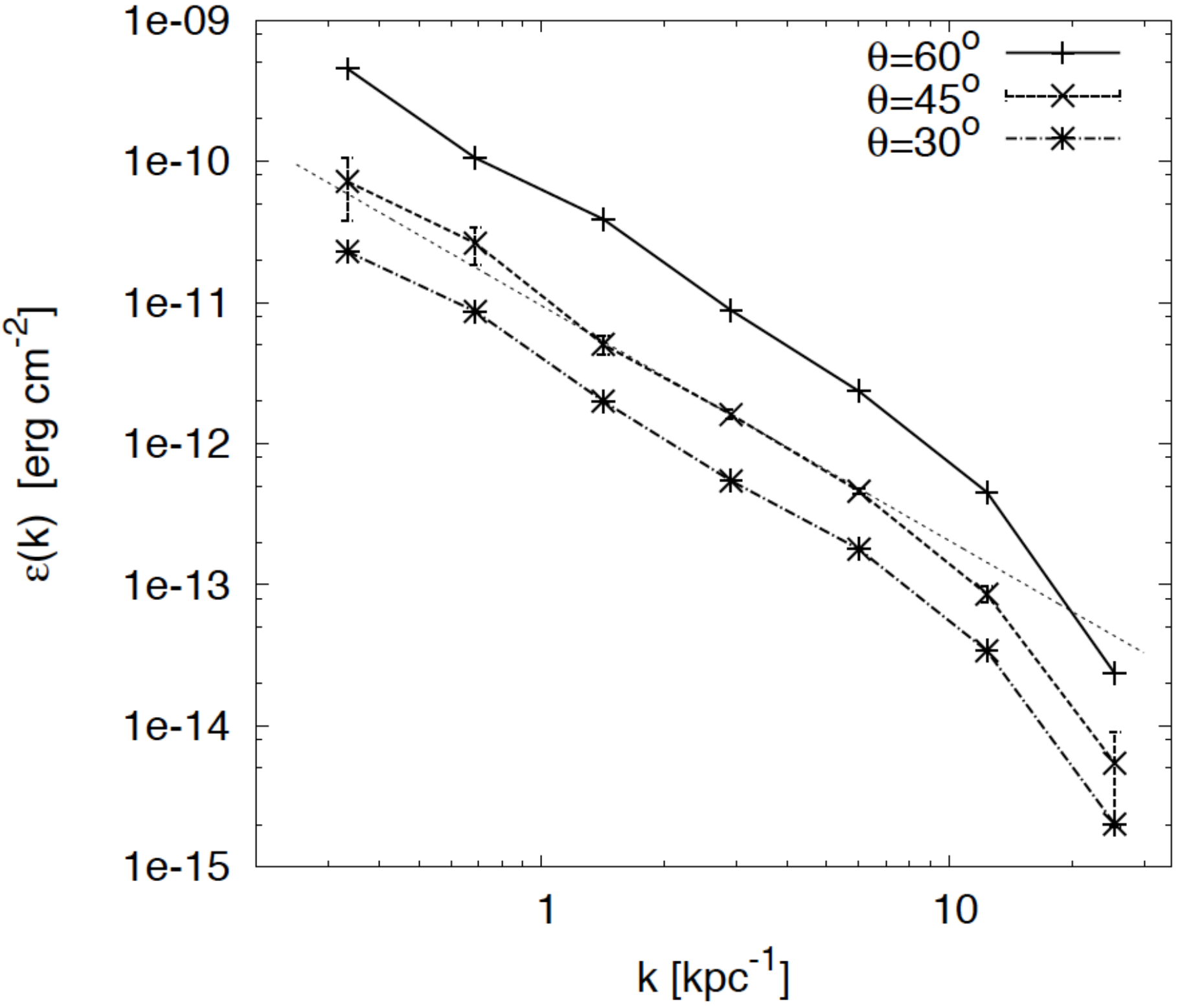
1e-09
1e-10
1e-11
1e-12
1e-13
1e-14
1e-15
ε(k) [erg cm-2]
1
10
k [kpc-1]
θ=60°
θ=45°
θ=30°

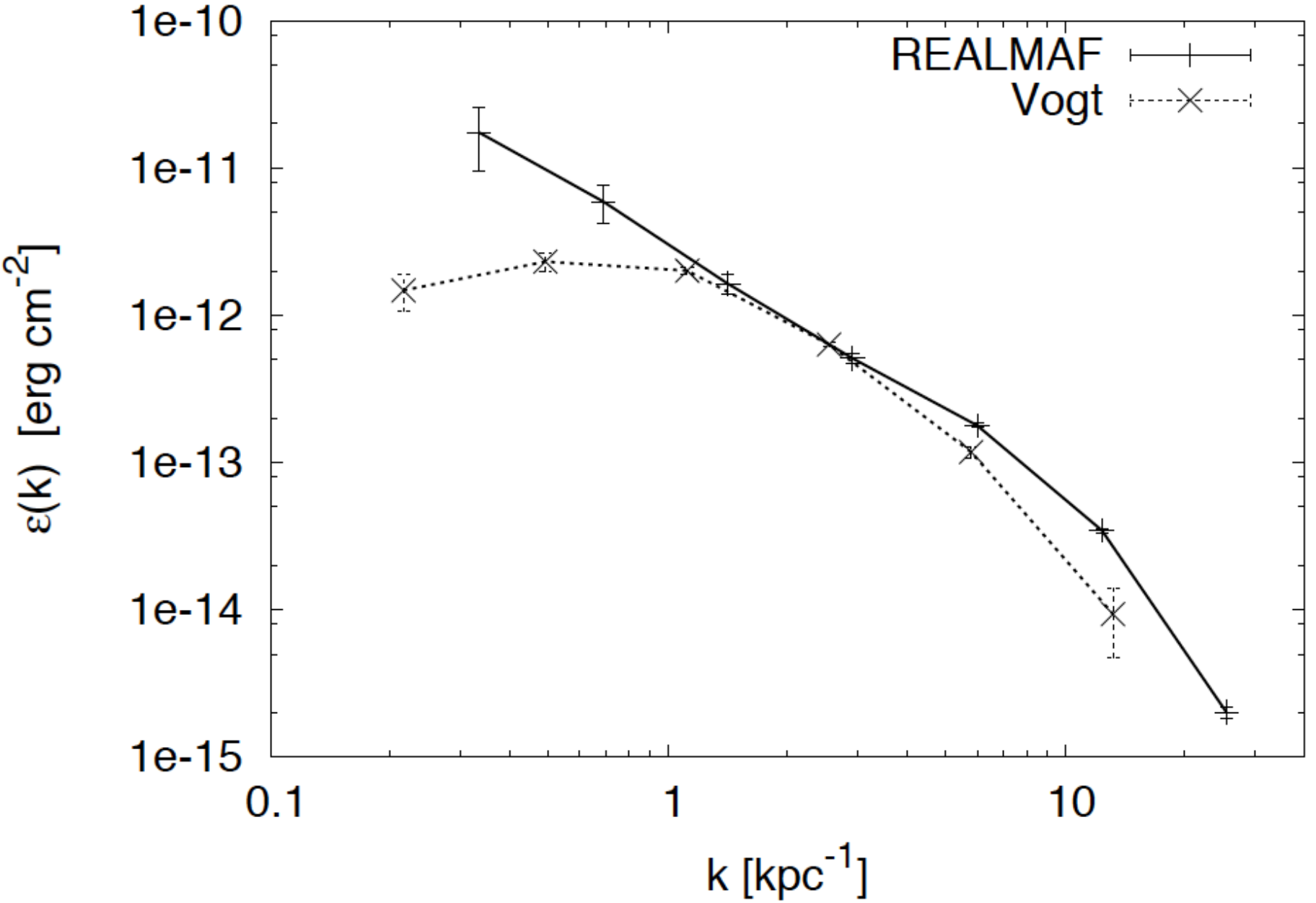

Fig. 10: Power spectrum with and without simplifications used in Vogt & Enßlin (2005) for $\alpha = 0.5$ and $\theta = 45^o$

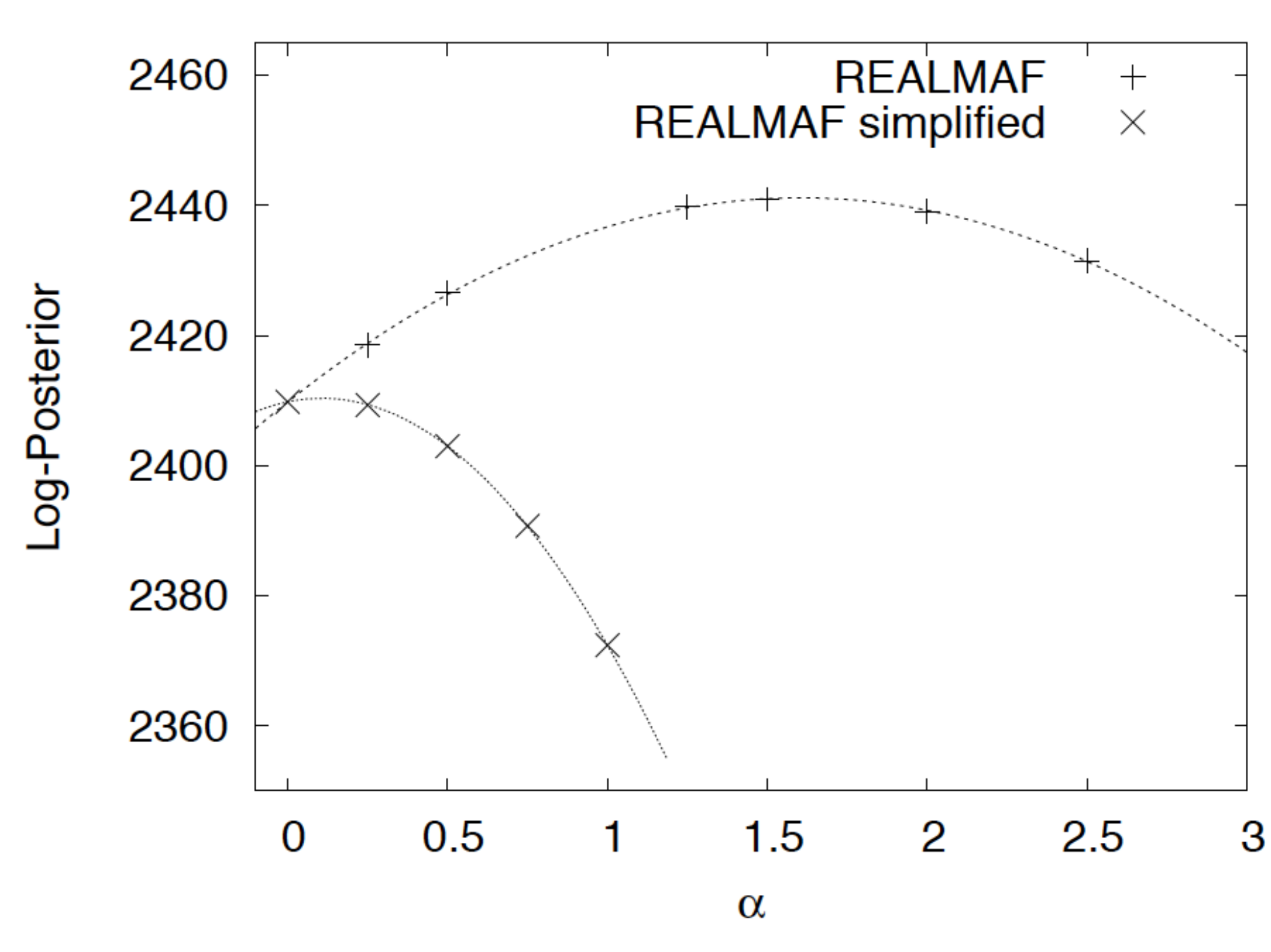
REALMAF
REALMAF simplified
Log-Posterior
2460
2440
2420
2400
2380
2360
0
0.5
1
1.5
2
2.5
3
α

	B_o [μG]	B_{50} [μG]	λ_B [kpc]	spectral index
$\theta = 30^o$	21 ± 1	9.3	5.0 ± 1.0	1.70 ± 0.14
$\theta = 45^o$	36 ± 2	16	5.2 ± 1.1	1.73 ± 0.13
$\theta = 60^o$	85 ± 5	37	5.3 ± 1.2	1.85 ± 0.14

Table 1: Magnetic field characteristics for most probable $\alpha = 1$

	B_o [μG]	B_{50} [μG]	λ_B [kpc]	spectral index
$\alpha = 0.5^o$	18 ± 1	12	4.8 ± 1.1	1.56 ± 0.14
$\alpha = 1.5^o$	70 ± 4	21	5.5 ± 1.2	2.06 ± 0.14

Table 2: Magnetic field characteristics for $\theta = 45^o$ and maximal and minimal possible α

	α	B_o in μG	spectral index	large-scale turnover
Kuchar	1.0	36	1.73	no
Laing	0.25	19	0.8	no
Vogt	0.5	7.3	1.67	yes

Table 3: Recent results of Hydra A for $\theta = 45^o$

Magnetic power spectrum in Hydra A cool core cluster

Kuchar & EnBlin (2009)

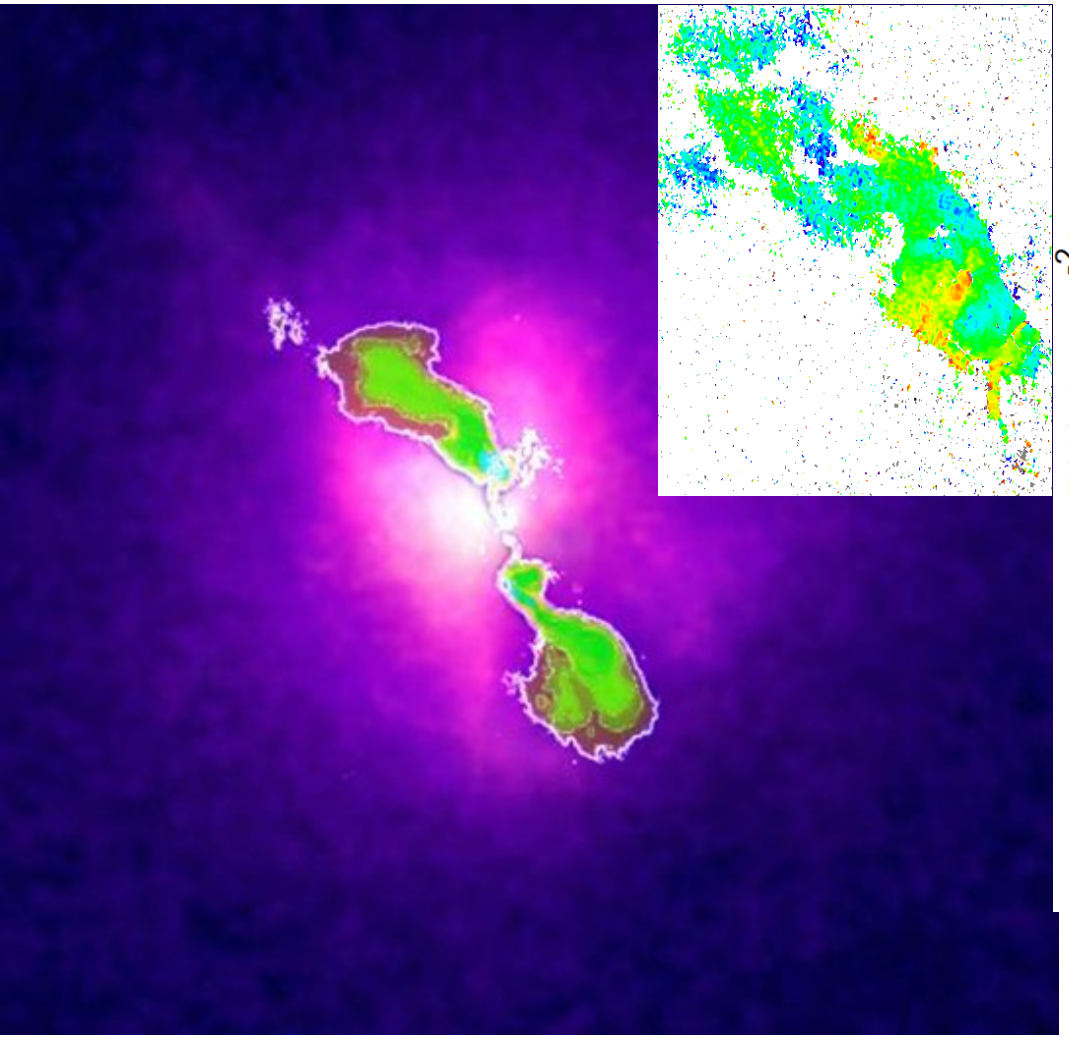

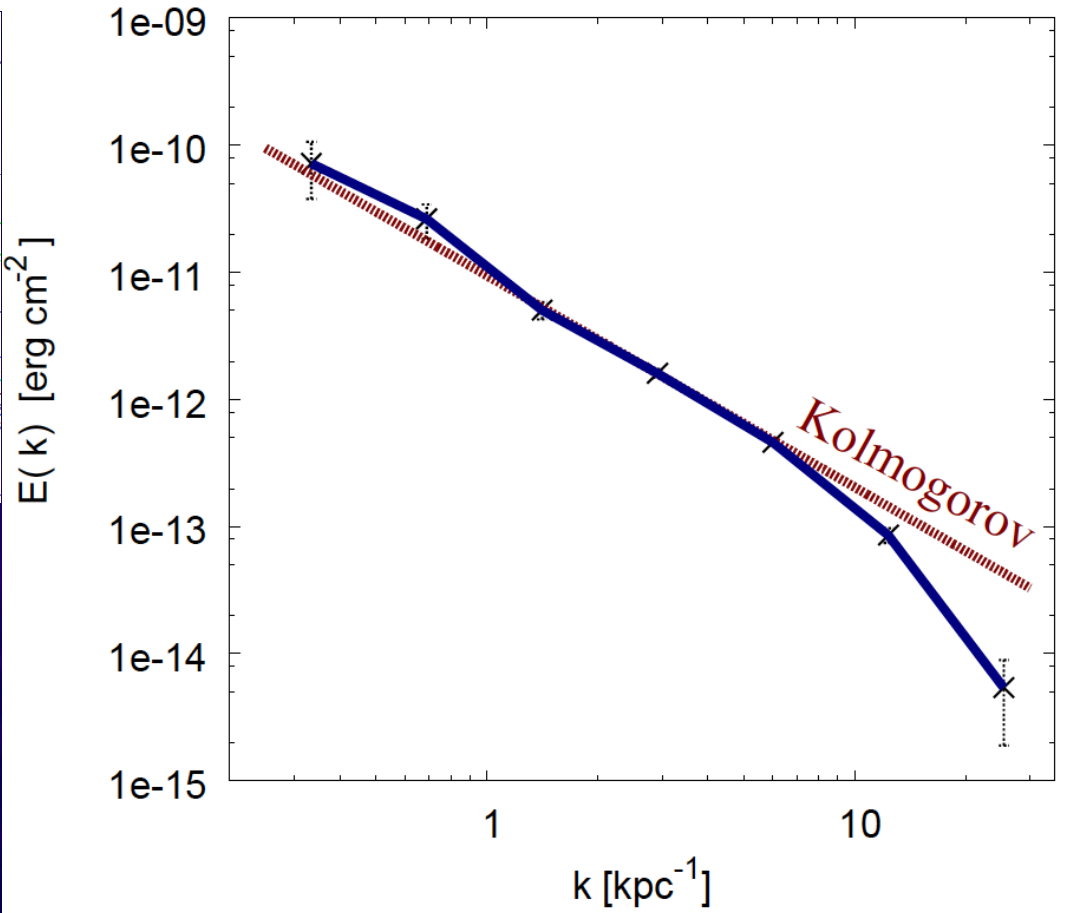

Magnetic turbulence in cool cores of galaxy cluster

Abell 400

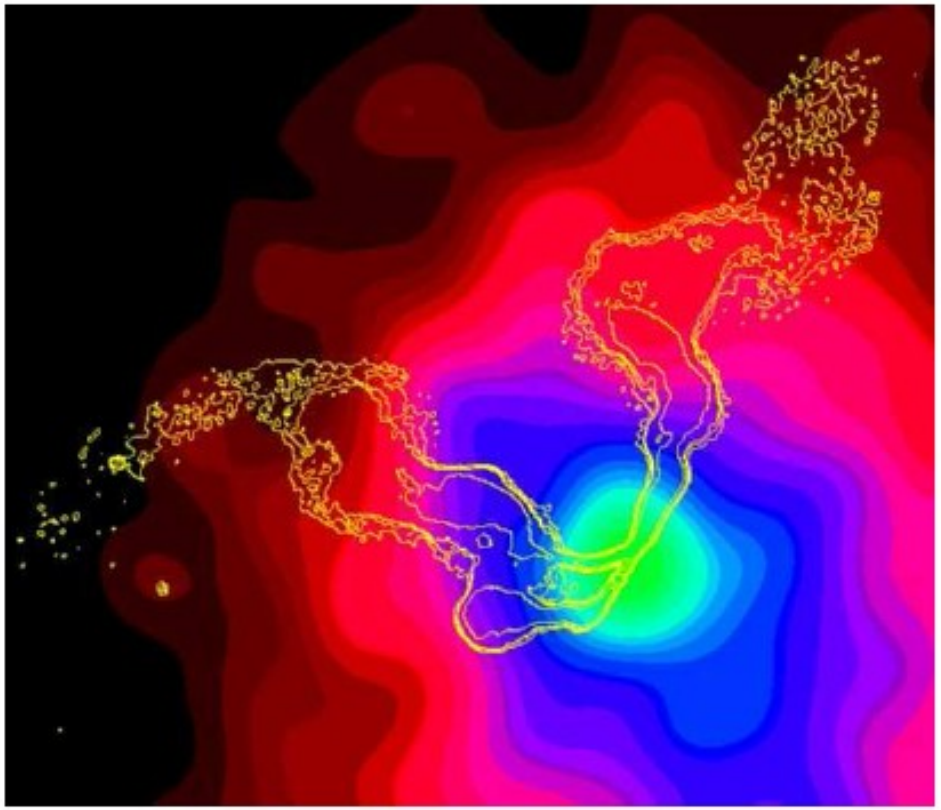

X-ray (colours)
radio (contours)

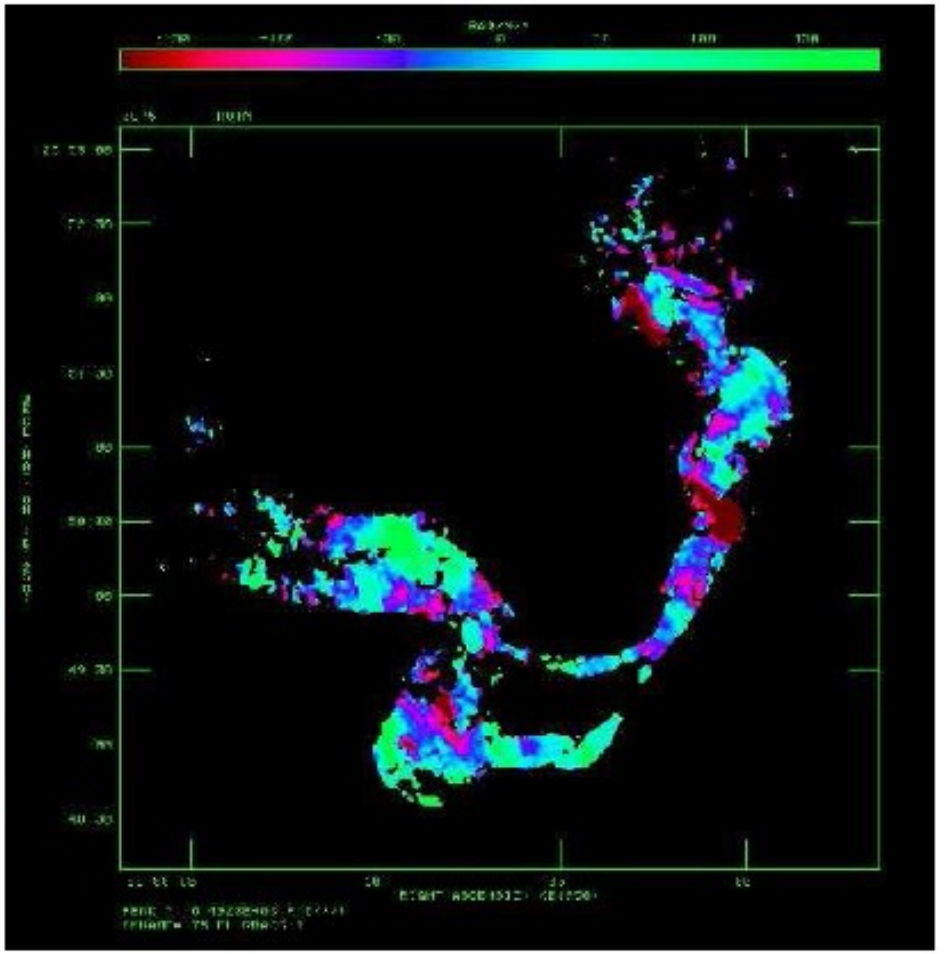

RM map: Eilek & Owen

Impact of tangled magnetic fields on AGN-blown bubbles

M. Ruszkowski,[1⋆] T.A. Enßlin[1], M. Brüggen[2], S. Heinz[3], & C. Pfrommer[4]

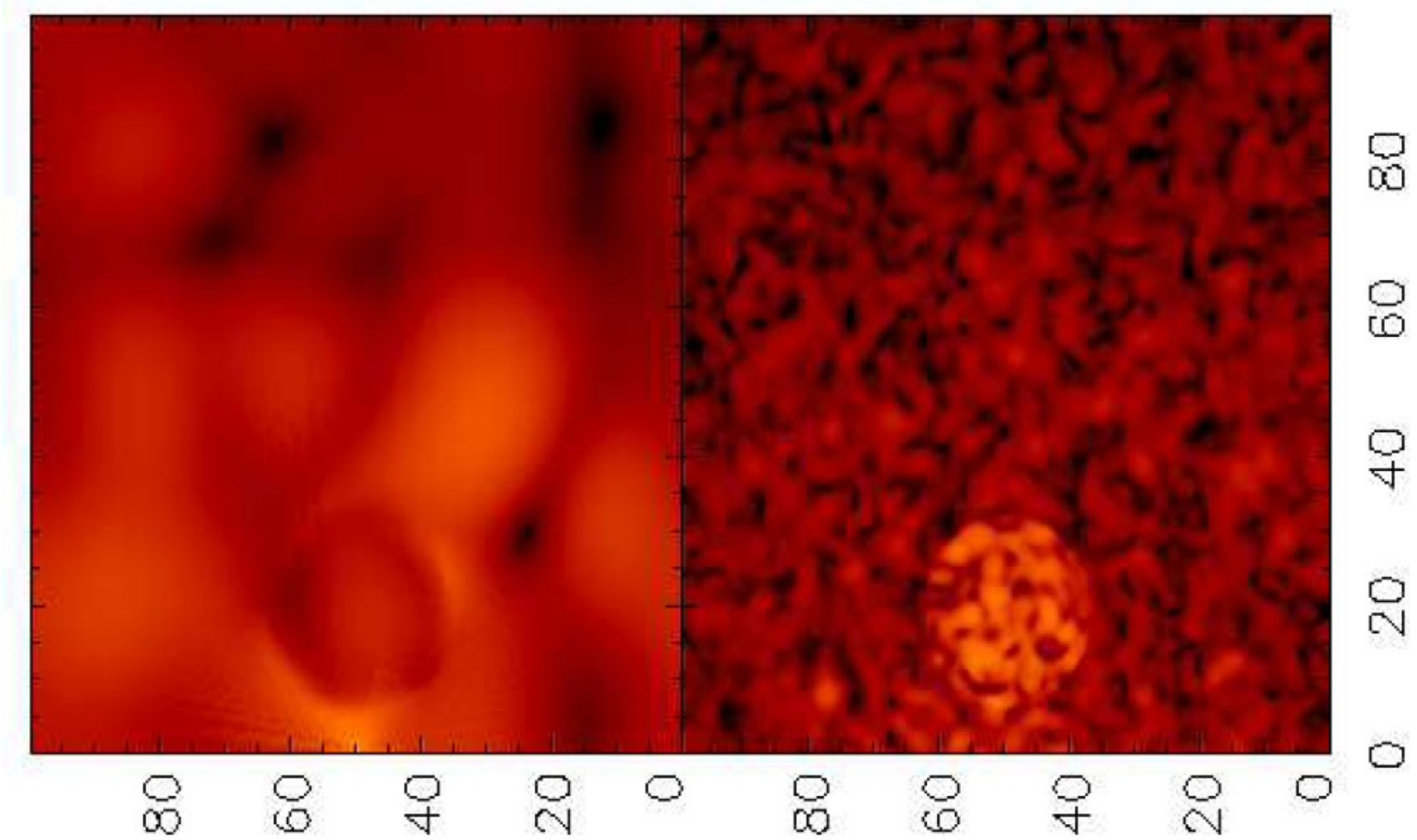

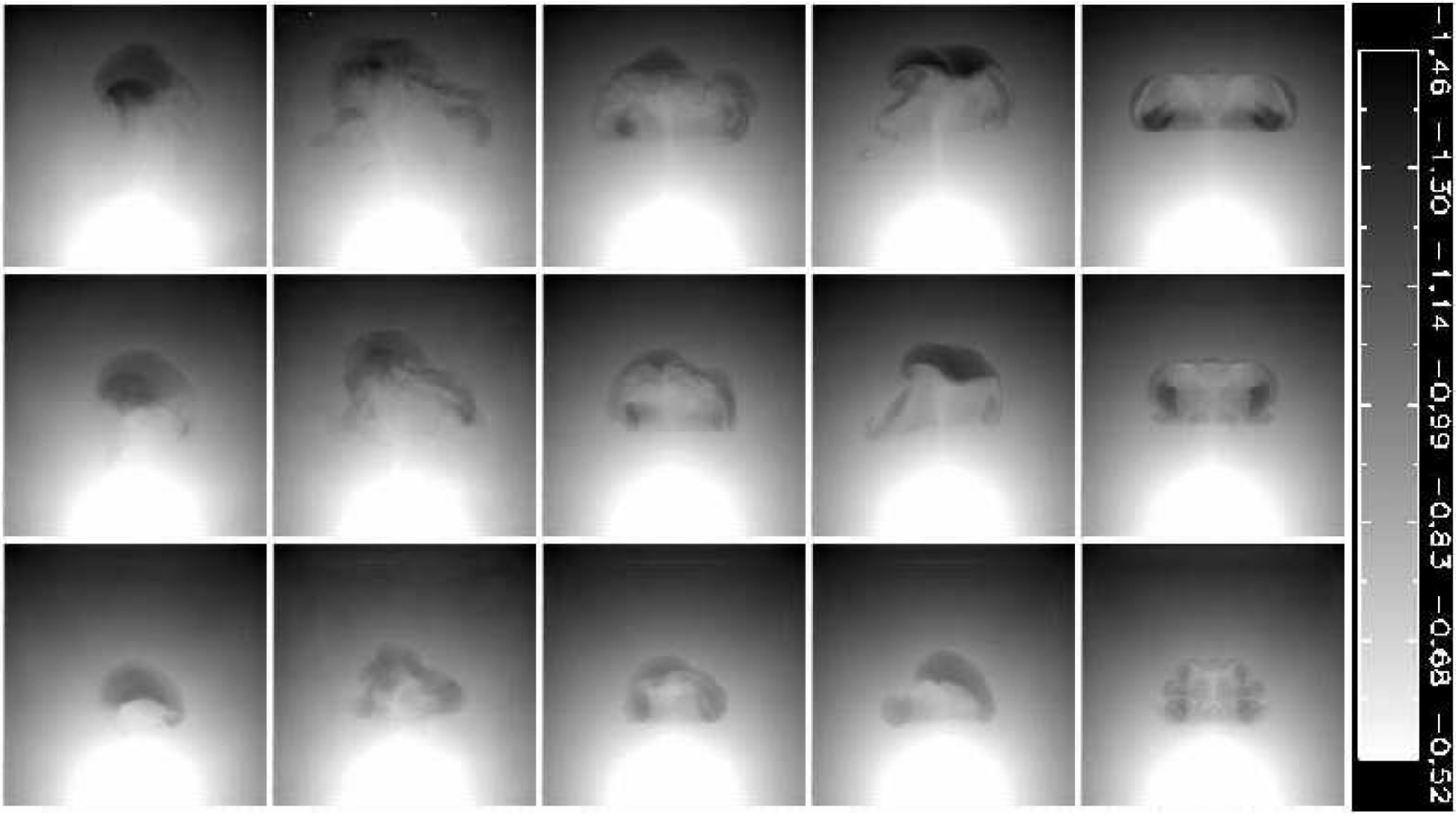

synthetic X-ray images

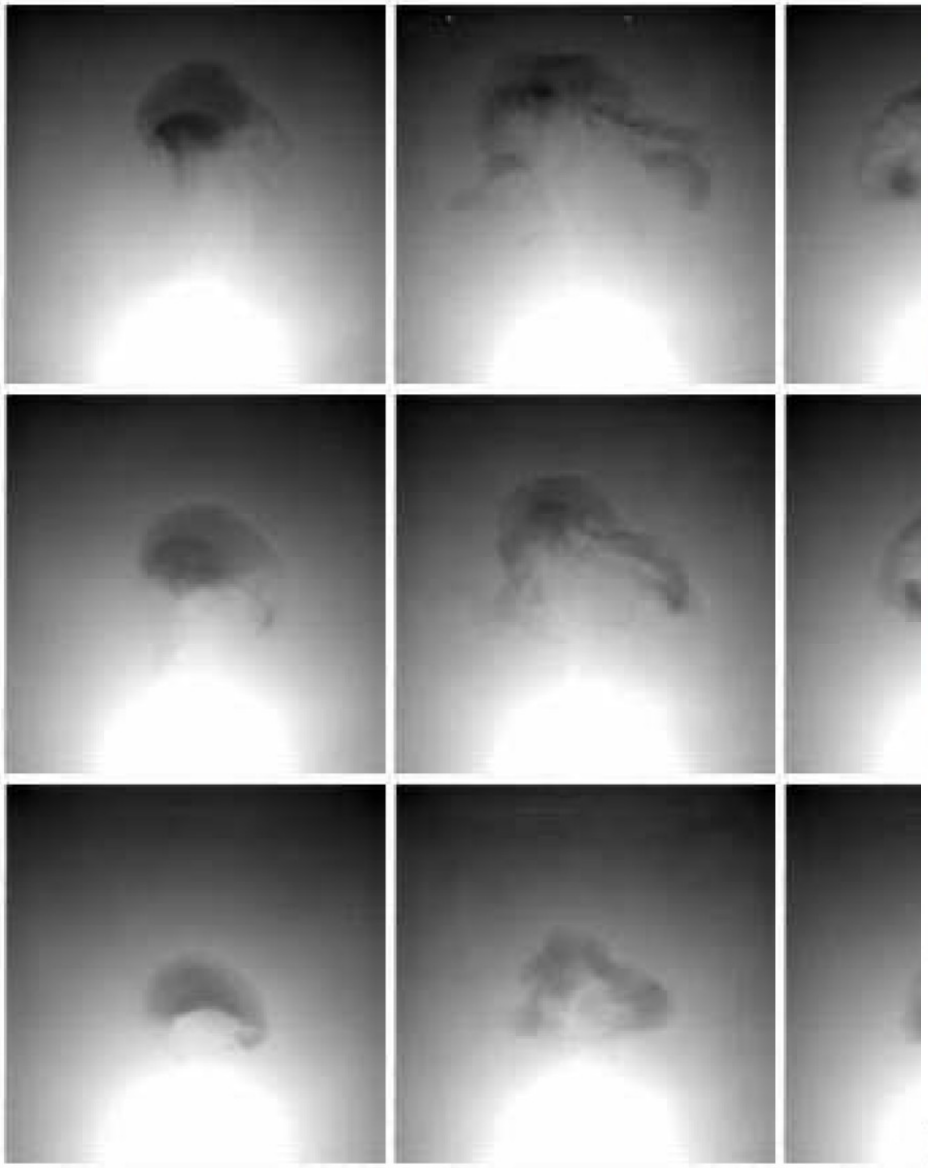

synthetic X-ray images

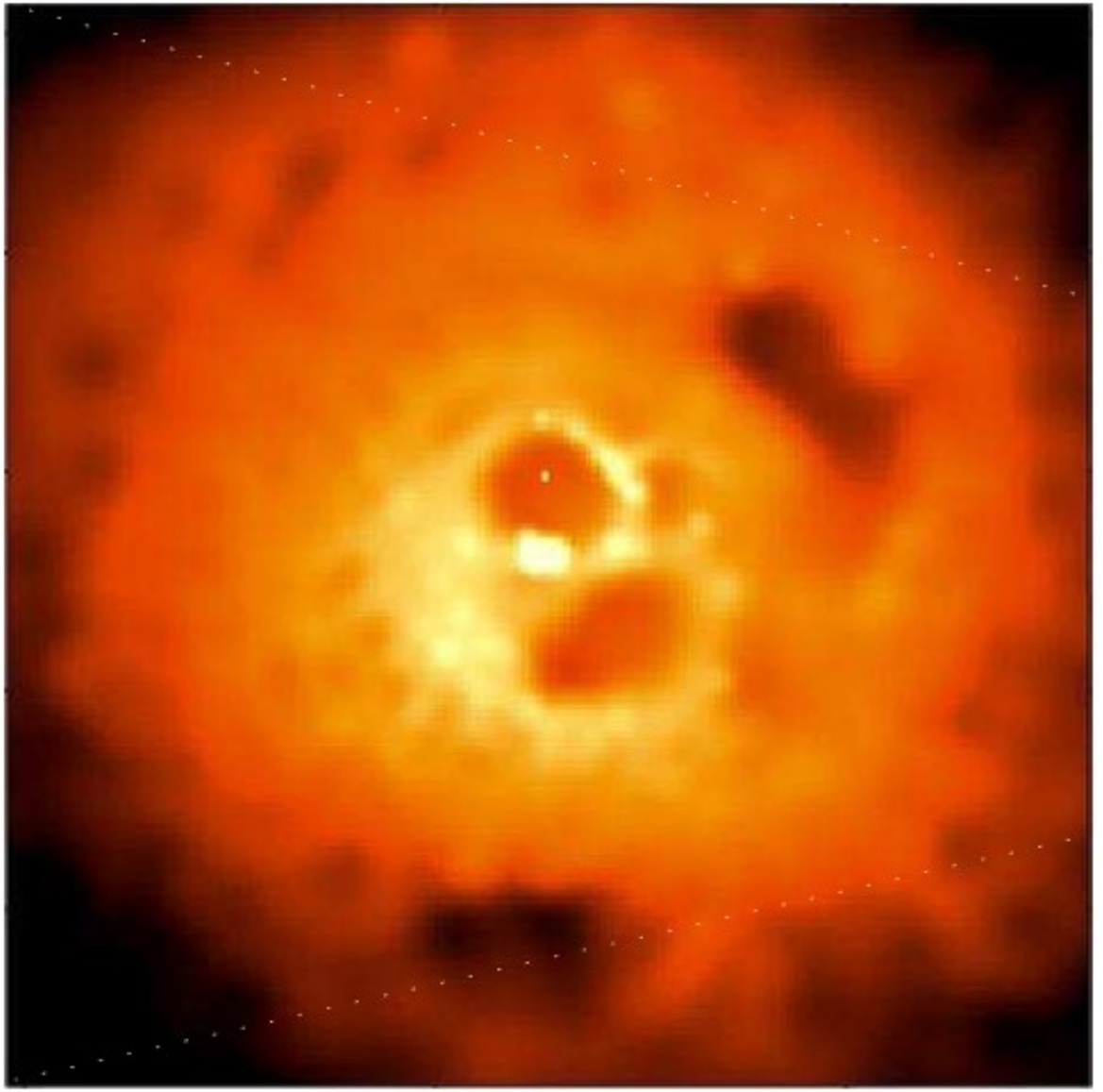

X-ray image of cool core with radio bubbles & ghost cavities
credit: Fabian et al./Chandra

Outline:

Cluster radio emission
& magnetic turbulence

Faraday rotation
& magnetic spectrum inference

Stokes correlators
& tension forces
A. Waelkens, A. Scheckochihin

Faraday-Stokes correlations
& magnetic helicity

RM Synthesis

de Bruyn & Brentjens (2005)

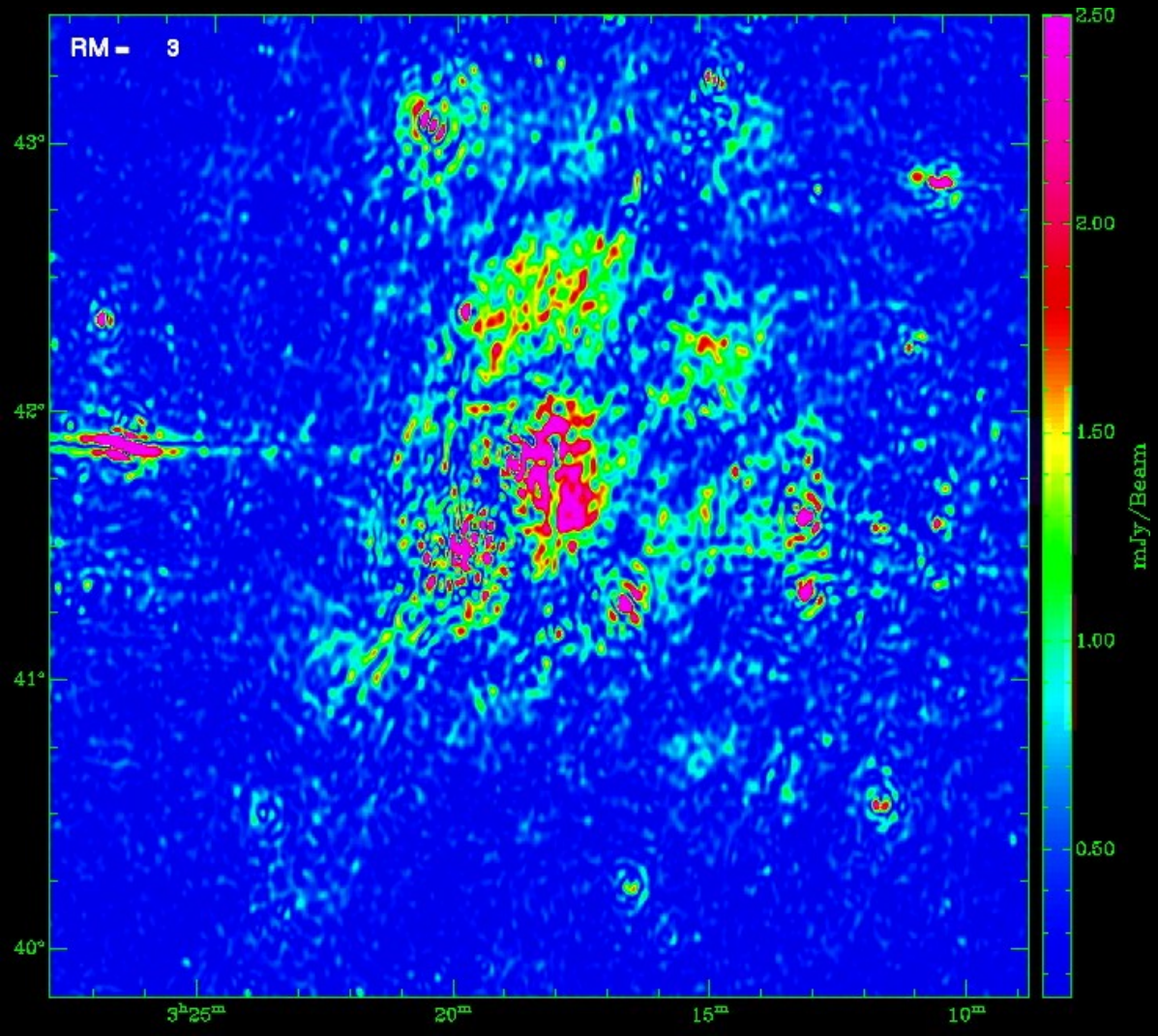

Where are we fishing?

Yousef, Rincon, Schekochihin 2007

What does the fish look like?

The magnetic power spectrum: $\langle \hat{B}_i(\vec{k}) \hat{B}_i^*(\vec{k}) \rangle = \langle |\hat{B}(\vec{k})|^2 \rangle$

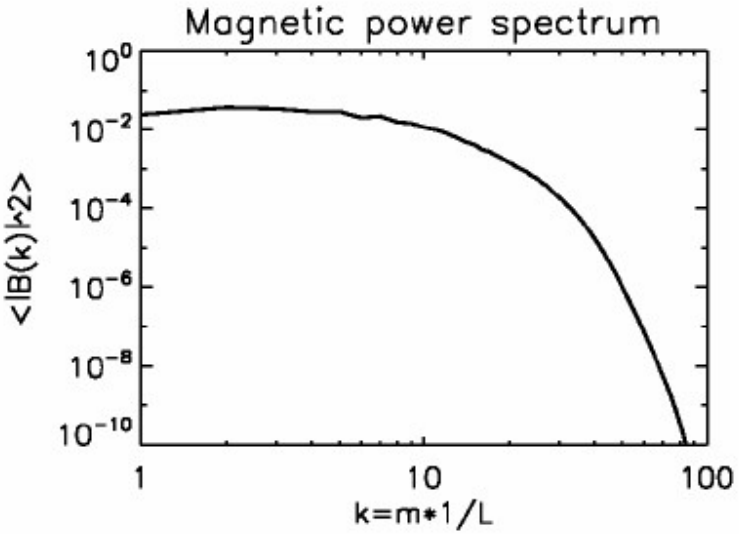

What does the fish look like?

The tension-force power spectrum: $\langle \hat{F}_i(\vec{k}) \hat{F}_i^*(\vec{k}) \rangle = \langle |\hat{F}(\vec{k})|^2 \rangle$

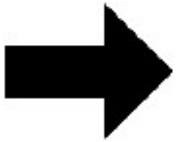

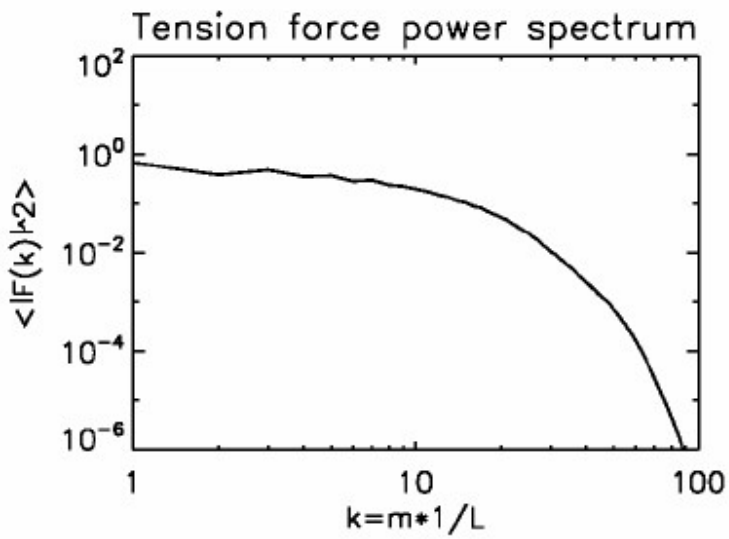

Tension force

$$\frac{1}{c}\vec{J}\times\vec{B} = -\nabla\frac{B^2}{8\pi} + \frac{1}{4\pi}\vec{B}\cdot\nabla\vec{B}$$

What does the tension force $\vec{F} = (1/4\pi)\left[(\vec{B}\nabla)\vec{B}\right]$ tell us?

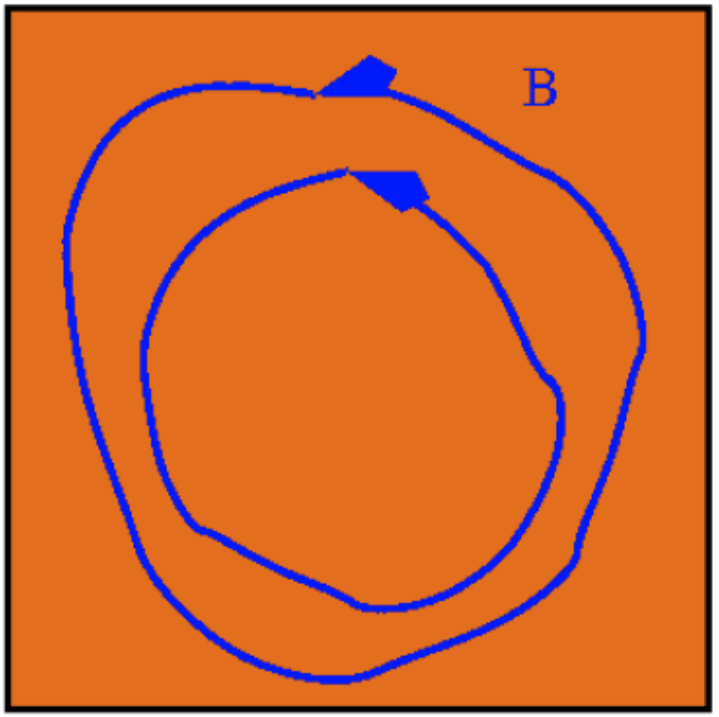

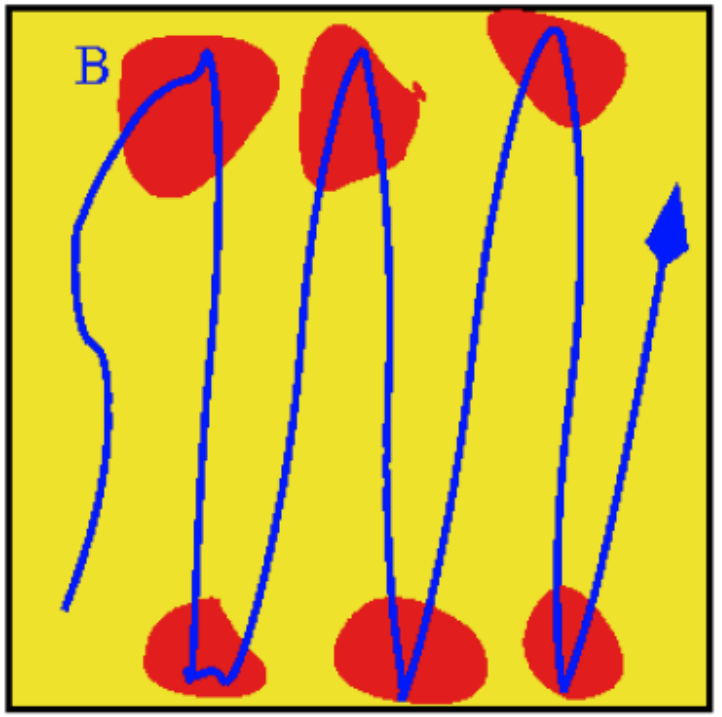

Tension force: $\vec{F} = (1/4\pi)\left[(\vec{B}\nabla)\vec{B}\right]$

MHD

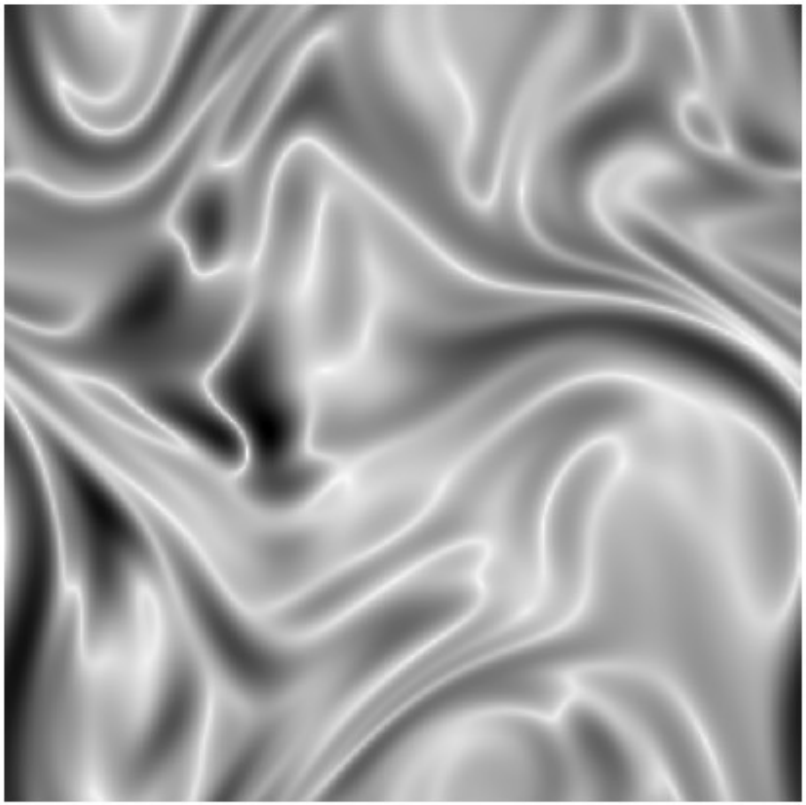

Gaussian

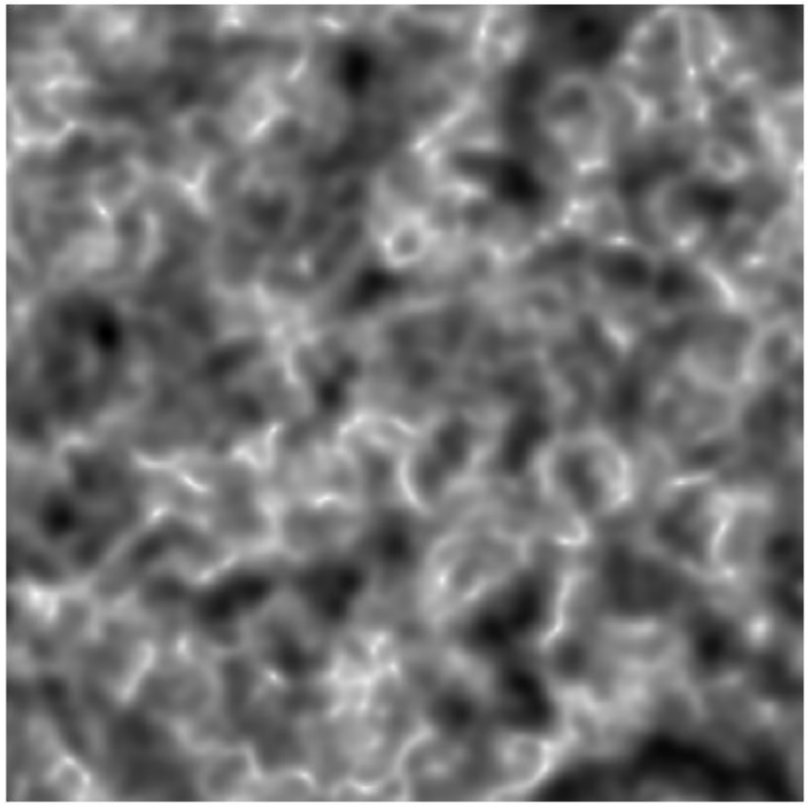

Tension force: $\vec{F} = (1/4\pi)\left[(\vec{B}\nabla)\vec{B}\right]$

MHD

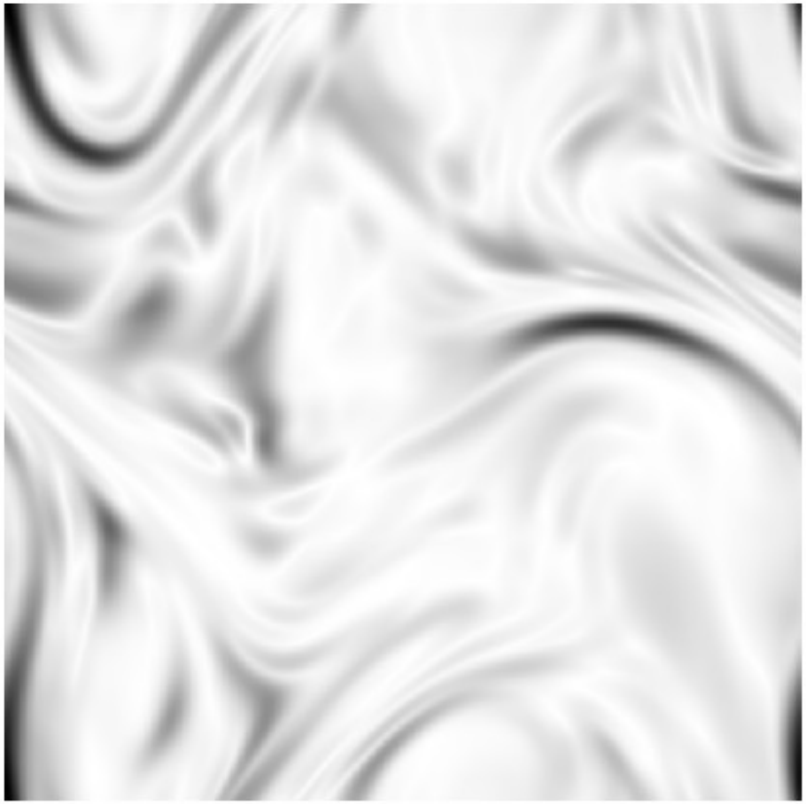

Gaussian

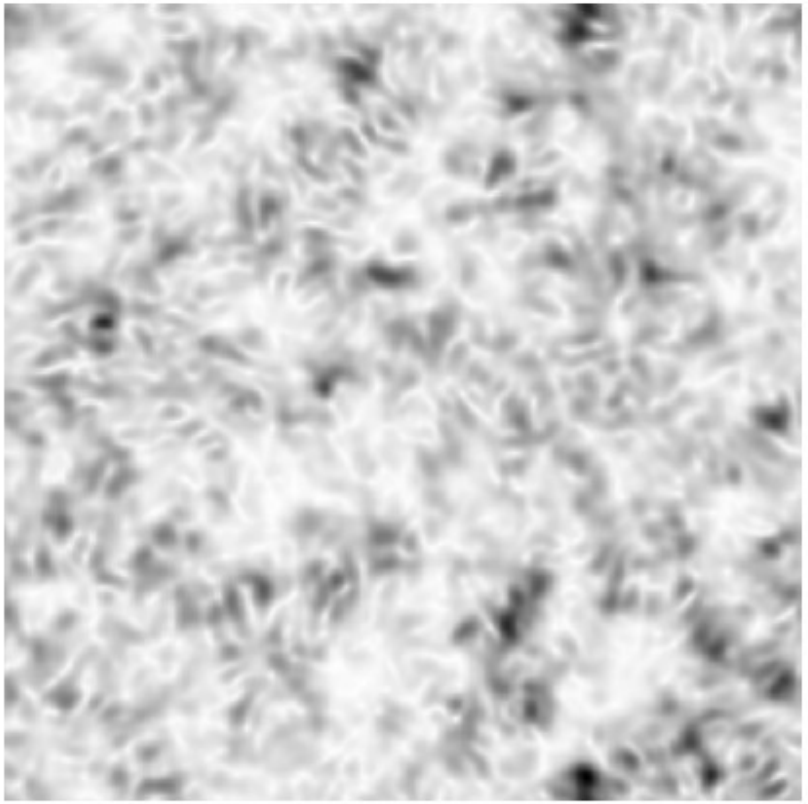

Tension force: $\vec{F} = (1/4\pi)\left[(\vec{B}\nabla)\vec{B}\right]$

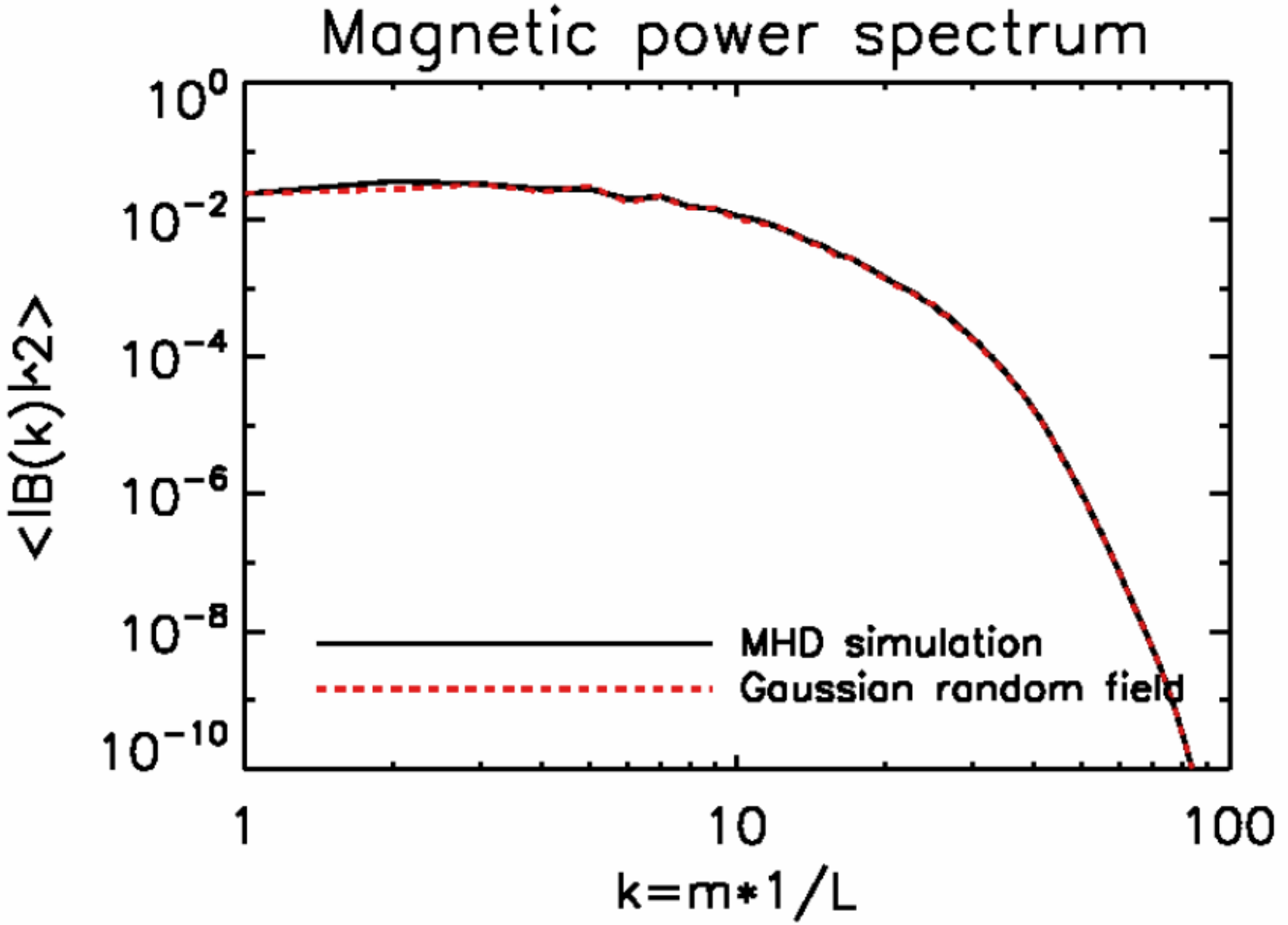

Tension force: $\vec{F} = (1/4\pi)\left[(\vec{B}\nabla)\vec{B}\right]$

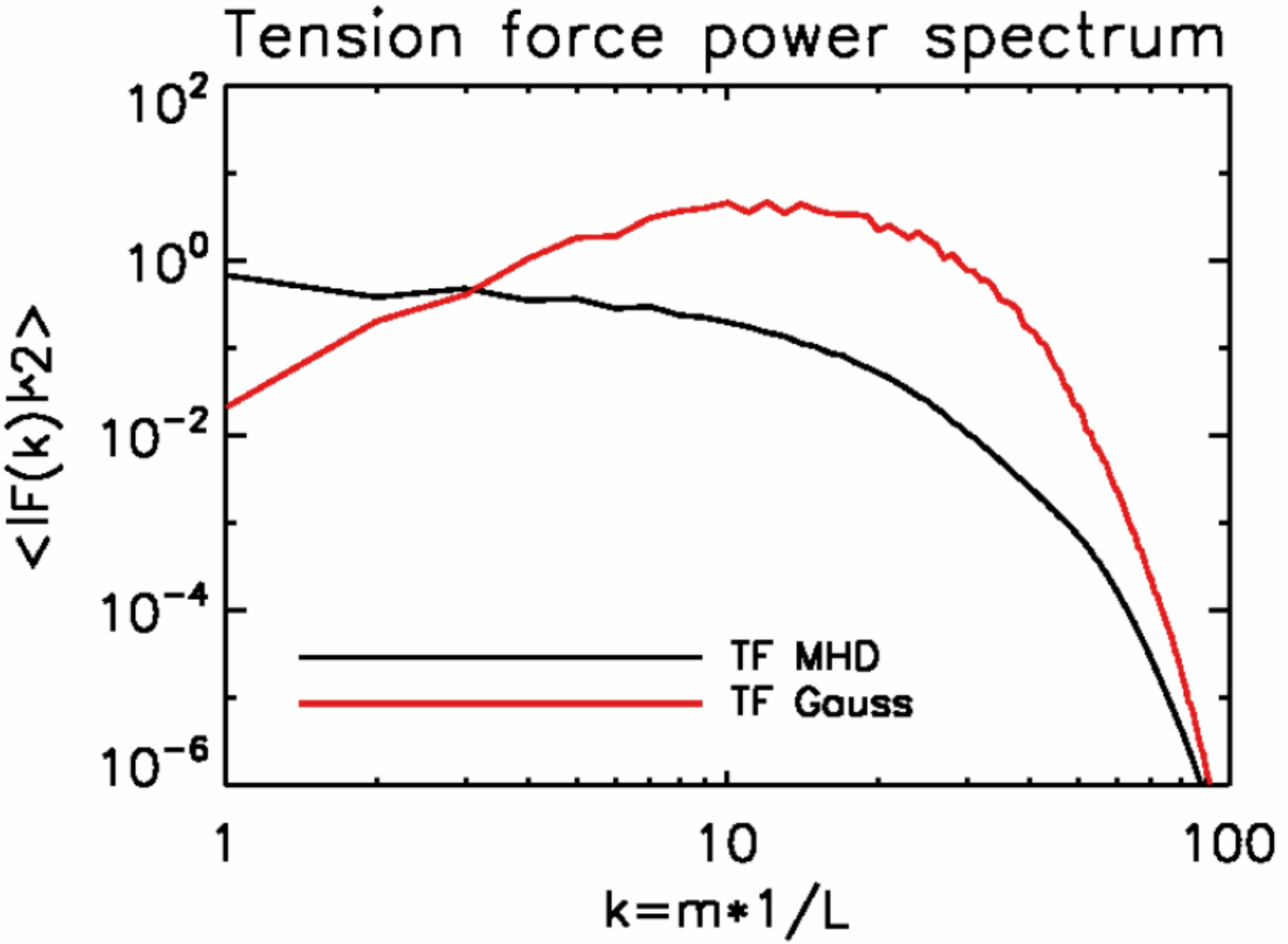

What are the conditions?

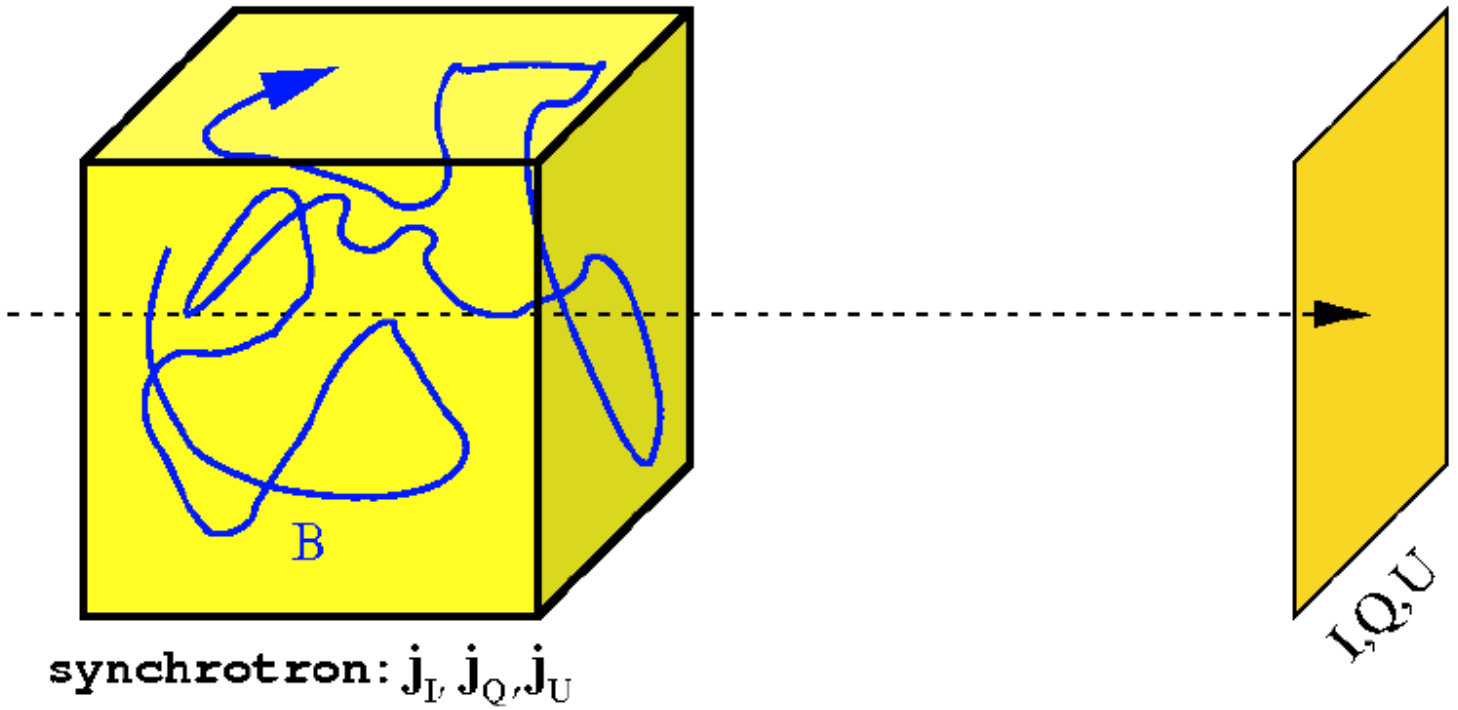

MHD

I, $p = 3$

Synthetic Gaussian

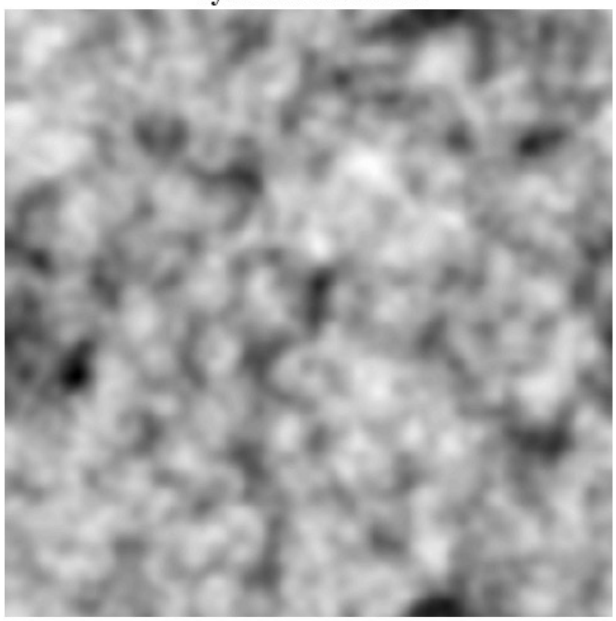

I, $p = 3$

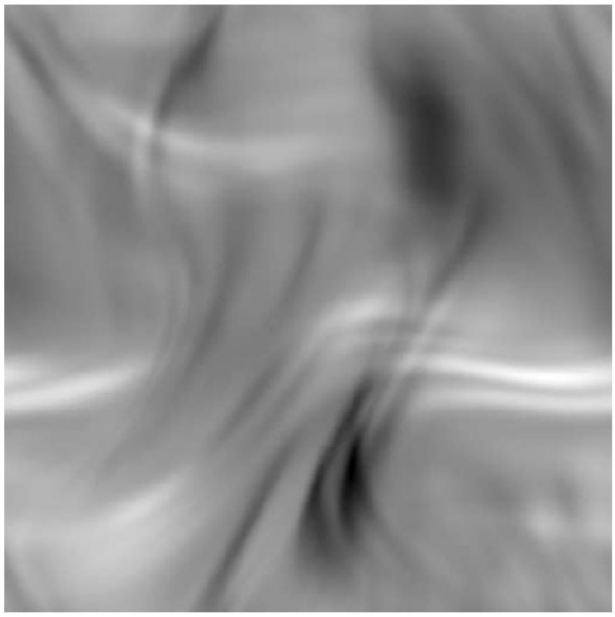

Q, $p = 3$

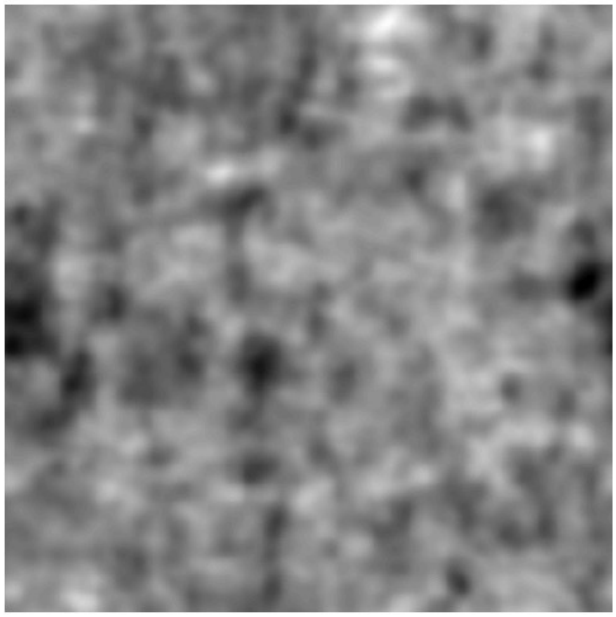

Q, $p = 3$

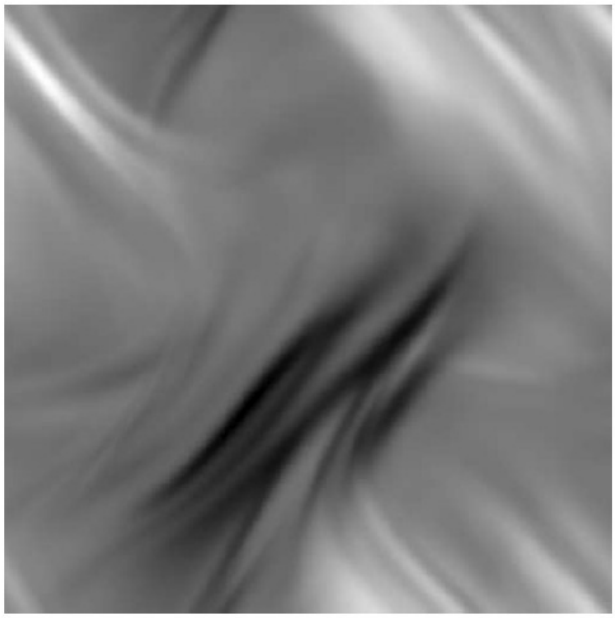

U, $p = 3$

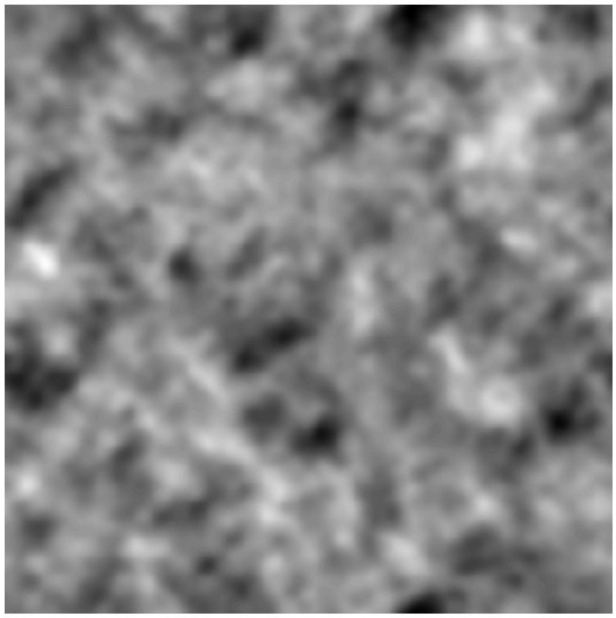

U, $p = 3$

What we measure:

Stokes parameters:

$$I(\vec{x}_\perp) \propto \int_{z_0}^{\infty} dz\, j_I(\vec{x}) \propto \int_{z_0}^{\infty} dz\, (\delta B_x^2(\vec{x}) + \delta B_y^2(\vec{x}))$$

$$Q(\vec{x}_\perp) \propto \int_{z_0}^{\infty} dz\, j_Q(\vec{x}) \propto \int_{z_0}^{\infty} dz\, (\delta B_x^2(\vec{x}) - \delta B_y^2(\vec{x}))$$

$$U(\vec{x}_\perp) \propto \int_{z_0}^{\infty} dz\, j_U(\vec{x}) \propto \int_{z_0}^{\infty} dz\, 2(\delta B_x(\vec{x}) \delta B_y(\vec{x}))$$

Isotropic case

The tension force power spectrum $\Phi_{ii}(k) = \langle \hat{F}_i^*(\vec{k}_\perp)\hat{F}_i(\vec{k}_\perp)\rangle$ for the isotropic case:

$$\begin{aligned}\Phi_{ii}(k) = \frac{V}{4L}\Big[& k_x^2\left(\hat{\Sigma}_{IQ}+\hat{\Sigma}_{IQ}^*+\hat{\Sigma}_{II}+\hat{\Sigma}_{QQ}+\hat{\Sigma}_{UU}\right) \\ & +2k_xk_y\left(\hat{\Sigma}_{IU}+\hat{\Sigma}_{IU}^*\right) \\ & +k_y^2\left(-\left(\hat{\Sigma}_{IQ}+\hat{\Sigma}_{IQ}^*\right)+\hat{\Sigma}_{II}+\hat{\Sigma}_{QQ}+\hat{\Sigma}_{UU}\right) \\ & \hat{\Sigma}_{UU}-\frac{2k_xk_y}{k_x^2-k_y^2}\hat{\Sigma}_{QU}\Big]\end{aligned}$$

Let's try it out!

MHD

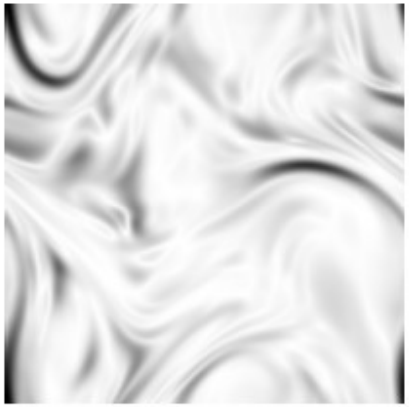

Gaussian

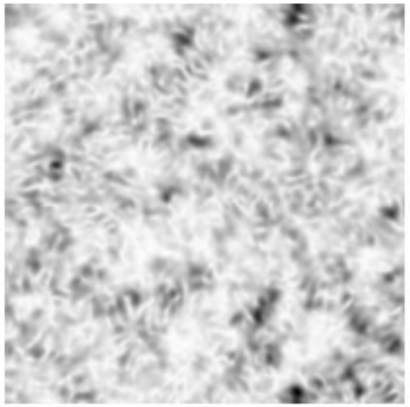

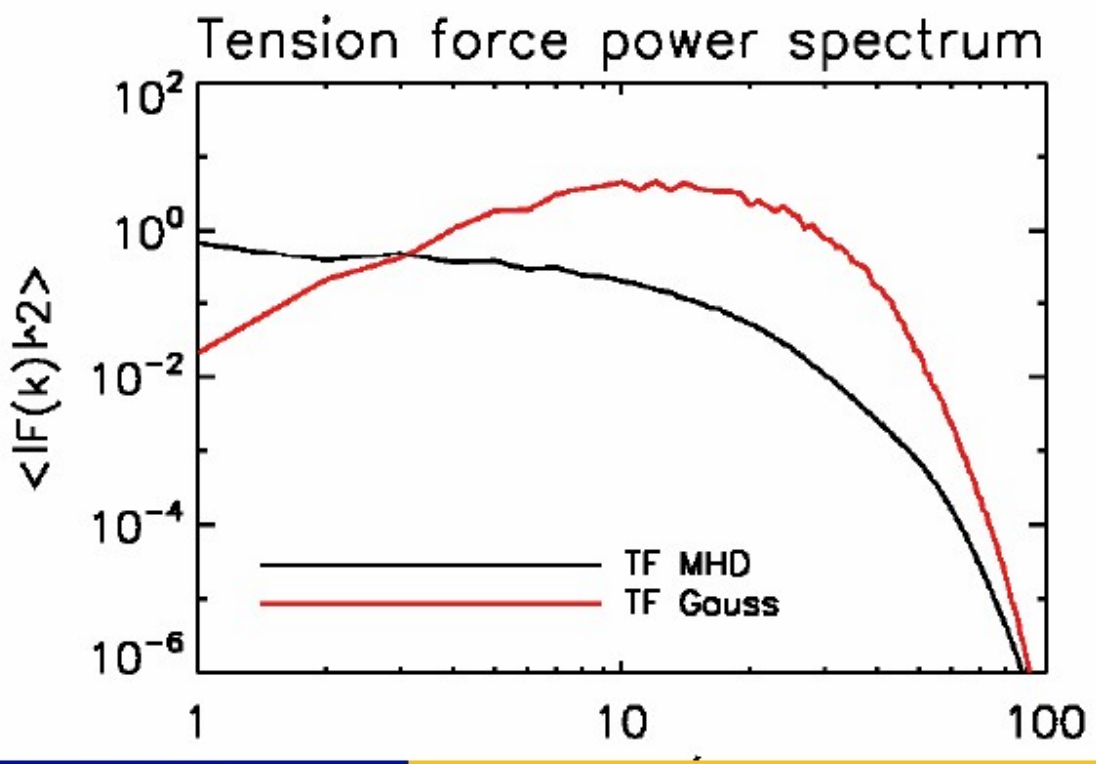

Let's try it out!

MHD

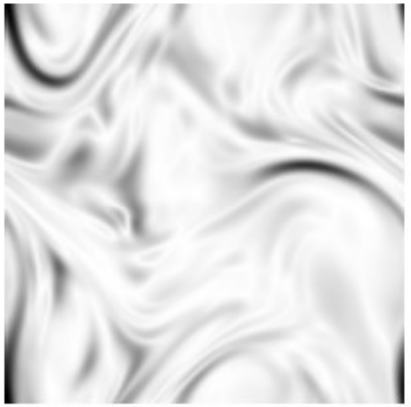

Gaussian

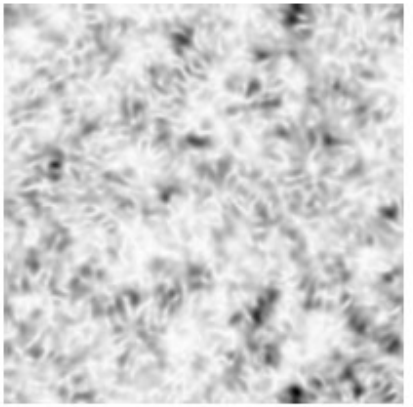

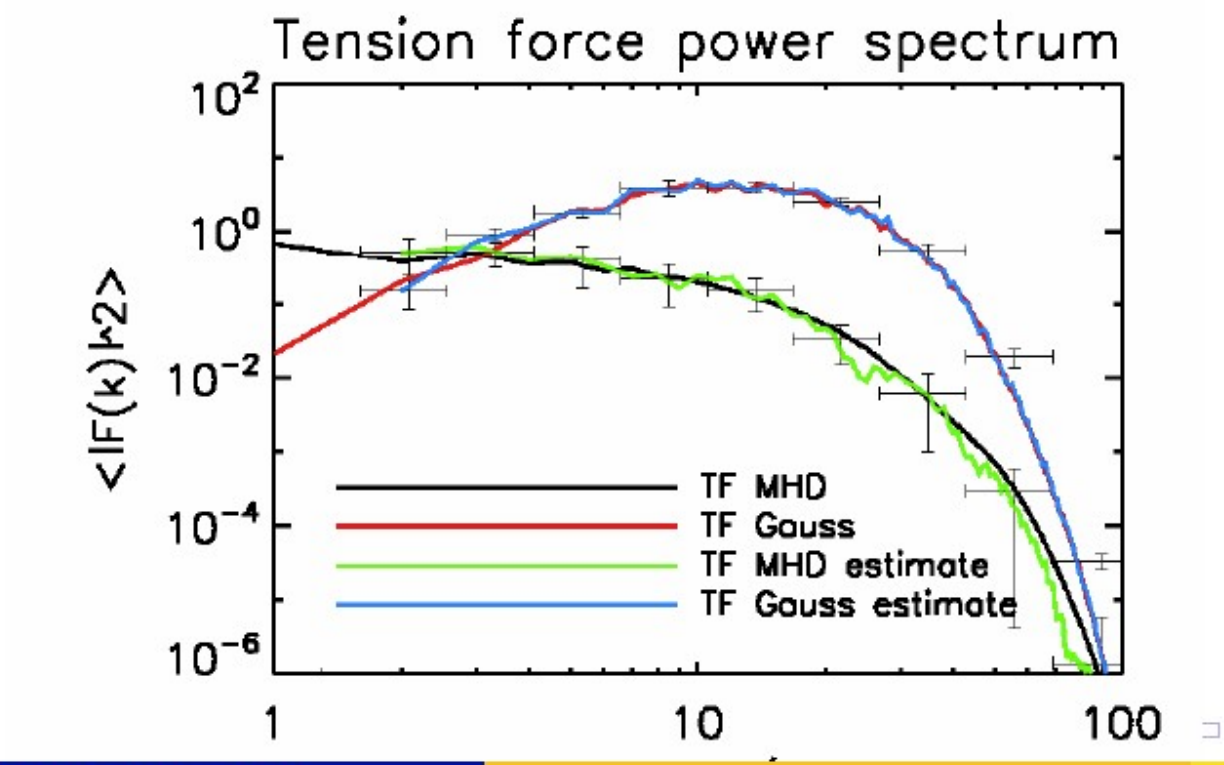

Outline:

Cluster radio emission
& magnetic turbulence

Faraday rotation
& magnetic spectrum inference

Stokes correlators
& tension forces

Faraday-Stokes correlations
& magnetic helicity

H. Junklewitz, N. Oppermann
(R. Stepanov)

Magnetic helicity

$$H = \int_V \mathbf{A} \cdot \mathbf{B} \; dx^3$$

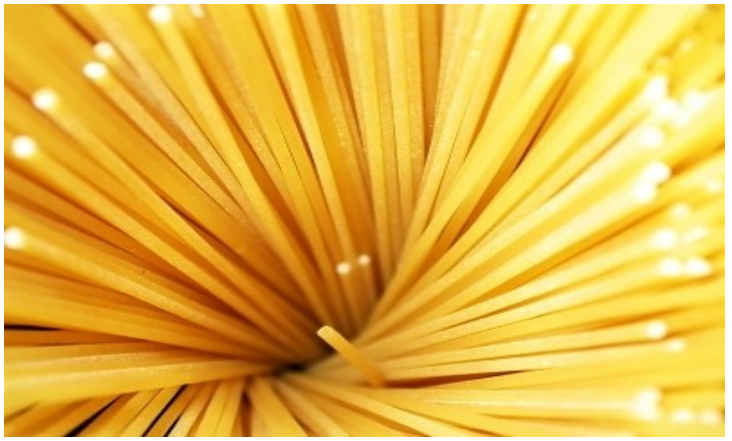

Observational situation

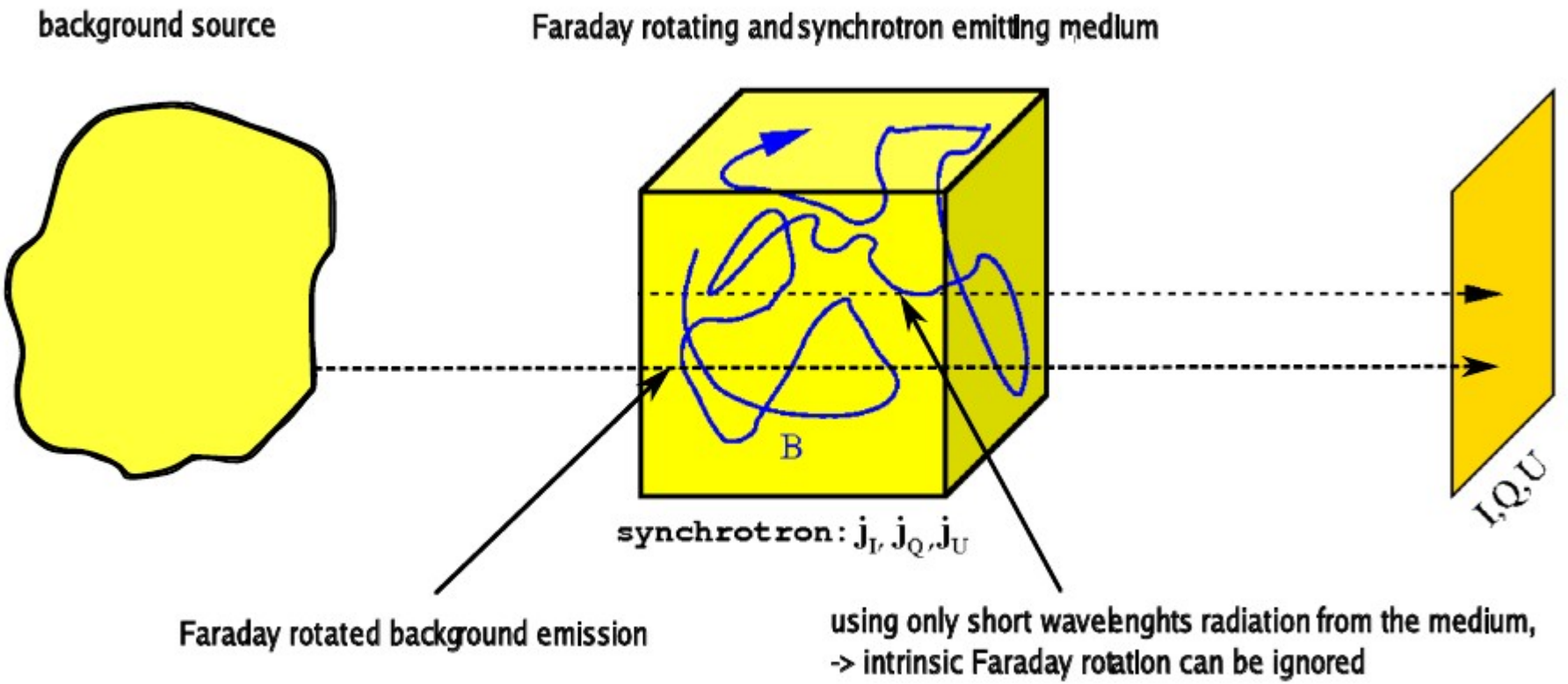

Total intensity $$I = \int dz \left(B_x^2 + B_y^2 \right)$$

Polarised intensity $$P = \int dz \left(B_x^2 - B_y^2 + 2iB_xB_y \right)$$

Faraday depth $$\phi = \int dz B_z$$

Helicity!

Aim: $$\langle P \rangle, \langle I\phi \rangle, \langle \phi\phi \rangle, \ldots, \langle I\phi\phi \rangle, \langle P\phi\phi \rangle$$

Spangler (1982,1983), Ensslin,Vogt (2003)
Eilek (1989a,b) , Waelkens et al. (2009)

Statistics I

- All calculations in Fourier space
- Gaussian magnetic field statistics
- Statistical homogeneity
- Constant electron density n
- Spectral index for the cosmic ray electron density p=3
- No intrinsic Faraday rotation, thus restriction to small wavelengths λ

Statistics II

$$\langle X(\mathbf{k}_\perp, \mathbf{k}'_\perp, \ldots)\rangle_B = \int \mathcal{D}B \; X(\mathbf{k}_\perp, \mathbf{k}'_\perp, \ldots)\; \mathcal{G}(\mathbf{B}, \mathbf{M})$$

e.g. $X(\mathbf{k}_\perp, \mathbf{k}'_\perp, \mathbf{k}''_\perp) = P(\mathbf{k}_\perp)\phi(\mathbf{k}'_\perp)\phi(\mathbf{k}''_\perp)$

$$\langle B_i B_j\rangle(\mathbf{k}) = \tilde{M}_{ij}(\mathbf{k}) = \tilde{M}_N(k)(\delta_{ij} - \frac{k_i k_j}{k^2}) - i\epsilon_{ijm}\tilde{H}(k)\frac{k_m}{k}$$

Statistics II

$$\langle B_i B_j \rangle(\mathbf{k}) = \tilde{M}_{ij}(\mathbf{k}) = \tilde{M}_N(k)(\delta_{ij} - \frac{k_i k_j}{k^2}) - i\epsilon_{ijm}\tilde{H}(k)\frac{k_m}{k}$$

Statistics III

$$\epsilon_B(k) = \frac{k^2 M_N(k)}{8\pi^3}$$

$$\epsilon_H(k) = -\frac{k^3 \hat{H}(k)}{\pi^2}$$

$$\epsilon_B(k) = \epsilon_0 \left(\frac{k}{k_0}\right)^{\beta} \left(1 + \left(\frac{k}{k_0}\right)^2\right)^{-\frac{(\alpha+\beta)}{2}}$$

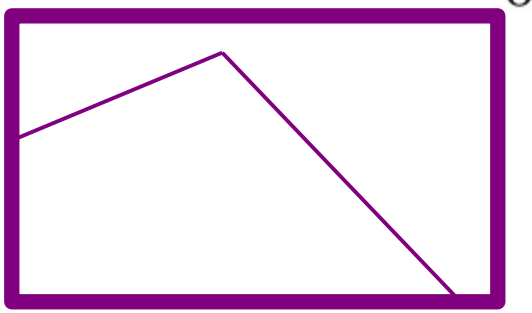

$$
\begin{aligned}
\langle I(\mathbf{k}_\perp)P(\mathbf{k}'_\perp)\rangle_{\mathbf{B}} &= \int dx^3 \int dx'^3 \exp\left[i(\mathbf{k}_\perp\mathbf{x}_\perp + \mathbf{k}'_\perp\mathbf{x}'_\perp)\right]\Big(\partial_1^2(\mathbf{x}) + \partial_2^2(\mathbf{x}\\
&\quad \Big(\partial_1^2(\mathbf{x}') - \partial_2^2(\mathbf{x}' + 2i\partial_1(\mathbf{x}')\partial_2(\mathbf{x}'))\Big)\exp\left[\frac{1}{2}\mathbf{J}^\dagger\mathbf{M}\mathbf{J}\right]|_{\mathbf{J}=0}\\
&= \int dx^3 \int dx'^3 \exp\left[i(\mathbf{k}_\perp\mathbf{x}_\perp + \mathbf{k}'_\perp\mathbf{x}'_\perp)\right]\Big[M_{11}^2(0) - M_{22}^2(0) + 2M_{11}^2(r) -\\
&\quad + 2M_{12}^2(r) - 2M_{21}^2(r) + 4iM_{21}(r)\Big(M_{11}(r) + M_{22}(r)\Big)\Big]\\
&= (2\pi)^2\delta^2(\mathbf{k}_\perp + \mathbf{k}'_\perp)L_z\int dr^3 \int \frac{dq^3}{(2\pi)^3}\int \frac{d\tilde{q}^3}{(2\pi)^3}\exp\left[i\mathbf{k}'_\perp\mathbf{r}_\perp\right]\exp\left[i\mathbf{r}(\mathbf{q}\right.\\
&\quad \Big[+ 2M_{11}(q)M_{11}(\tilde{q}) + 2M_{22}(q)M_{22}(\tilde{q}) + 2M_{12}(q)M_{12}(\tilde{q}) - 2M_{21}(q)\\
&\quad + 4iM_{21}(\tilde{q})\Big(M_{11}(q) + M_{22}(q)\Big)\Big]\\
&= (2\pi)^2\delta^2(\mathbf{k}_\perp + \mathbf{k}'_\perp)L_z\int \frac{dq^3}{(2\pi)^3}\int \frac{dq'^3}{(2\pi)^3}\ (2\pi)^3\delta^2(\mathbf{q}_\perp + \tilde{\mathbf{q}}_\perp + \mathbf{k}'_\perp)\\
&\quad \delta(q_z + \tilde{q}_z)\Big[2M_{11}(q)M_{11}(\tilde{q}) + 2M_{22}(q)M_{22}(\tilde{q}) + 2M_{12}(q)M_{12}(\tilde{q})\\
&\quad - 2M_{21}(q)M_{21}(\tilde{q}) + 4iM_{21}(\tilde{q})\Big(M_{11}(q) + M_{22}(q)\Big)\Big]\\
&= (2\pi)^2\delta^2(\mathbf{k}_\perp + \mathbf{k}'_\perp)L_z\int \frac{dq^3}{(2\pi)^3}\Big[2M_{11}(q)M_{11}(a)\\
&\quad + 2M_{22}(q)M_{22}(a) + 2M_{12}(q)M_{12}(a) - 2M_{21}(q)M_{21}(a)\\
&\quad + 4iM_{21}(a)\Big(M_{11}(q) + M_{22}(q)\Big)\Big]\\
&= (2\pi)^2\delta^2(\mathbf{k}_\perp + \mathbf{k}'_\perp)L_z\int \frac{dq^3}{(2\pi)^3}\Big[\frac{M_N(q)M_N(a)}{q^2a^2}\Big[2(q_2^2 + q_3^2)(a_2^2 + a_3^2)\\
&\quad + 2(q_1^2 + q_3^2)(a_1^2 + a_3^2) - 4i(q_1^2 + q_2^2 + 2q_3^2)a_2a_3\Big] + 2\frac{M_N(q)H(a)}{q^2a}\\
&\quad \Big[iq_1q_2a_3 - 2(q_1^2 + q_2^2 + 2q_3^2)a_3\Big] + \frac{M_N(a)H(q)}{q^2a}\Big[ia_1a_2q_3\Big]\Big]\\
&= (2\pi)^2\delta^2(\mathbf{k}_\perp + \mathbf{k}'_\perp)L_z\int \frac{dq^3}{(2\pi)^3}\Big[\frac{M_N(q)M_N(a)}{q^2a^2}\Big[2(q_2^2 + q_3^2)(a_2^2 + a_3^2)
\end{aligned}
$$

. . .

Results I

$$\langle I(\mathbf{k}_\perp)\rangle_{\mathbf{B}} = 2(2\pi)^2\delta(\mathbf{k}_\perp)L_z M_N(0)$$

$$\langle P(\mathbf{k}_\perp)\rangle_{\mathbf{B}} = 0$$

$$\langle \phi(\mathbf{k}_\perp)\phi(\mathbf{k}'_\perp)\rangle_{\mathbf{B}} = (2\pi)^2\delta^2(\mathbf{k}_\perp + \mathbf{k}'_\perp)L_z\tilde{M}_{33}(\mathbf{k}'_\perp, 0)$$

$$\langle I(\mathbf{k}_\perp)I(\mathbf{k}'_\perp)\rangle_{\mathbf{B}} = (2\pi)^2\delta^2(\mathbf{k}_\perp + \mathbf{k}'_\perp)L_z \int \frac{dq^3}{(2\pi)^3}\Big(2\big(\tilde{M}_{11}(\mathbf{q})\tilde{M}_{11}(\mathbf{a}) + \tilde{M}_{22}(\mathbf{q})\tilde{M}_{22}(\mathbf{a})\big) + 4\tilde{M}_{21,\mathrm{isym}}(\mathbf{q})\tilde{M}_{21,\mathrm{isym}}(\mathbf{a})\Big)$$

$$\langle P(\mathbf{k}_\perp)\overline{P}(\mathbf{k}'_\perp)\rangle_{\mathbf{B}} = \frac{8}{2\pi}\delta^2(\mathbf{k}_\perp - \mathbf{k}'_\perp)L_z \int dq^3\big(\tilde{M}_{11}(\mathbf{q})\tilde{M}_{11}(\mathbf{a}) + \tilde{M}_{22}(\mathbf{q})\tilde{M}_{22}(\mathbf{a}) + \tilde{M}_{22}(\mathbf{q})\tilde{M}_{11}(\mathbf{a}) + \tilde{M}_{22}(\mathbf{a})\tilde{M}_{11}(\mathbf{q})\big)$$

$$\mathbf{a} = (-\mathbf{q}_\perp - \mathbf{k}'_\perp, -q_z)$$

Results II

$$\langle I(\mathbf{k}_\perp)P(\mathbf{k}'_\perp)\rangle_{\mathbf{B}} = (2\pi)^2\delta^2(\mathbf{k}_\perp+\mathbf{k}'_\perp)L_z\int\frac{dq^3}{(2\pi)^3}\Big[2\tilde{M}_{11}(q)\tilde{M}_{11}(a) + 2\tilde{M}_{22}(q)\tilde{M}_{22}(a) + 2\tilde{M}_{12}(q)\tilde{M}_{12}(a) - 2\tilde{M}_{21}(q)\tilde{M}_{21}(a) + 4i\tilde{M}_{21}(a)\Big(\tilde{M}_{11}(q)+\tilde{M}_{22}(q)\Big)\Big]$$

$$\langle\phi(\mathbf{k}_\perp)\phi(\mathbf{k}'_\perp)\phi(\mathbf{k}''_\perp)\phi(\mathbf{k}'''_\perp)\rangle_{\mathbf{B}} = (2\pi)^4\Big[\delta^2(\mathbf{k}''_\perp+\mathbf{k}'''_\perp)\delta^2(\mathbf{k}_\perp+\mathbf{k}'_\perp)\tilde{M}_N(\mathbf{k}'''_\perp,0)\tilde{M}_N(\mathbf{k}',0) + \delta^2(\mathbf{k}'''_\perp)+\mathbf{k}'_\perp)\delta^2(\mathbf{k}''_\perp+\mathbf{k}_\perp)\tilde{M}_N(\mathbf{k}'''_\perp,0)\tilde{M}_N(\mathbf{k}''_\perp) + \delta^2(\mathbf{k}''_\perp+\mathbf{k}'_\perp)\delta^2(\mathbf{k}'''_\perp+\mathbf{k}_\perp)\tilde{M}_N(\mathbf{k}''',0)\tilde{M}_N(\mathbf{k}'_\perp,0)\Big]$$

$$\mathbf{a} = (-\mathbf{q}_\perp - \mathbf{k}'_\perp, -q_z)$$

Results III

$$\langle I(\mathbf{k}_\perp)\phi(\mathbf{k}'_\perp)\phi(\mathbf{k}''_\perp)\rangle_{\mathbf{B}} = L^2(2\pi)^4\delta^2(\mathbf{k}'_\perp+\mathbf{k}''_\perp)\delta^2(\mathbf{k}_\perp)\tilde{M}_N(u)2M_N(0)$$
$$- 2L_z(2\pi)^2\delta^2(\mathbf{k}_\perp+\mathbf{k}'_\perp+\mathbf{k}''_\perp)\tilde{H}(k''_\perp)\tilde{H}(k'_\perp)/k''_\perp k'_\perp$$
$$\left(k''_1k'_1+k''_2k'_2\right)$$

$$\langle P(\mathbf{k}_\perp)\phi(\mathbf{k}'_\perp)\phi(\mathbf{k}''_\perp)\rangle_{\mathbf{B}} = 2L_z(2\pi)^2\delta^2(\mathbf{k}_\perp+\mathbf{k}'_\perp+\mathbf{k}''_\perp)$$
$$\tilde{H}(k''_\perp)\tilde{H}(k'_\perp)/k''_\perp k'_\perp\ \Big(\left(k''_1k'_1-k''_2k'_2\right)$$
$$+\,i\left(k''_1k'_2+k''_2k'_1\right)\Big)$$

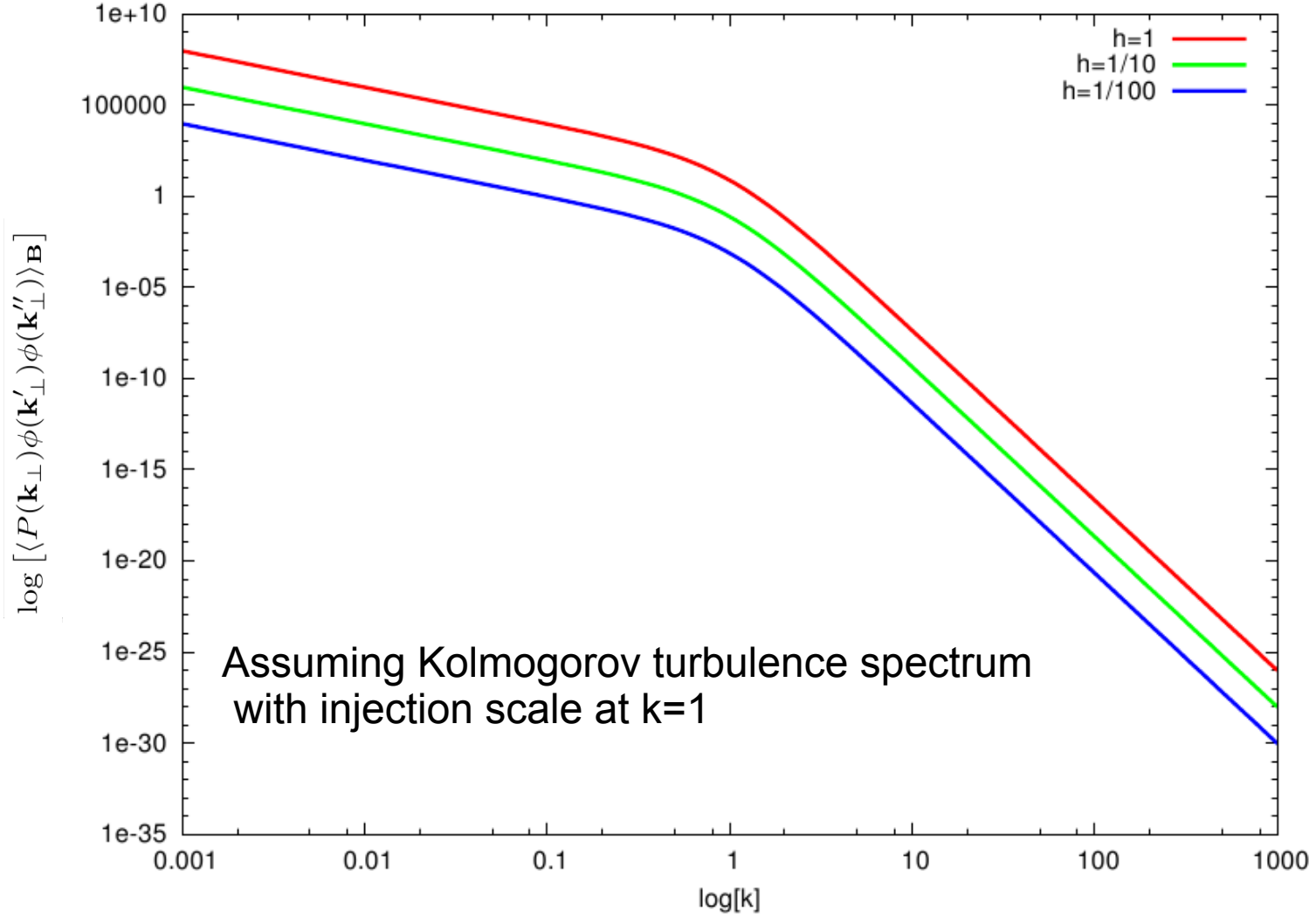

$$(\mathrm{c})\ \alpha = 5/3$$

$$\delta^2(\mathbf{k}_\perp + \mathbf{k}'_\perp + \mathbf{k}''_\perp) \longrightarrow \mathbf{k}_\perp = 0$$

$$\mathbf{k} = k\ \mathbf{e}_y$$

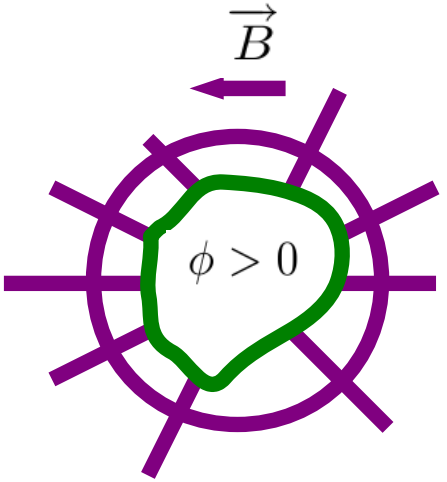
$\vec{B}$
$\phi > 0$

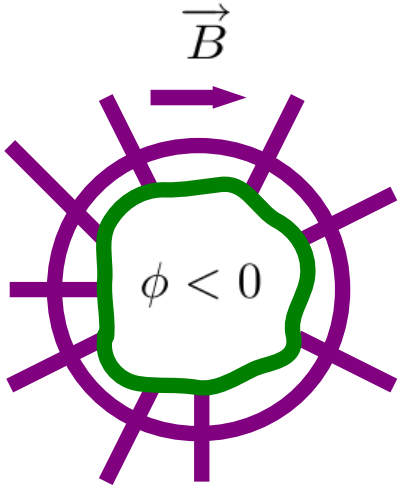
$\vec{B}$
$\phi < 0$

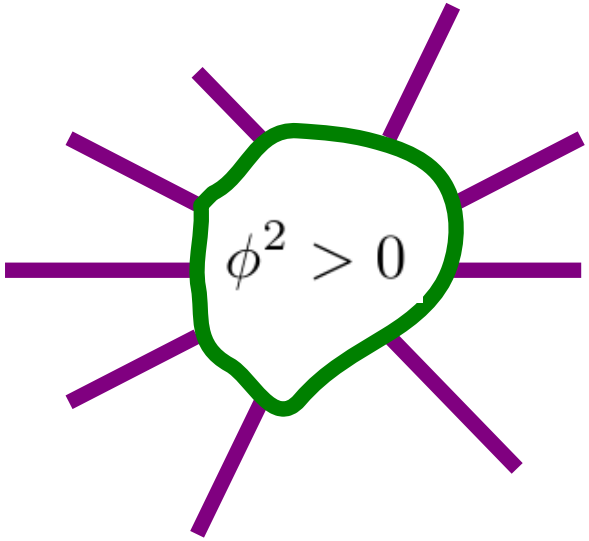
$\phi^2 > 0$

The Acidtest

- First numerical test of our method
- Easily applicable to real data to test for helicity

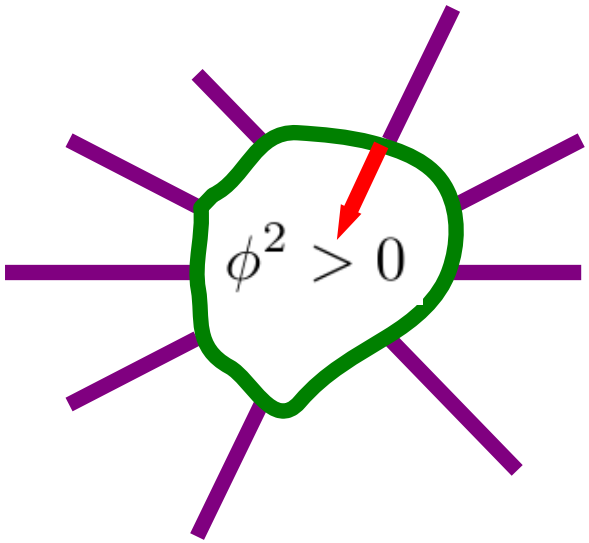

Gradient of RM^2

$$\mathbf{G} = |\overrightarrow{G}| \exp[2i\alpha] \quad \text{with} \quad \alpha = \tan^{-1} \frac{\overrightarrow{G}_y}{\overrightarrow{G}_x}$$

$$\mathbf{P} = |\overrightarrow{P}| \exp[2i\chi]$$

$$\left\langle (\mathbf{GP}^*) \right\rangle_{\text{Hel}} > 0 \quad \text{and} \quad \left\langle (\mathbf{GP}^*) \right\rangle_{\text{Nohel}} = 0$$

Intensity without helicity

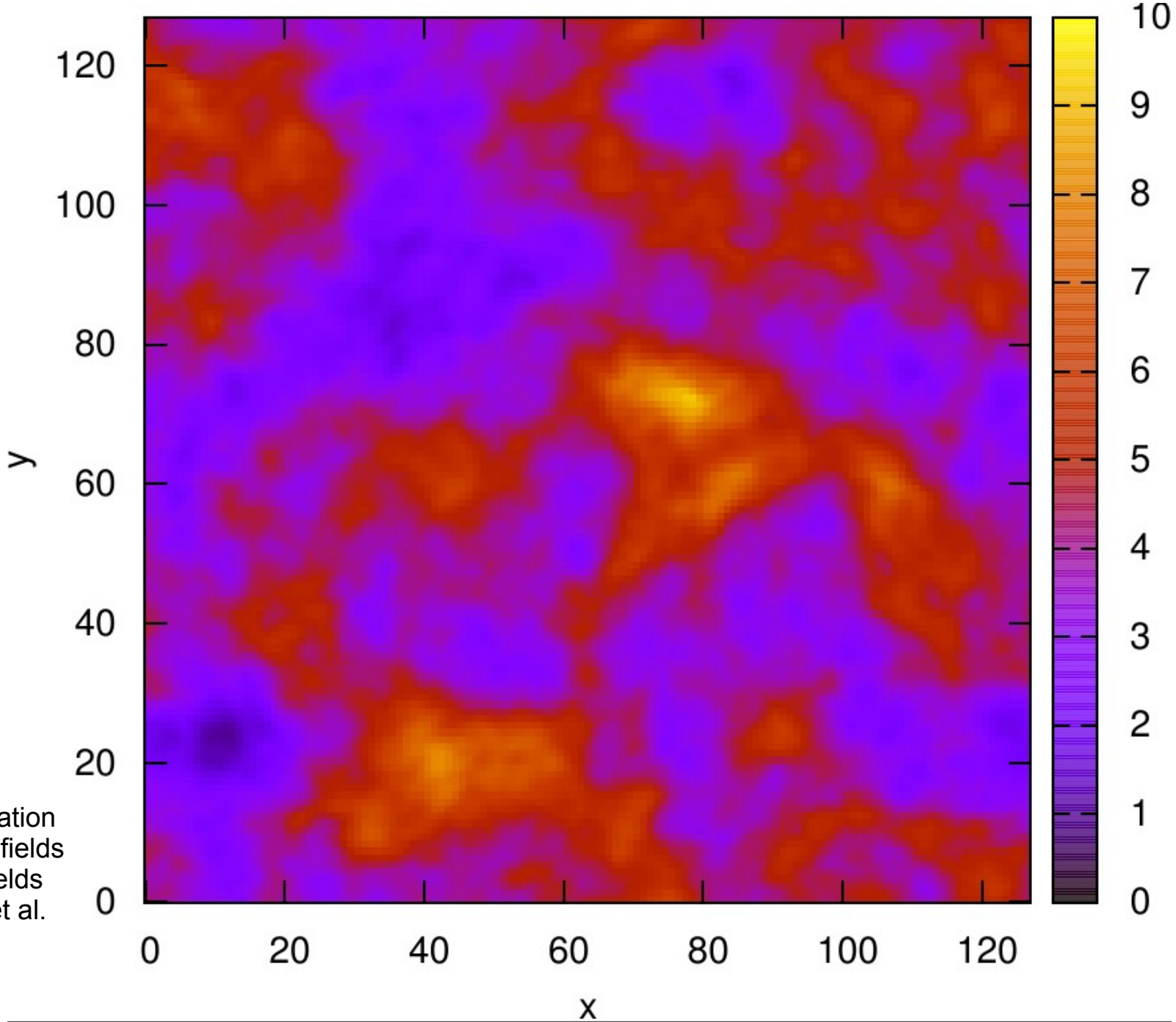

Based on a 128^3 simulation of magnetic fields using GarFields (Waelkens et al. 2009)

Faraday Rotation without helicity

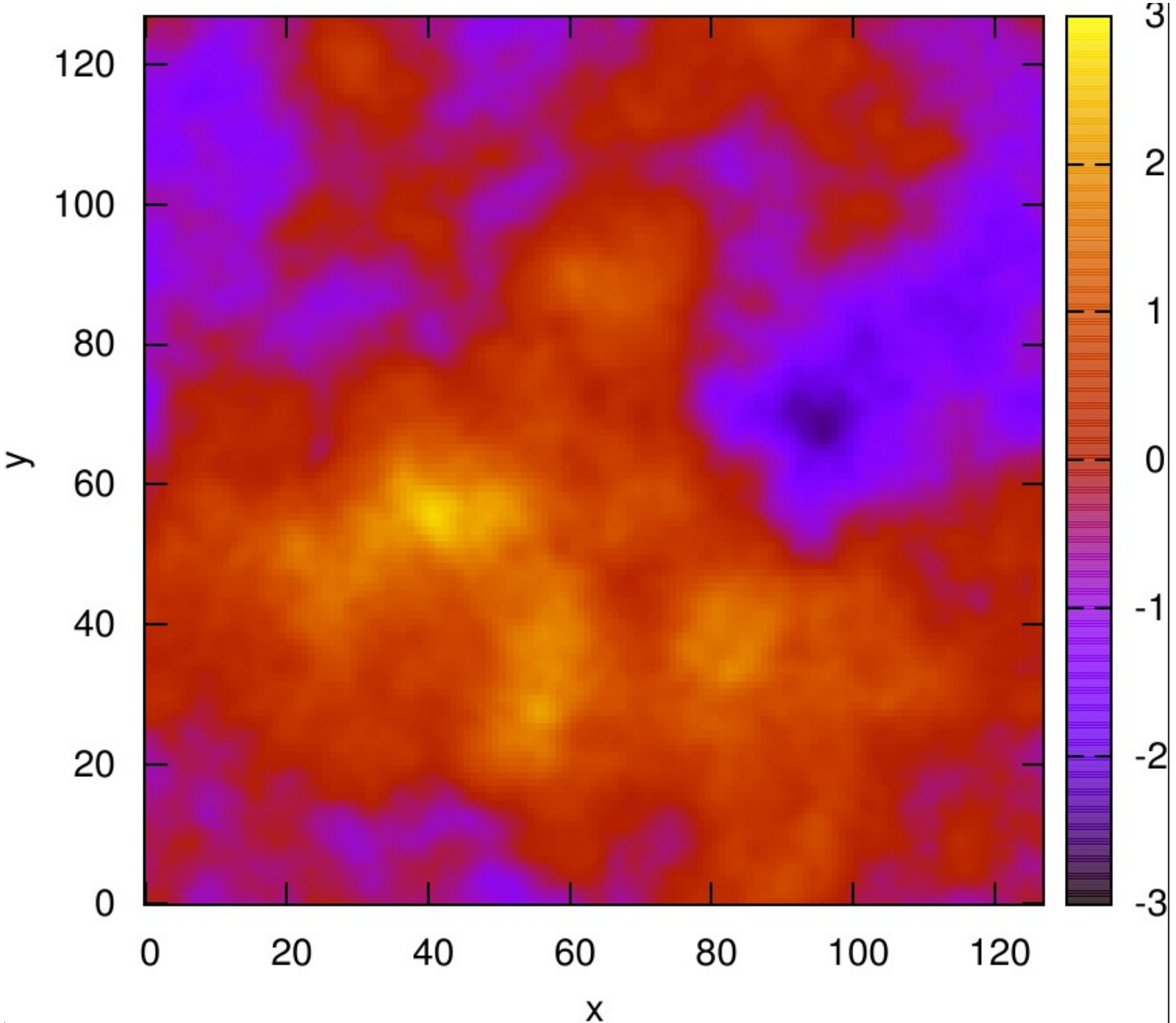

Absolute value of polarised intensity without helicity

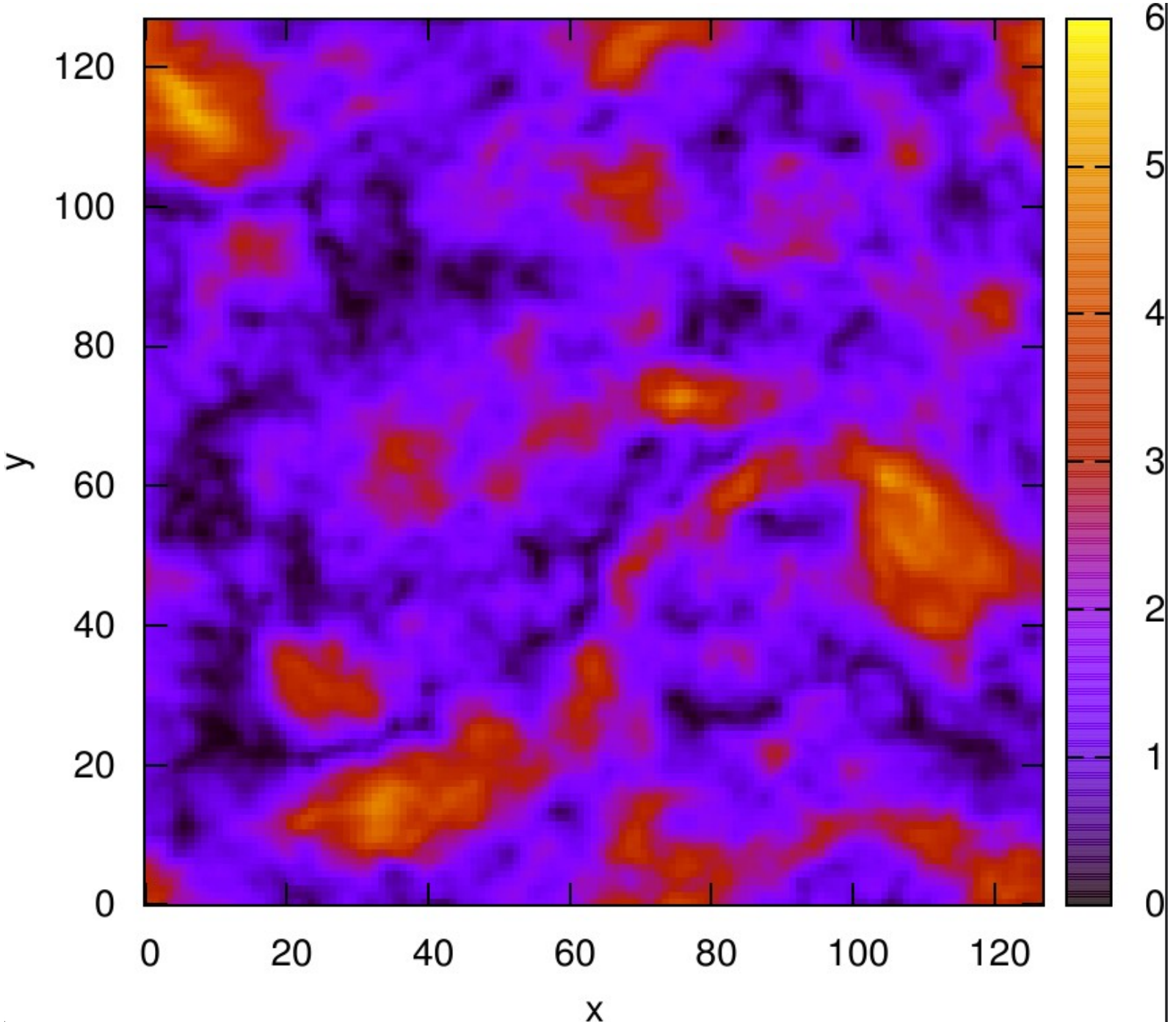

Acid-test: Real part without helicity

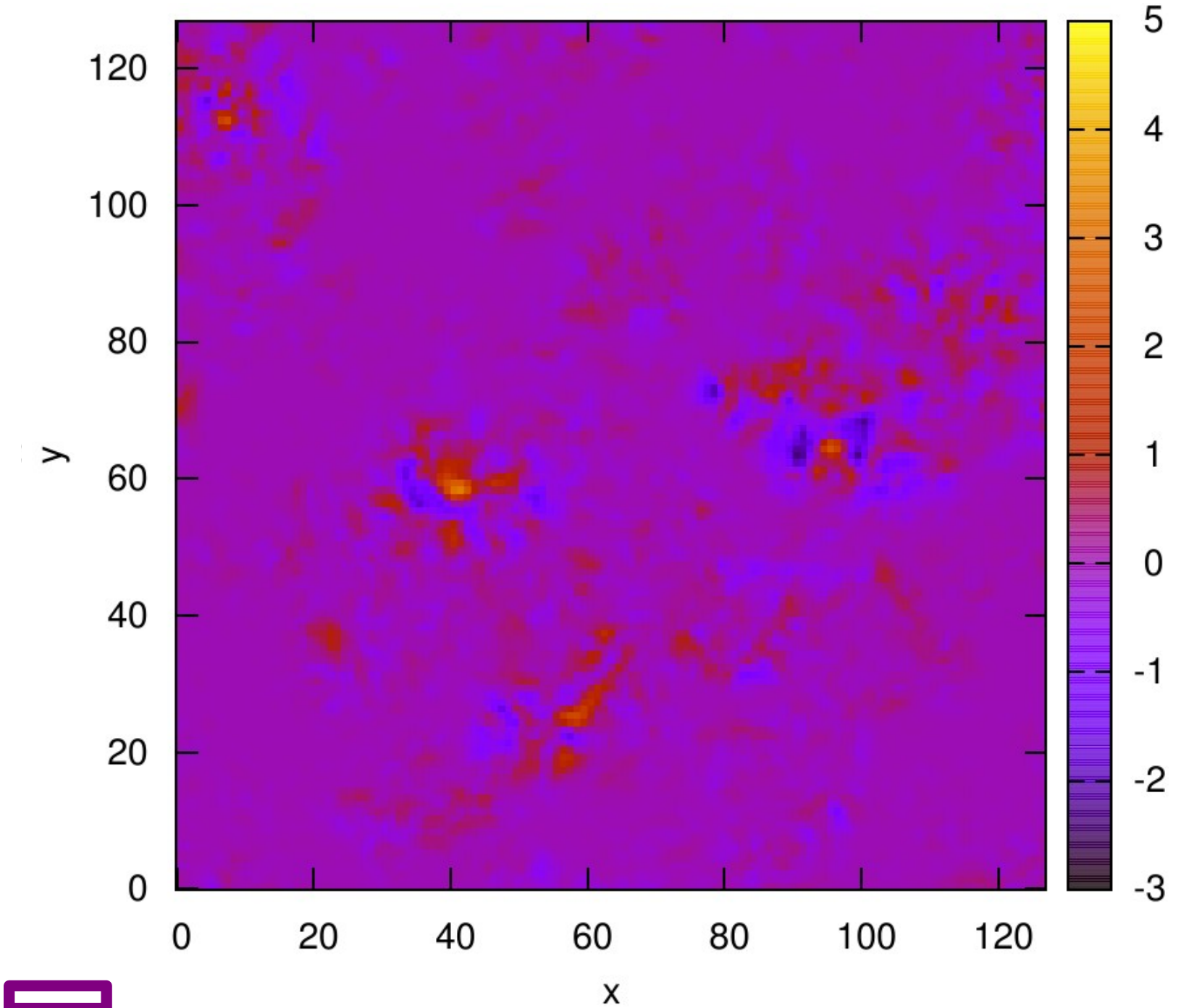

Intensity with helicity

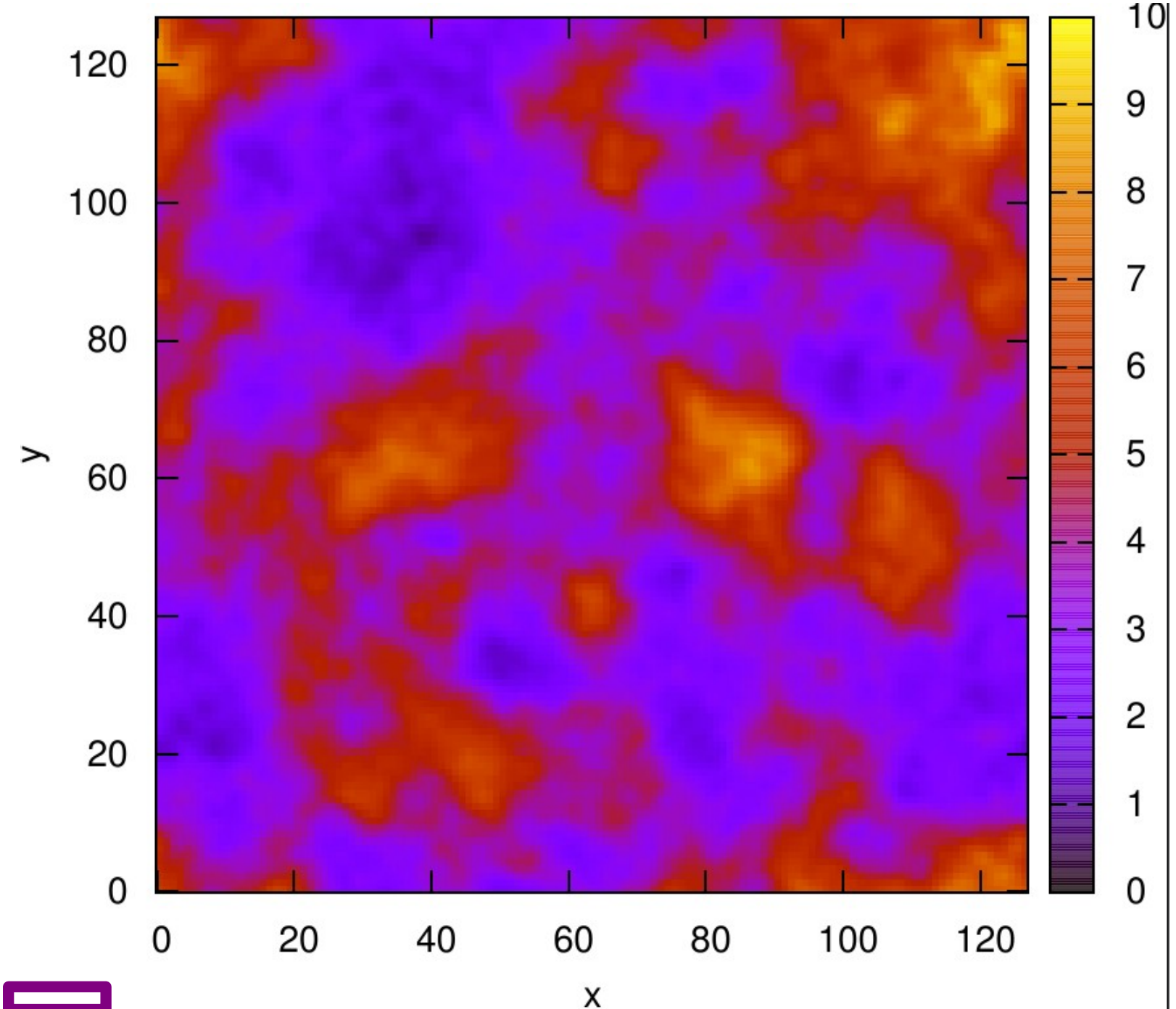

Faraday Rotation with helicity

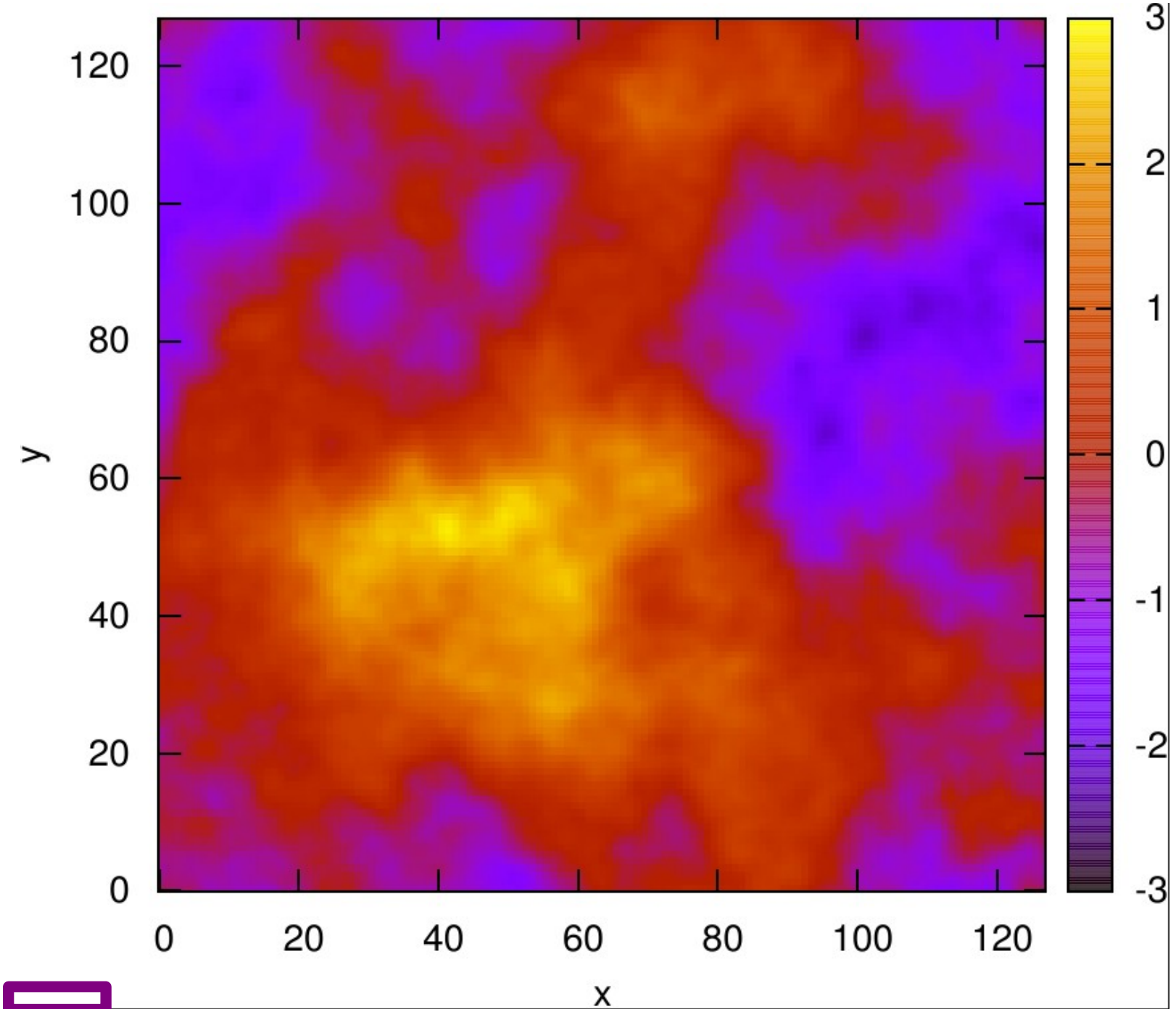

Absolute value of polarised intensity with helicity

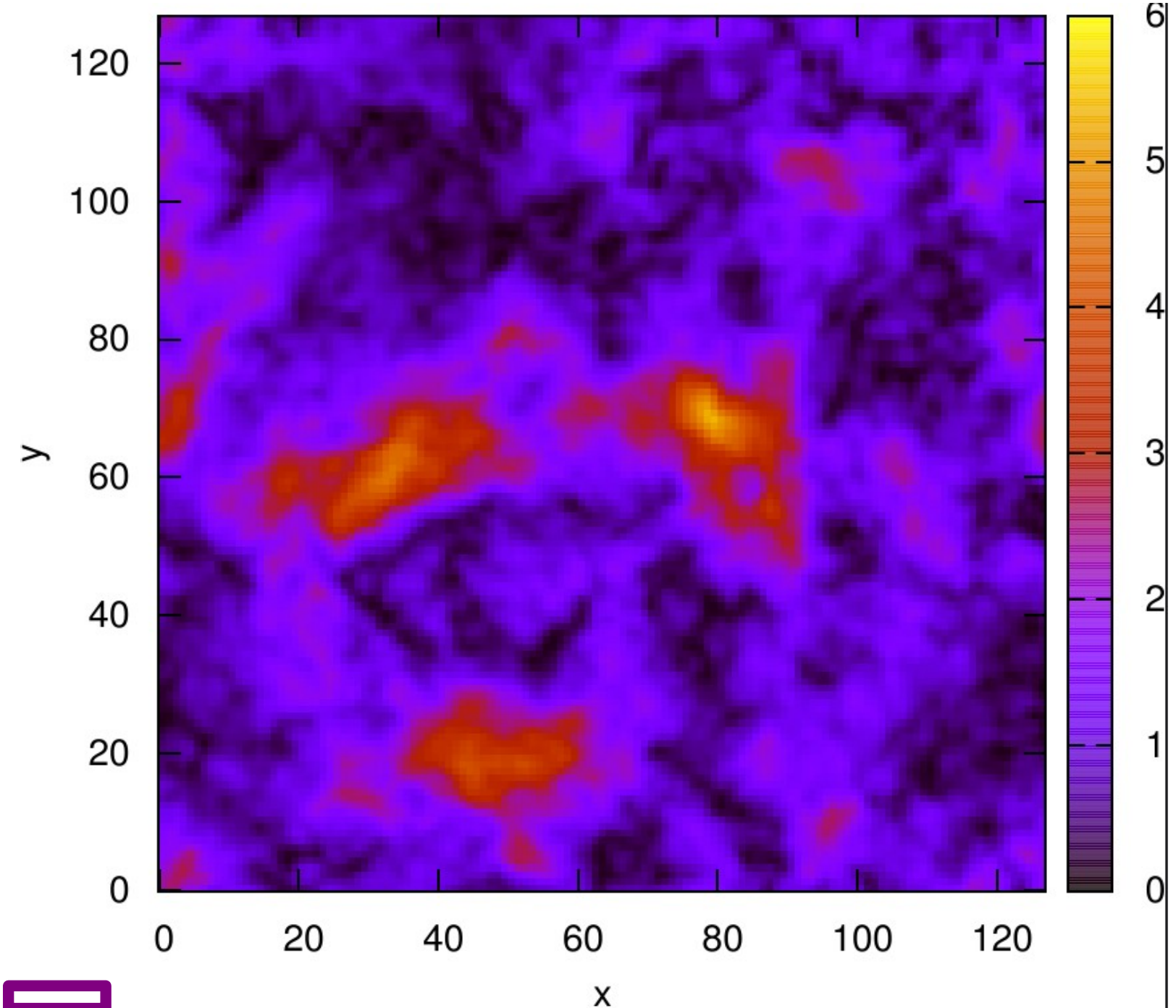

Real part with helicity

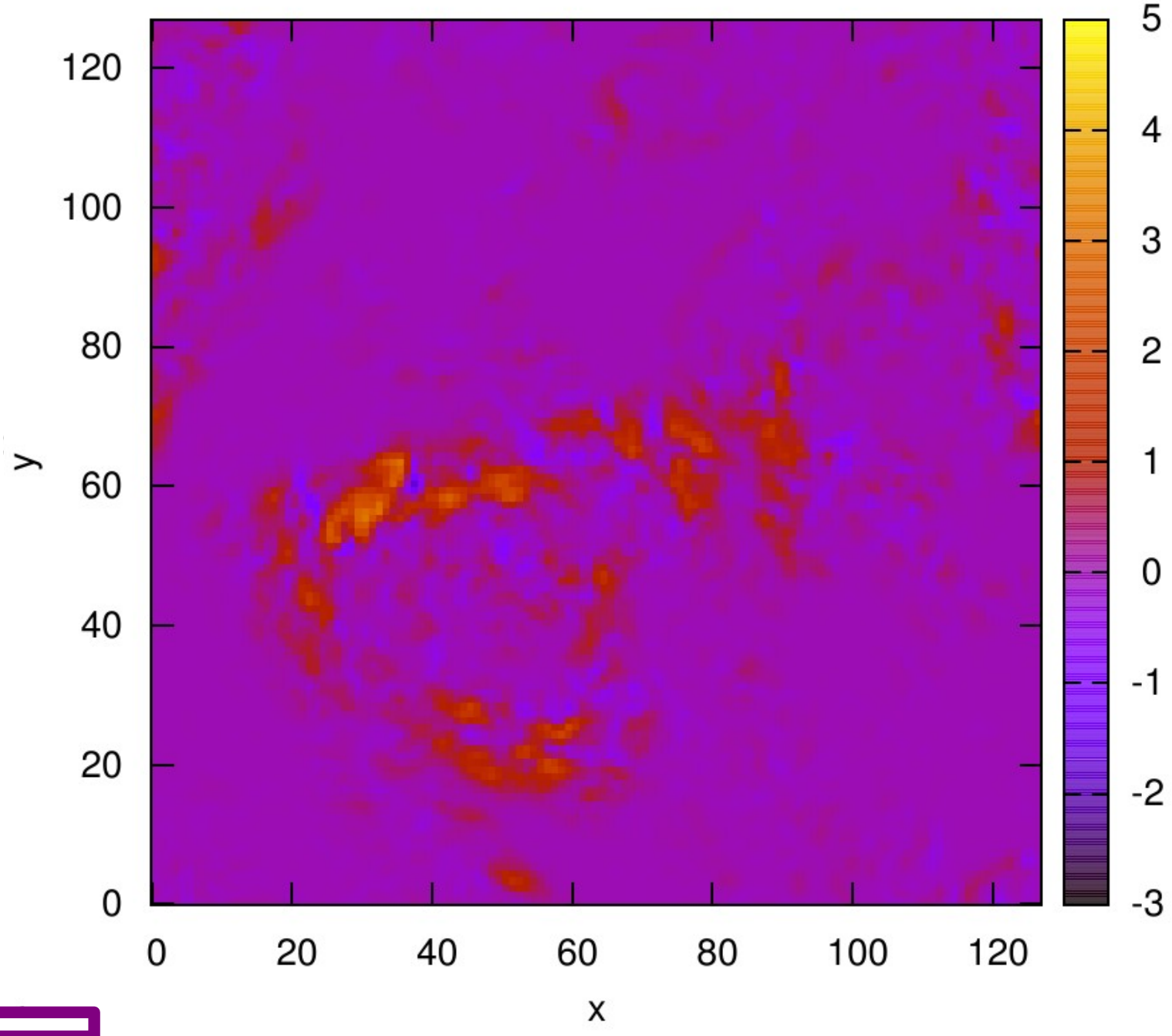

Real part with helicity

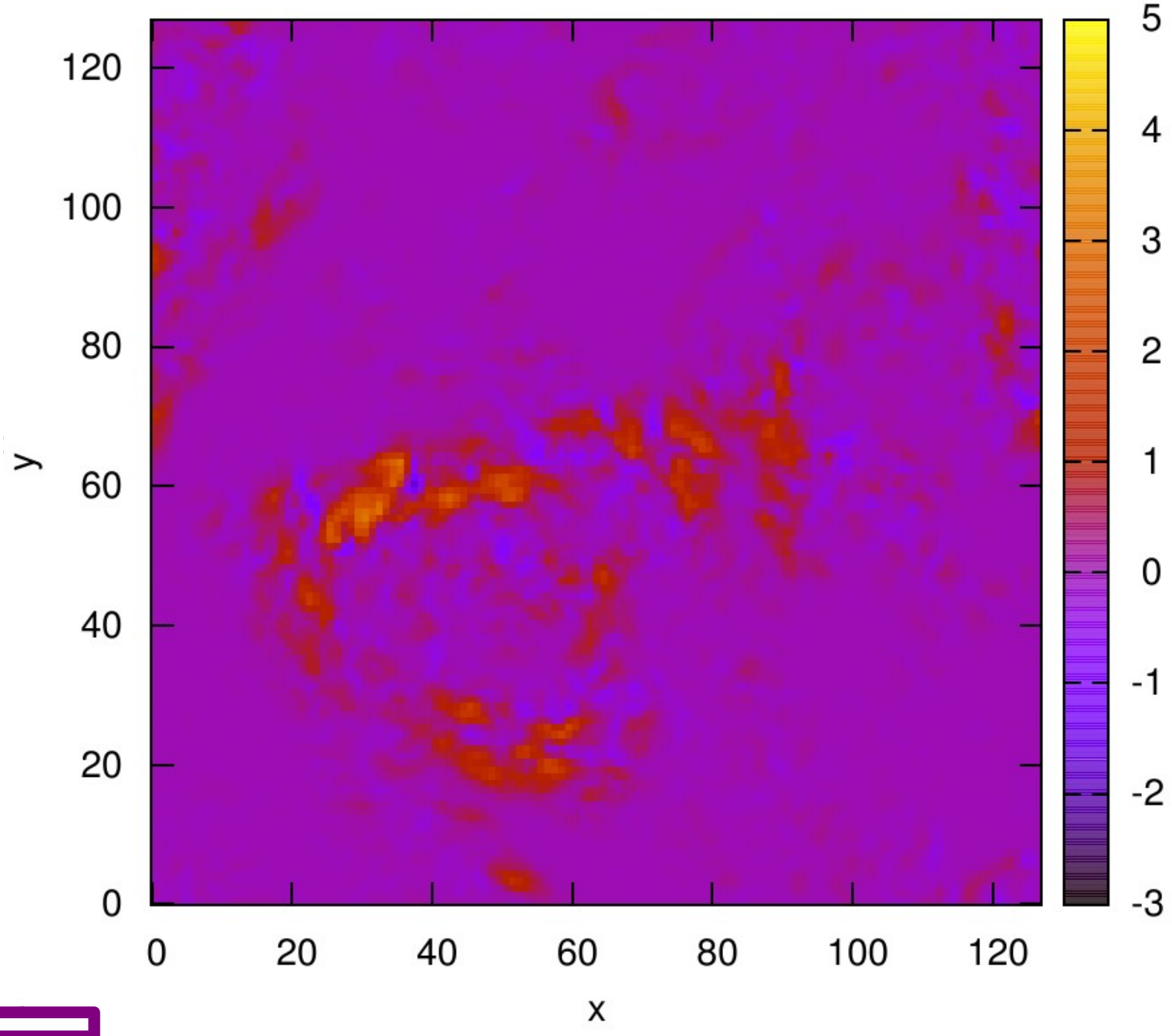

Real part without helicity

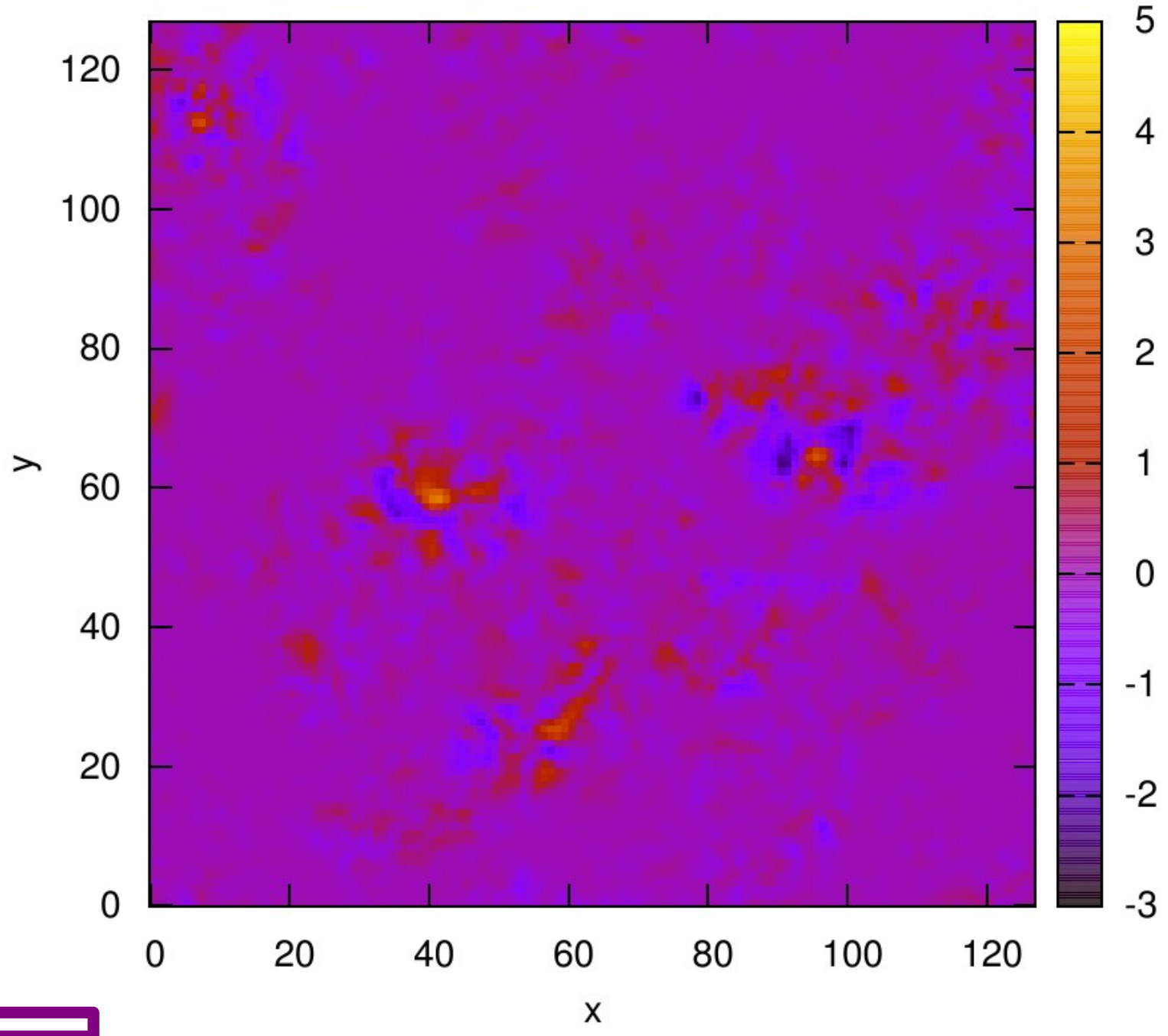

Results of the Acidtest with simulated data

- In total 18 samples to improve the statistics
- All samples show the same trend in accordance with our predictions
- Total mean with helicity: m= 0.078
- Total mean without helicity: m= -0.003

Conclusions:

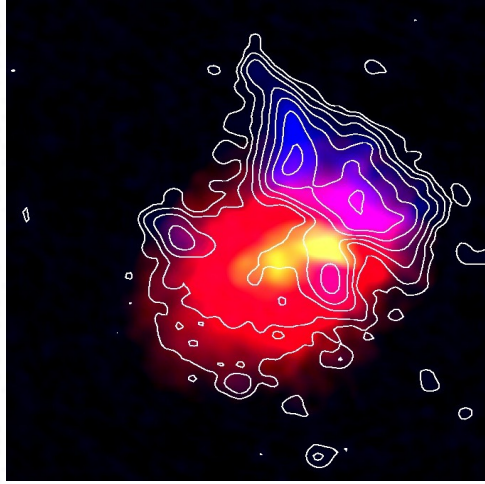

cluster radio emission & magnetic turbulence

- structure formation drives turbulence & shocks
- radio halos & relics trace magnetic fields & CR within cluster volume & slices, respectively

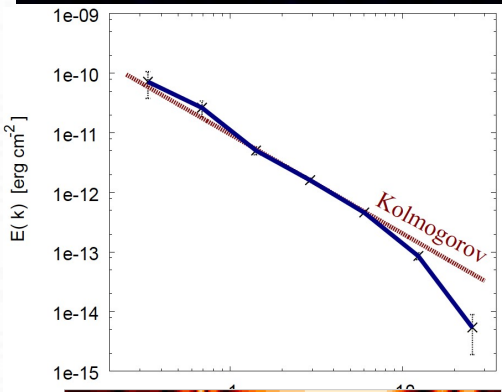

Faraday rotation & magnetic inference

- Kolmogorov-like magnetic spectrum in cool cores
- similar spectra found in non-cool core clusters

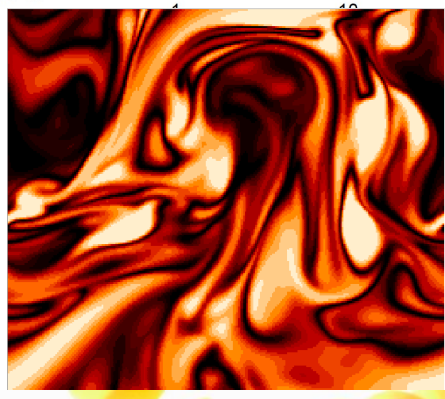

Stokes correlators & turbulent magnetic forces

- synchrotron emission reveals magnetic forces
- tension force power spectrum should be measurable

Faraday-Stokes correlations & magnetic helicity

- magnetic helicity imprints on radio observables
- helicity spectrum is observable
- simple acid-test for helicity presented

Thank you!

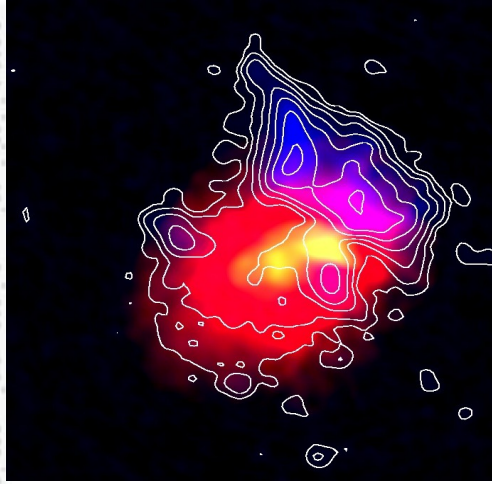

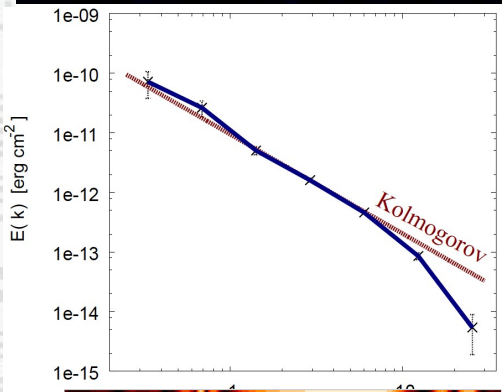

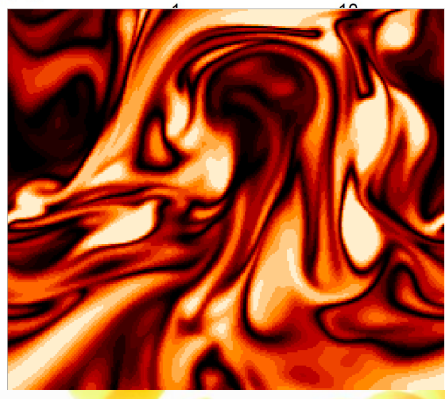

Thank you!

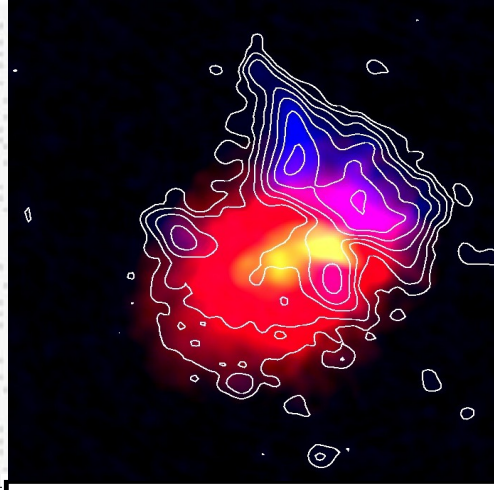

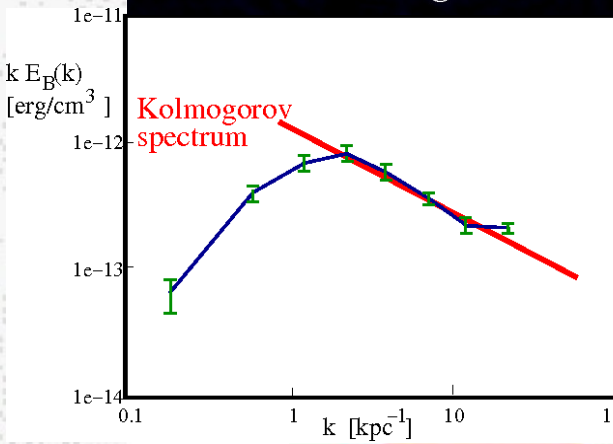
1e−11
k E_B(k)
[erg/cm^3]
Kolmogorov
spectrum
1e−12
1e−13
1e−14
0.1
1
10
k [kpc^−1]

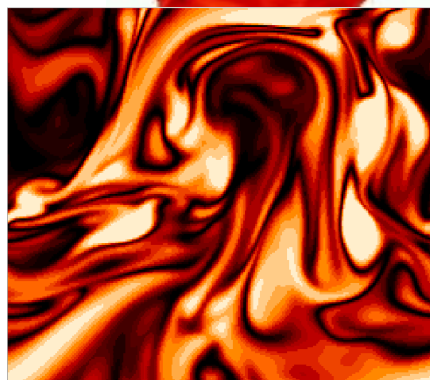

The Acidtest with real data

Taylor,Stil,Sunstrum 2009

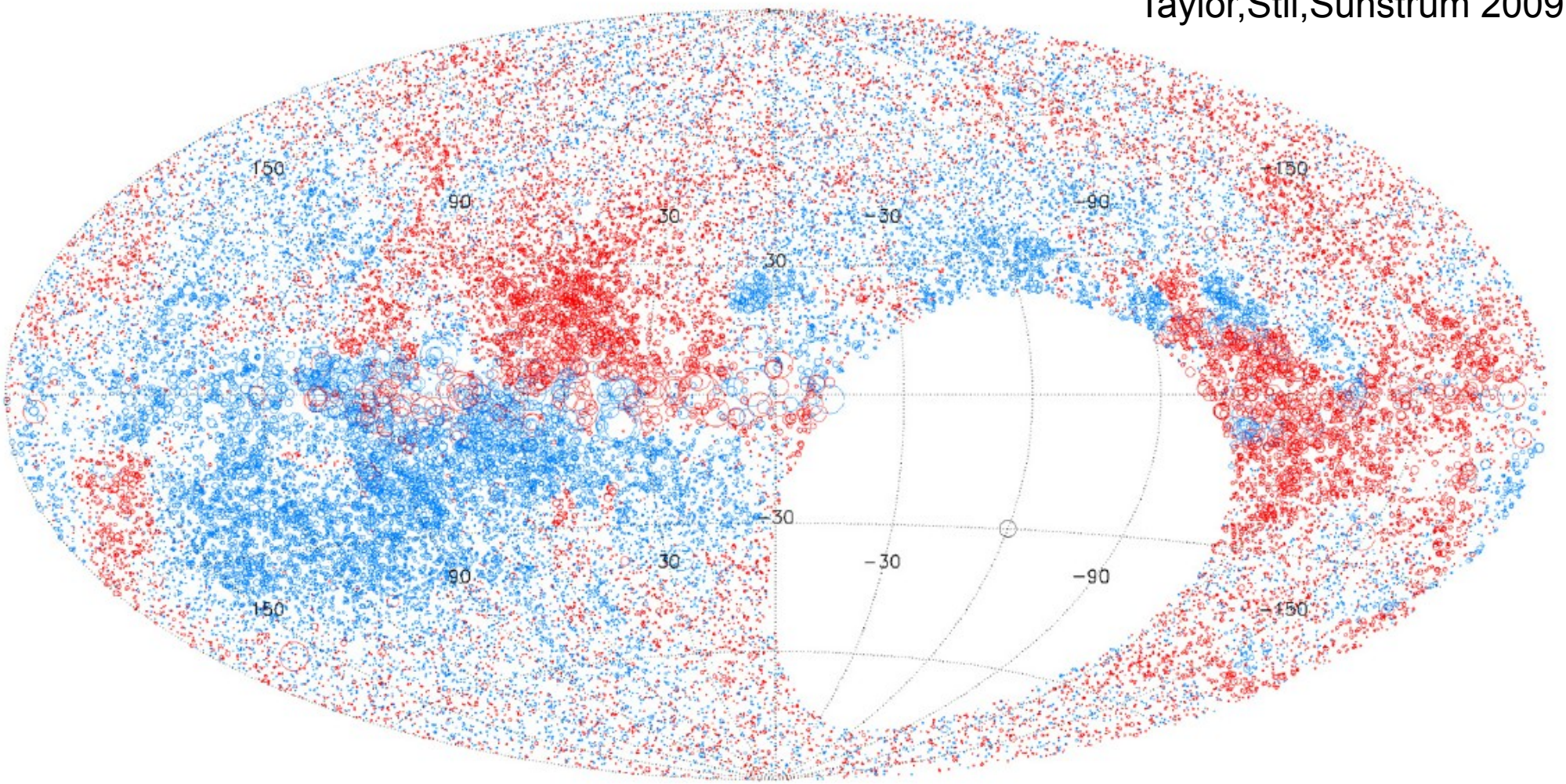

37,534 RM extragalactic RM-sources in the northern sky

The Acidtest with real data

Taylor,Stil,Sunstrum 2009

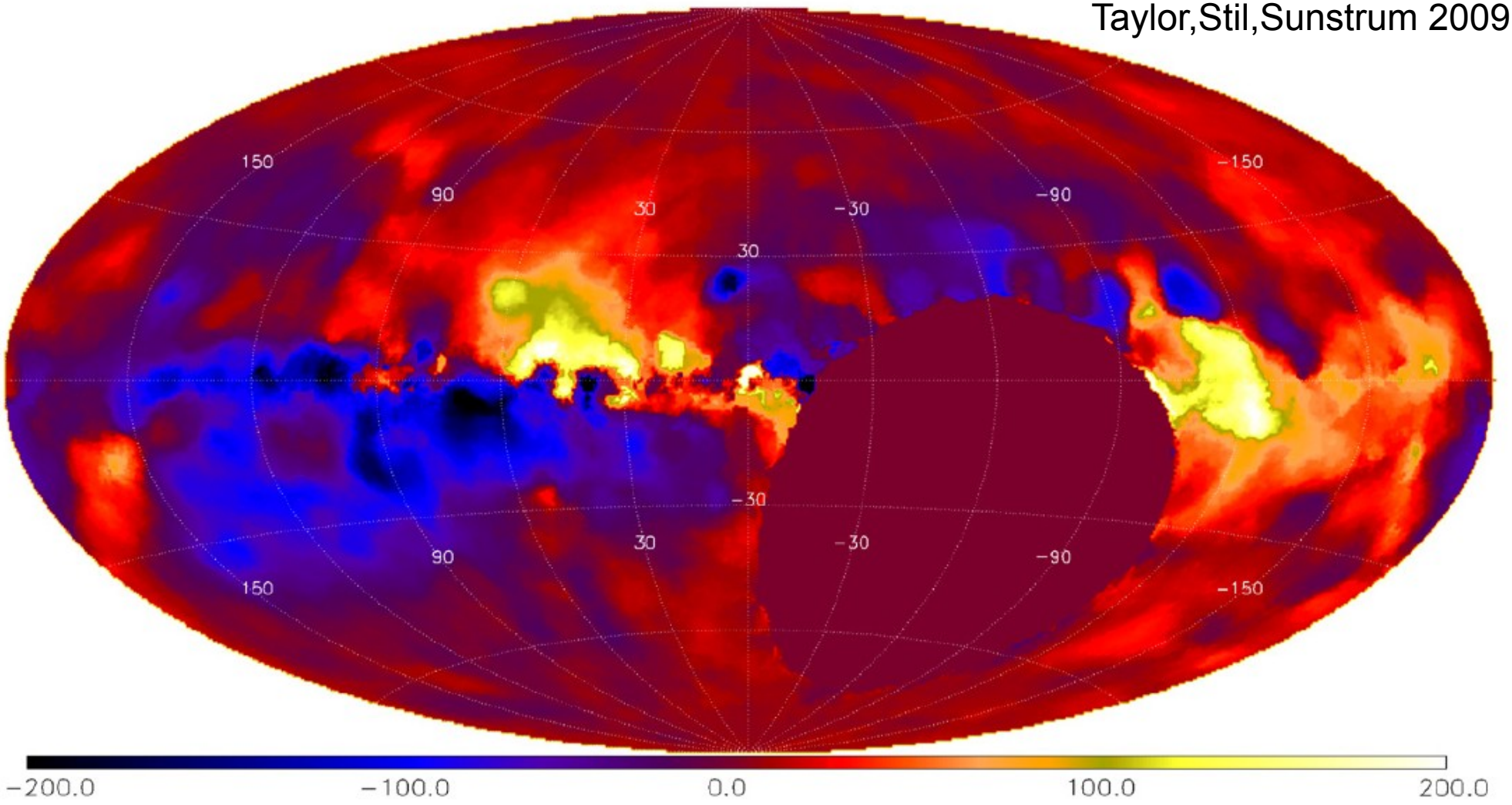

Image of the median value of RM

The Acidtest with real data

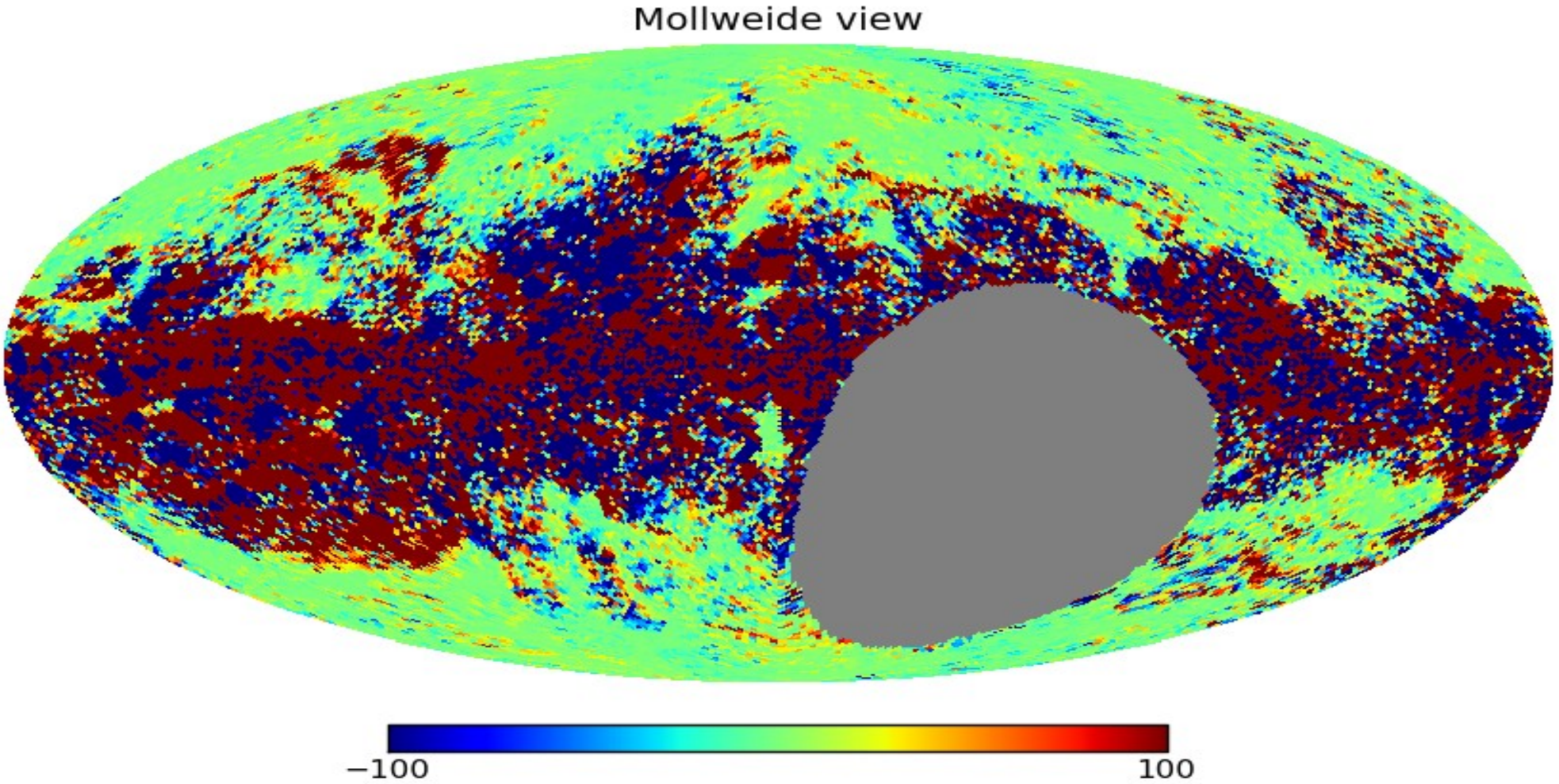

real part

The Acidtest with real data

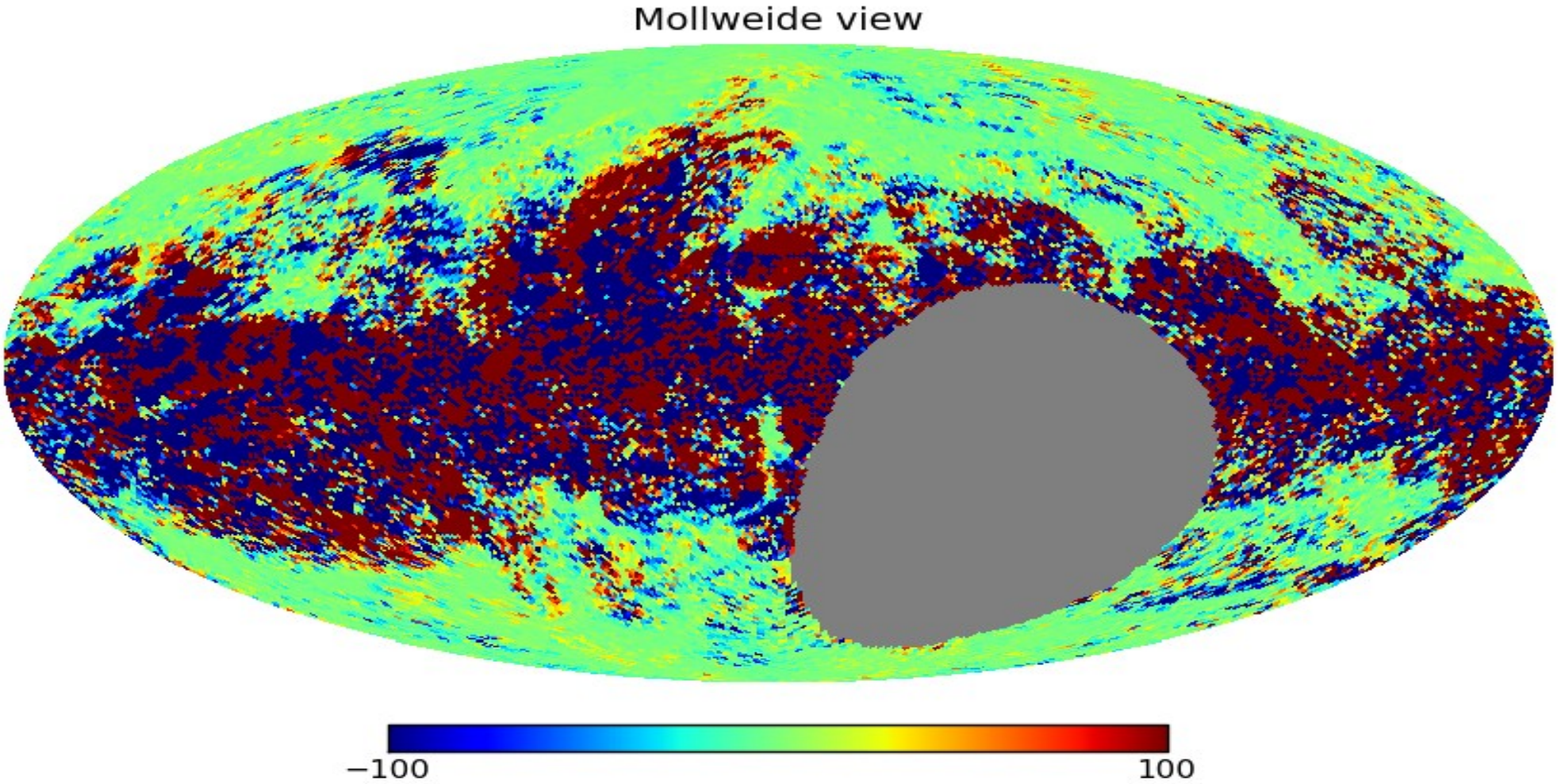

imaginary part

The Acidtest with real data

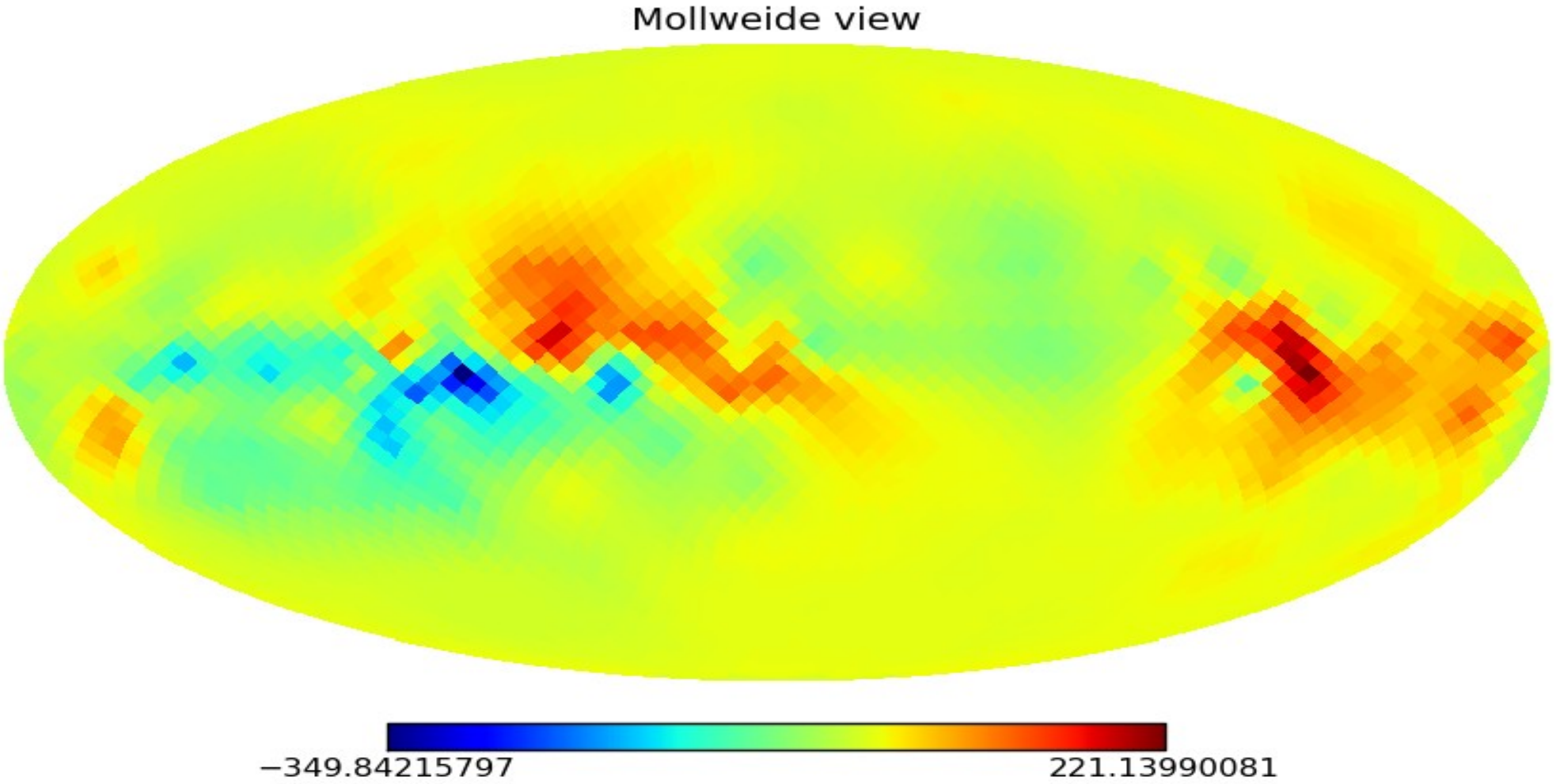

Wiener filtered RM-map with infered power spectrum

The Acidtest with real data

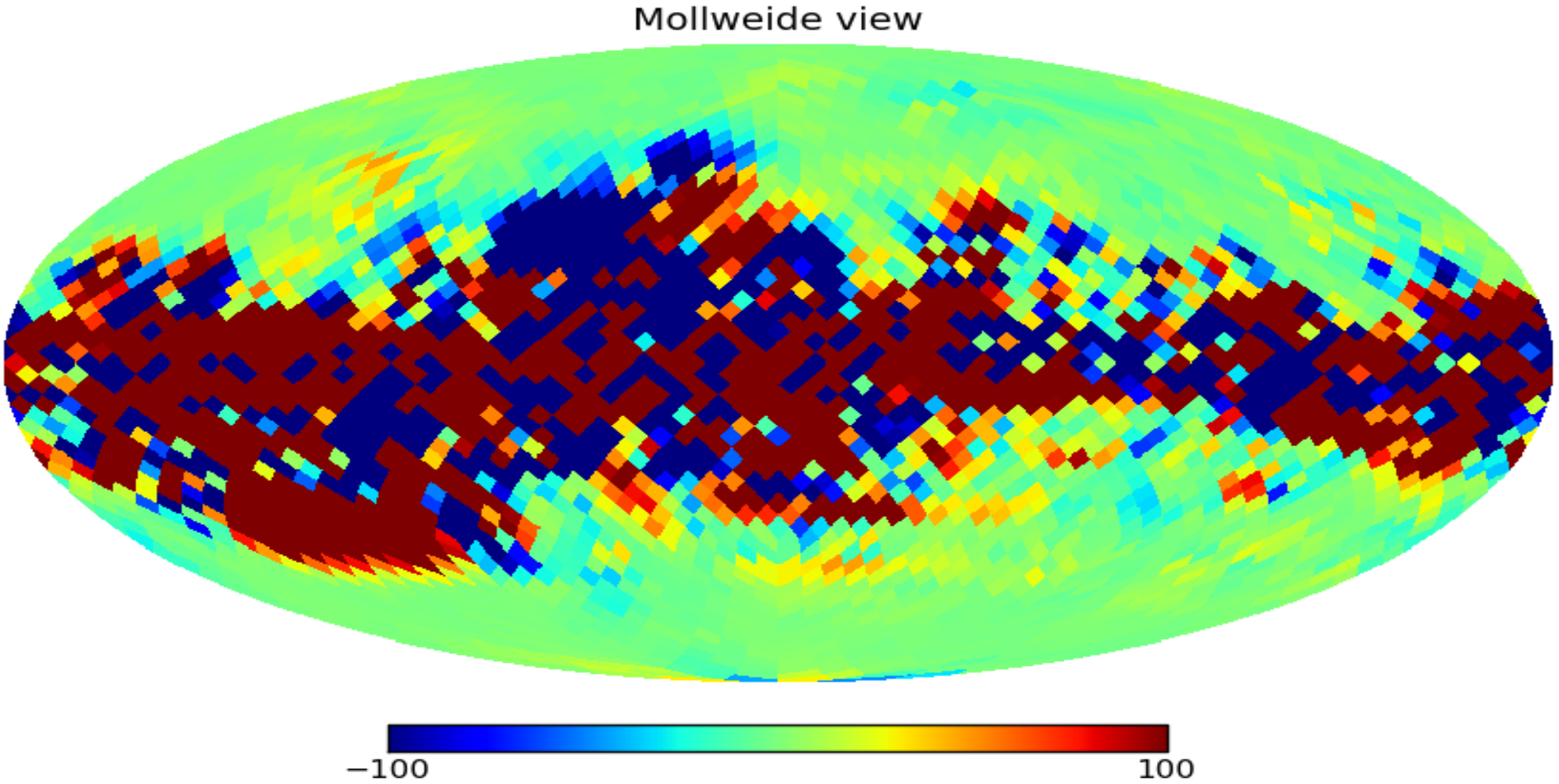

real part calculated with the Wiener filtered map

The Acidtest with real data

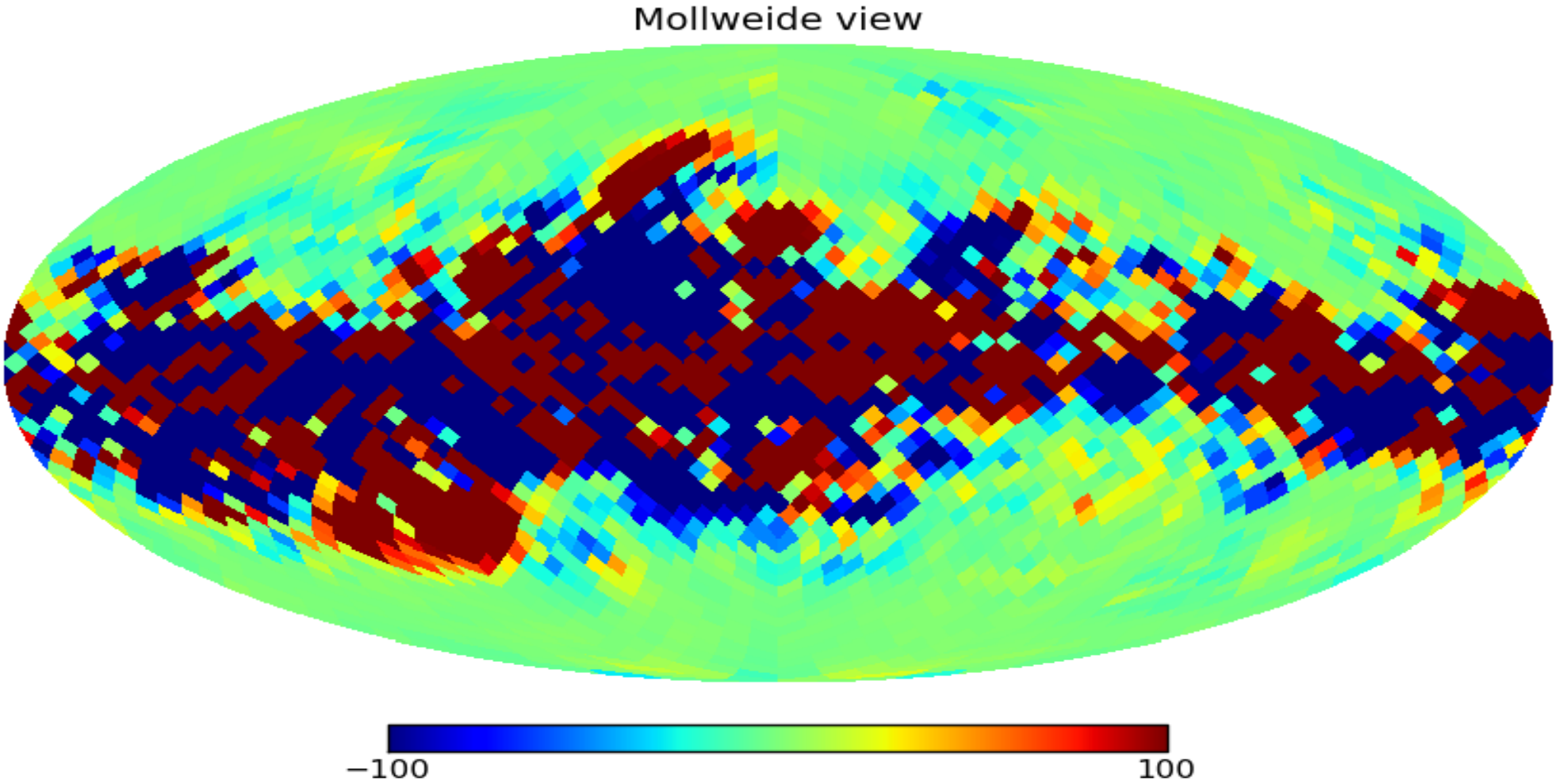

imaginary part calculated with the Wiener filtered map

The Acidtest with real data

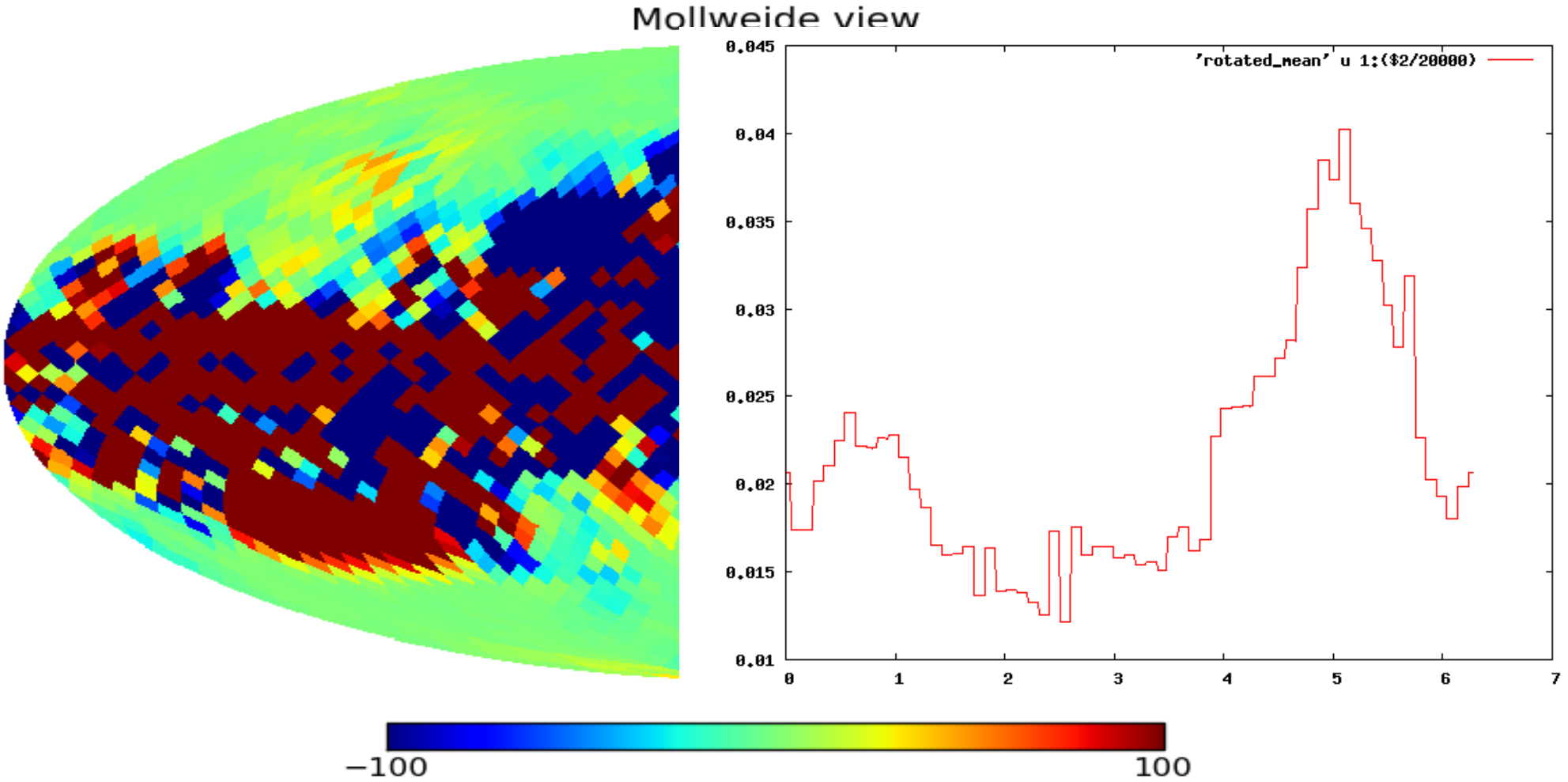

real part calculated with the Wiener filtered map